Superoxide as a Messenger of Endothelial Function

DISSERTATION

zur Erlangung des akademischen Grades
des Doktors der Naturwissenschaften
an der Universität Konstanz
Mathematisch-Naturwissenschaftliche Sektion
Fachbereich Biologie

vorgelegt von

Markus Michael Bachschmid

Tag der mündlichen Prüfung: 15. Mai 2003
Referent: Prof. Dr. V. Ullrich
Referent: Prof. Dr. W. Hofer
Referent: Prof. Dr. J. Pfeilschifter

Acknowledgment

The current work was carried out at the Department of Biological Chemistry of the University of Konstanz during the period of 1999-2002. Working there was at the same time instructional and fun, both of which being constantly upheld by my supervisor Prof. Dr. Volker Ullrich. Besides instructions, I like to thank him for his excellent support and working facilities he provided.

I am grateful to all of my colleagues and co-workers for their friendship, collaboration and support especially to Dr. Dr. M. Zou, E. Müßig, D. Namgaladze, P. Schmidt, C. Kavakli, V. E. Dormeneva, R. Hölz, G. von Scheven and G. Naschwitz. I like to thank also my diploma candidates for their very dedicated cooperation and the numerous overtimes, S. Schildknecht, K. Heinz, S. Schwarz and A. Baumann.

I like to thank Prof. Dr. Lüscher, Helen Greutel and Dr. Francesco Cosentino for the excellent and very successful collaboration. The permanent contact, scientific discussions and friendship of Bernd van der Loo is gratefully acknowledged.

I like to thank Prof. Dr. Przybylski and Nikolay Youhnovski for their kind collaboration in performing mass spectroscopy.

I had the privilege to become a member of the “Graduiertenkolleg Biochemische Pharmakologie” and I profited very much from the collaborations and support among the members, its seminars, its courses and the attendance of national and international congresses. I wish to thank the organisers Prof. Dr. Wendel, Prof. Dr. Nicotera and Prof. Dr Ullrich for their professional running the “Kolleg”.

I like to acknowledge the friendship and scientific help of K. Eichert, G. Dünstel, Dr. J. Hamacher and Dr. E. May.

Last and final thanks go to my beloved family.

Contents

Superoxide as a Messenger of Endothelial Function

The results of this thesis have been published as contributions to the following papers:

1. Bachschmid M, Thurau S, Zou M, Ullrich V. Endothelial cell activation by endotoxin involves superoxide/NO mediated nitration of prostacyclin synthase and thromboxane receptor stimulation. FASEB (Submitted and accepted at the first levels reviewing) 2002

2. Cosentino F., Van der Loo, Bachschmid M Ullrich V, Luscher T. Submitted to Circulation

3. Bachschmid M, van der Loo B, Thurau S. Luscher T, Ullrich V. Oxidative stress-associated vascular aging is independent of the Protein Kinase C/ NAD(P)H oxidase pathway. Submitted to Mech. Aging Develop.

4. Daiber A, Zou MH, Bachschmid M, Ullrich V. Ebselen as a peroxynitrite scavenger in vitro and ex vivo. Biochem Pharmacol. 2000 Jan 15;59(2):153-60.

5. Zou MH, Bachschmid M. Hypoxia-reoxygenation triggers coronary vasospasm in isolated bovine coronary arteries via tyrosine nitration of prostacyclin synthase. J Exp Med. 1999 Jul 5;190(1):135-9.

6. Ullrich V, Bachschmid M. Superoxide as a messenger of endothelial function. Biochem Biophys Res Commun. 2000 Nov 11;278(1):1-8. Review.

7. van der Loo B, Labugger R, Skepper JN, Bachschmid M, Kilo J, Powell JM, Palacios-Callender M, Erusalimsky JD, Quaschning T, Malinski T, Gygi D, Ullrich V, Luscher TF. Enhanced peroxynitrite formation is associated with vascular aging. J Exp Med. 2000 Dec 18;192(12):1731-44.

8. Ullrich V, Zou MH, Bachschmid M. New physiological and pathophysiological aspects on the thromboxane A(2)-prostacyclin regulatory system. Biochim Biophys Acta. 2001 May 31;1532(1-2):1-14. Review.

9. van der Loo B, Labugger R, Aebischer CP, Skepper JN, Bachschmid M, Spitzer V, Kilo J, Altwegg L, Ullrich V, Luscher TF. Cardiovascular aging is associated with vitamin E increase. Circulation. 2002 Apr 9;105(14):1635-8.

1 Introduction

1.1 The Blood Vessel

1.1.1 Overview

Blood vessels are highly regulated elastic tubes for the transport of blood from the heart to the organs via arteries (high pressure system) and back to the heart via veins (low pressure system). In between, the terminal vessels from the microcirculation are responsible for the metabolite exchange. The blood vessel system can be subdivided as follows:

Arteries (high pressure system)
”Elastic type” = arteries
“Muscular type” = arteries

Terminal vessels (= microcirculation)
Arterioles
Capillaries
Venoles

Veins (low pressure system)
Peripheral veins (capacity system)
Big veins

Depending on the function of the vessel, their architecture varies a lot and the transition between different vessel types is continuous. Therefore this classification is just a formal and stereotype simplification and does not account for the large variations of vessel physiology.
The circulatory system fulfills a series of functions like exchange of metabolites, gases, transport, participation in the immune response, mechanical tasks and triggering of the spontaneous arrest of bleeding. The general composition of a blood vessel is morphologically divided into three sections. Beginning from the luminal site, there is the **intima**, **media** and **adventitia**.

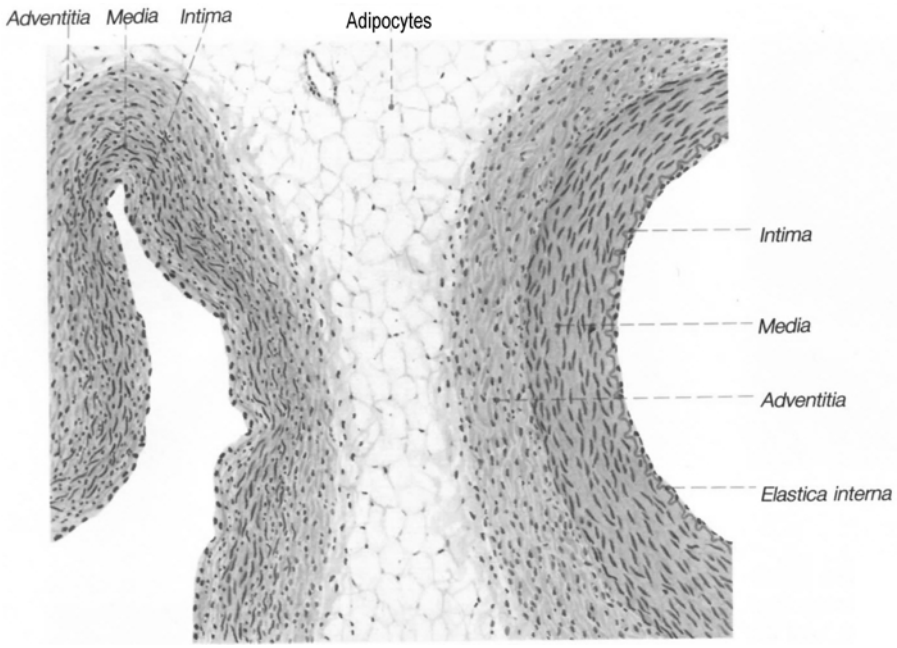

Figure 1.1

General organisation of blood vessels (hematoxylin-eosin staining) in tunica intima, media and adventitia. Cores of the endothelium appear spherical shaped, whereas cores of the smooth muscle cells are ellipsoidal and elongated. Under the fluorescence microscope the basal lamina exerts a relative strong green auto-fluorescence, that makes discrimination easy between media and intima. After Sobotta, 1997

1.1.2 The Intima or Tunica Interna

One can histologically distinguish between the endothelial monolayer and the basal lamina. Endothelial cells exhibit an apical-basal orientation and can be easily distinguished from the media under the microscope (fig. 1.1), because the basal lamina exhibits a strong green auto-fluorescence and appears as a continuous green line dividing intima from media.

In the past, researchers had a very simplified view of the endothelial cell layer, regarding only its barrier function and assigning the active regulatory part of vessel tone to the smooth muscle cell layer. Meanwhile, this opinion has changed, since the most potent vasoactive molecules are endothelium-derived and had been first named after the action they exerted (endothelium-derived relaxation factor [**EDRF**] or endothelium-derived hyperpolarisation factor [**EDHF**]). After their identification and the elucidation of the regulatory pathways, the crucial role of the endothelial cell layer and its contribution to many pathophysiological events like hypertension, atherosclerosis etc. becomes more obvious.

The endothelium has plenty of versatile functions, which are either organ and/or vessel size specific. Therefore a generalization often leads to controversies. For example, a capillary is simply composed of the intima and podocytes (supporting cells). Even this vessel type shows a highly sophisticated adaptation for local requirements, such as the fenestrated type in glands to simplify hormone secretion, for ultrafiltration in the kidney, or in case of the endothelial cells in brain microcirculation, forming the blood-brain barrier by very tight ligation to each

other (tight junctions). The most important functions of the endothelium are summarized as follows:

Angioneogenesis
Regulation of cell adhesion and modulation of local immune function
Regulation of thrombosis (synthesis and release of pro- and/or antithrombotic substances)
Barrier function (regulation of vessel permeability and metabolite exchange)
Synthesis of the basal membrane (Collagen IV and V, proteoglycans, laminin etc.)
Regulation of vessel tone (autacoids, angiotensin converting enzyme etc.)
Growth- regulation of media's smooth muscle cells
Degradation of blood lipids

To take over such complex tasks, the endothelium has developed many specific molecules, mechanisms, and structures like the fuzzy coat named glycocalyx. Its specific sugar groups and membrane proteins are involved in the adhesion of leukocytes to the luminal surface. The endothelium also contains the preformed Weibel-Palade bodies, serving as a storage system for endothelin, von-Willebrand factor and P-selectin. Upon stimulation the vesicles translocate to the membrane, release the factors and present P-selectin on the surface within a few minutes. Another important structure are the vesiculae superficiales or caveolae. These are small spherical to egg-shaped static invaginations of the plasmamembrane (av. diam. 100-200 nm) which are wrapped up by caveolin. Some of them are partially closed by thin membranes of glycoproteins important for signaling and receptor mediated potocytosis, e.g. folic acid is enriched by binding to receptors within the caveolae and cellular uptake is carried out by transport proteins. Endothelial cells also pose intermediate filaments of the vimentin-type and a strongly developed contractile filament system (actin-myosin) for regulation of the intercellular gap and resorption of shear forces.
The basal lamina (membrana elastica interna, basal membrane, lamina elastica) is synthesized by the endothelium and contains specific matrix proteins like collagen IV. This layer functions as an adapter between the intima's endothelial cells and smooth muscle cells of the media, building a "flooding"-like basis to withstand the fluid shear stress.

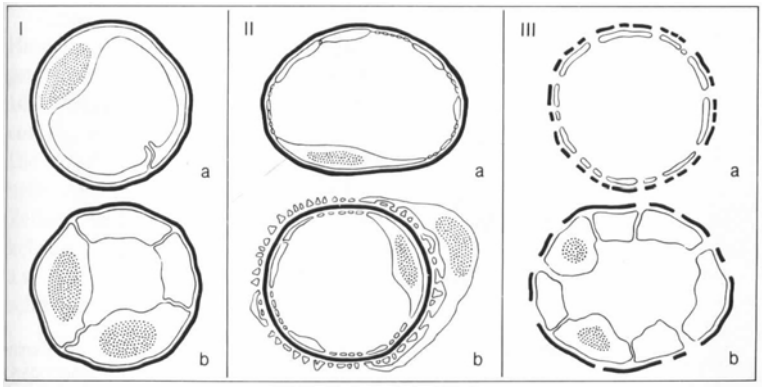

Figure 1.2

Scheme of different capillary types. (I) Closed endothelial cell unit with continuous basal membrane; big variations in cell thickness are possible. (a and b: Skeletal muscle, myocardium, skin, lung). (II) Here and there strongly flattened endothelial cell bodies which either contain membrane closed fenestrations or regular pores (a Glands with internal secretion; b Capillaries of the glumerulum). (III) The endothelial layer has irregular intercellular gaps and sits on an discontinuous basal membrane (a Sinusoids of the liver; b Sinusoids of the spleen). After Benninghoff, 1994.

Sinzinger and coworkers [personal commun.] have shown that the so-called “endothelial dysfunction” parallels stiffening of the matrix and impaired mobility of the endothelial cell layer on top of the media. Endothelial dysfunction is characterized by an inappropriate reaction of the endothelium upon stimulation with agonists or shear stress to release endothelium-derived mediators (PGI_2, NO, EDHF) for maintenance of vascular homeostasis. It sometimes is used synonymously with “endothelial cell activation”, which contains related mechanisms.

Further, the matrix also serves as a storage structure for growth factors, mediators (bFGF, von-Willebrand factor etc.), which are activated and released after endothelial cell injury.

1.1.3 Tunica Media

Depending on the vessel type, the media contains smooth muscle cells ,collagen fibrils of type I and III and elastic material in different amounts. The media of the aorta (elastic type vessel in proximity of the heart) is very rich in elastic fibers to smoothen the waves caused by the beating heart, and therefore generating a relative constant blood pressure and flow (“Windkessel”, elastic buffer). Nevertheless, the aorta participates actively in blood pressure regulation by its contractile smooth muscle cells and functions not just as a simple rubber tube. In contrast, the pulmonary or coronary arteries (muscular type) exhibit a high content of smooth muscle cells (myocytes) for flow regulation and blood distribution by actively varying the vessel diameter. On the other hand, veins serve as a blood storage system (low pressure capacity system) and the media of this vessel type contains high amounts of fibers, so that the vessel is able to expand like a balloon. In contrast to the arteries, the vessel walls of veins are much thinner and regularly arranged valves prevent a back flow of the blood.

1.1.4 The Adventitia

The adventitia serves a connector and interface between blood vessels and the surrounding tissue. It contains mainly fibrocytes that synthesize collagen fibrils and a loose elastic fiber net. Depending on the tissue, a few invaded mast cells can be observed. In many model systems the function of the adventitia is neglected for practical reasons. Isometric tension measurements require an isolated vessel, where the adventitia is often removed during preparation. Some researchers have observed that this layer also plays an important role in oxygen radical production etc. that may in fact influence vessel function (R. Cohen, personal commun.). For future work, this should also be taken into consideration.

1.1.5 Effects of Agonist on the Endothelium and Endothelium-Derived Mediators

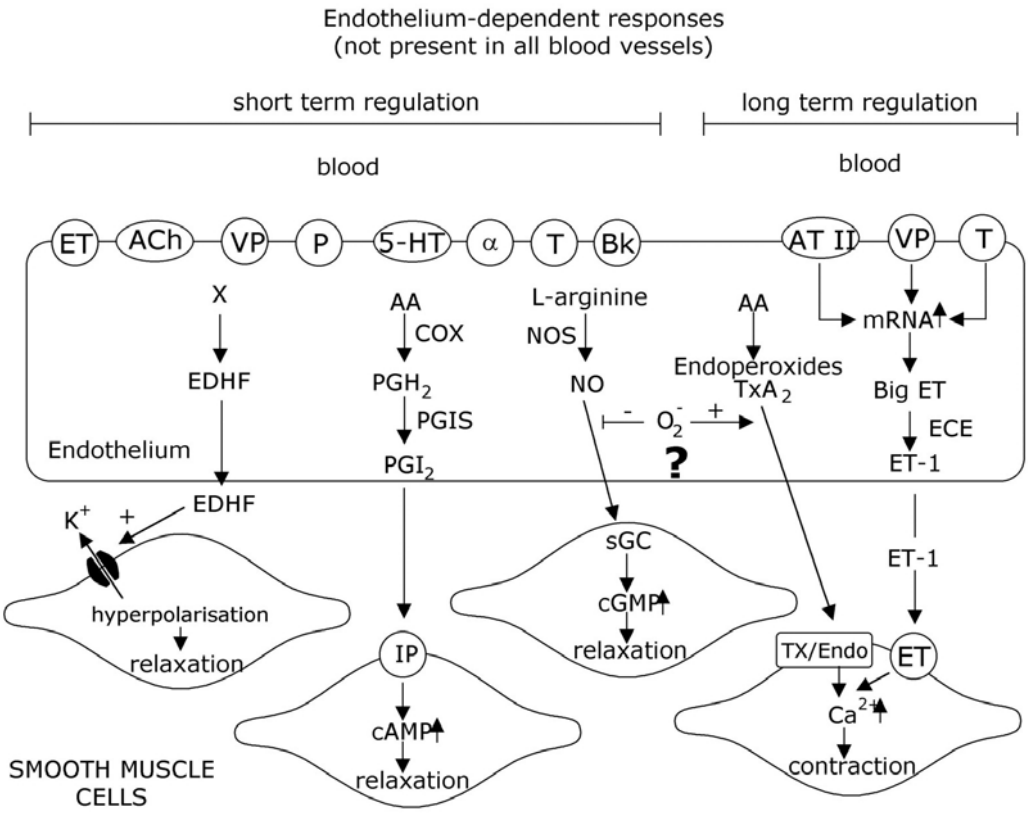

Figure 1.3

Multiplicity of endothelium derived relaxing and contracting factors. α = alpha adrenergic; AA = arachidonic acid; ACh = acetylcholine; AT II = angiotensin II; Bk = bradykinin; COX = cyclooxygenase; ECE = endothelin converting enzyme; EDHF = endothelium derived hyperpolarizing factor; ET = endothelin-1; 5-HT = serotonin; P = purines; T= thrombin; VP = vasopressin, PGI_2 = prostacyclin; PGH_2 = prostaglandin endoperoxide H_2; PGIS = PGI_2 synthase; NOS = NO synthase. After Vanhoutte, 1998.

Many substances (agonists), like acetylcholine, bradykinin, purines (summarized in fig. 1.3), are able to alter vascular function (tone, barrier function, adhesive properties etc.) by modulating endothelium-derived mediators (NO, prostacyclin, EDHF, endothelin). The contribution of the corresponding receptors of the agonists varies for different blood vessel types and species, so that only a very crude overview can be given. Many of these agonists like angiotensin II can have short term effects like alteration of the vessel tone (< 1h), but also long-term effects like induction of endothelin synthesis, VSMC growth (>2-3h) etc. This, as it is the case for angiotensin II, is simply determined by the duration of the stimulus. A short stimulation (30 min.) increases vascular tone whereas stimulation for 4h increases superoxide formation via induction of vascular NADPH-oxidase.

Usually, the endothelium maintains an active cross talk with smooth muscle cells to preserve vascular homeostasis via endothelium-derived mediators. These mediators are very potent, even at very low concentrations (nM to pM range) but belong to different substance classes like radicals, peptides and lipids. Agonists of the endothelium can modulate the generation and synthesis of these endothelium-derived mediators, which leads to alterations in vessel function. These factors can be divided into “good” and “bad” mediators as summarized in table 1.1 and figure 1.3.

	Endothelial Homeostasis	Endothelial Cell Activation
Effects	Vasorelaxation	vasoconstriction
	anti adhesive	adhesive
	anti thrombotic	pro-thrombotic
		mitogenic
Mediator		
	Prostacyclin	superoxide
	nitric oxide	thromboxane A_2
	EDHF	endoperoxides
		endothelin

Table 1.1

The term “good factors” points out that these mediators preserve vascular homeostasis, ensured via anti-adhesive, anti-thrombotic, anti-proliferative and vaso-relaxing properties, whereas “negative factors” cause the opposite effects. Although this classification is very tentative and pragmatic, it helps to underline the aim of this thesis work, which was to

elucidate whether the appearance of these factors is rather a physiologic regulation or part of a more pathophysiological function. Only when changes become systemic and irreversible the term “endothelial dysfunction” seems to be appropriate. In the following chapters, attention is focused on the prostanoid, nitric oxide, and superoxide pathways as mediators of vessel tone and on the changes that may lead to responses of the endothelium under the influence of hypoxia/ reoxygenation injury, alterations or aging.

1.2 Prostaglandins

Historically the first chemically identified mediator of vessel relaxation was prostacyclin (PGI_2), one of the five representatives of the prostaglandins (PG), which were first discovered by von Euler in the prostate secret. They represent a class of highly active lipid mediators and physiological messengers derived from arachidonic acid (AA), and involved in a complex network of regulation. The two isoforms of prostaglandin endoperoxide synthase, better known as cyclooxygenase (COX-1 and COX-2) are the key enzymes for the prostanoid metabolic pathway.

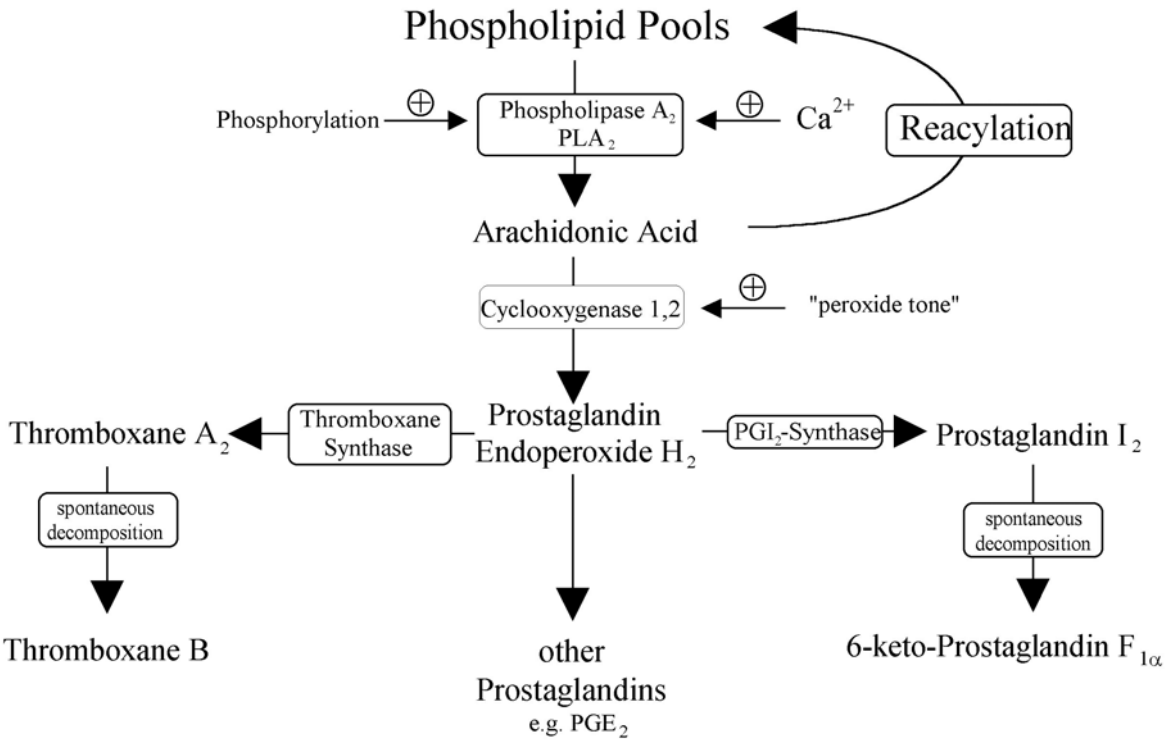

Figure 1.4 After Ullrich et al., 2001.

Both are of high pharmacological impact, since the beneficial and adverse effects of non-steroidal anti-inflammatory drugs (NSAIDs) are based on the inhibition of either enzyme. COX-1 represents the constitutive isoform, whereas COX-2 is upregulated under inflammatory conditions, explaining the antipyretic and antiphlogistic effects of NSAIDs. Since the function, regulation, receptors etc. of prostaglandins are manifold and depend on the tissue or cell type just a short summary of the most important ones, namely prostacyclin (PGI_2), thromboxane (TxA_2), prostaglandin H_2 and E_2, can be given, since they are key compounds for the present work.

Starting with AA as the substrate, a rise in intracellular Ca^{2+} is considered the initial event leading to activation of phospholipase A_2 (PLA_2) and AA liberation (fig. 1.4). Newer additions to this simple scheme involve different Ca^{2+}-pools from which the influx of extracellular Ca^{2+} has a major and the primary release from intracellular stores has a minor effect on the activation of phospholipase A_2 (PLA_2). Phosphorylation is another pathway for PLA_2 activation, but not yet fully understood. Meanwhile more than ten PLA_2 isoenzymes are known which possibly act on different phospholipid pools. This has led to the concept that AA is not equally distributed in the cell but may be compartmentalized through metabolism, reacylation or due to the presence of special fatty acid binding proteins. Certainly, PLA_2 activity is the first step for PG biosynthesis and sometimes can limit the availability of PGs, but generally the rate-limiting step is the subsequent irreversible cyclisation to 15-OH-prostaglandin-9-11-endoperoxide (PGH_2) by the two COX isoenzymes. Interestingly resting cells contain low levels of free AA, which is not converted by the enzyme. The explanation for this phenomenon is the so called “peroxide tone” leading to an activation of the enzyme (the ferric enzyme is converted into a ferryl-tyrosyl radical state). The levels for both enzymes are different and will usually not be reached in a resting cell (COX-1 ≈ 21nM; COX-2 ≈ 2.3nM). Also the Km for COX-1 is higher than for COX-2, which means the consumption of AA by induced COX-2 is preferred.

Finally, the last step in the synthesis of TxA_2, and PGI_2 involves two isomerases which possess similar biochemical and mechanistic properties . Both enzymes convert the same PG-endoperoxide (PGH_2) by a heme-thiolate (P450 family) dependent mechanism, but its rearrangement leads to the two different products with antagonistic properties. TxA_2, in the circulatory system mainly synthesized by platelets and macrophages, activates the TxA_2-receptor (TP), leading to increased levels in inositol trisphosphate (IP_3) and Ca^{2+}. TxA_2 belongs to the most potent vasoconstrictors and effectors of platelet shape change causing thrombus formation. All prostanoid receptors belong to the class of seven loop

transmembrane spanning G-protein coupled receptors (GPCRs). Differences in their C-terminal cytosolic tail region mediates different G-protein coupling and is responsible for different answers in different cells. From the TP receptor two isoforms derived from differential splicing are known, called TPα (343 aa) and TPβ (369 aa). Both forms increase inositol phosphates, but in the case of TPα cAMP levels are lowered whereas TPβ does the opposite. Surprisingly and most relevant for our results, both receptors can react with the chemically different PGH_2 and also with some isoprostanes (Takahashi et al., 1992) derived from AA cyclizations caused by free radicals. Therefore many assumptions and conclusions in literature are misleading, since they were simply attributed to TxA_2 instead of isoprostanes or PGH_2 respectively (see Aims).

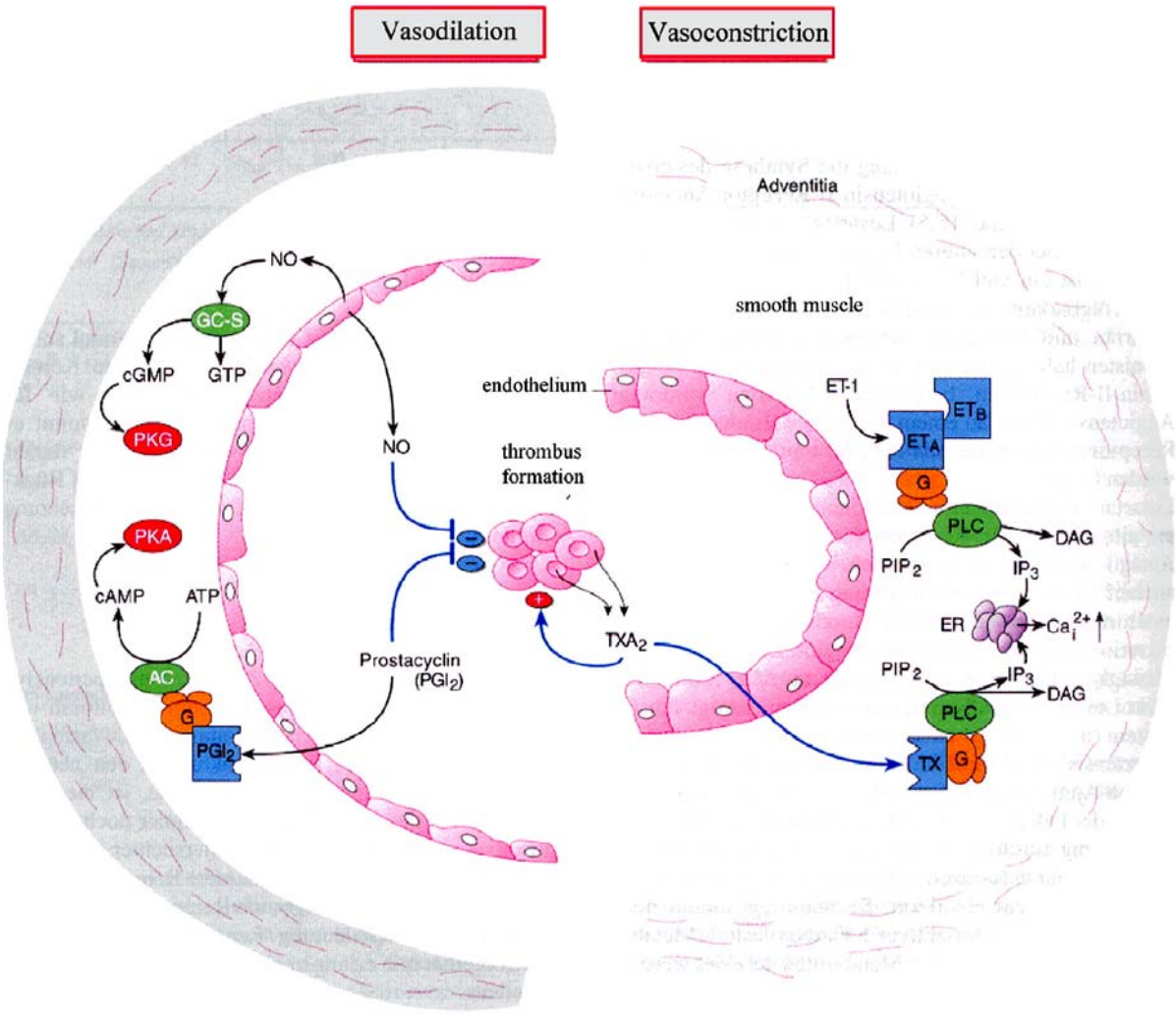

Figure 1.5
GC-S = soluble guanylyl cyclase; PKC = protein kinase C; PKG = protein kinase G; ET-1 = endothelin 1; ER = endoplasmatic reticulum; DAG = diacyl glycerol; PIP_2 = Phosphatidyl inositol phosphate; PLC = phospholipase C; G = G protein. After Forth et al., 1998

PGI_2 which antagonizes the TxA_2 effects, leads to increased levels of cAMP via PGI_2 receptor (IP) activation. The TxA_2-PGI_2 system plays an important role in regulation of hemodynamics

and hemostasis. PGI_2 is considered to be the major vasorelaxant of larger vessels (organism-dependent), whereas the microcirculation seems to prefer NO. In the rat lung, PGI_2 plays an important role as anticoagulant to maintain constant blood flow. Nevertheless, NO and PGI_2 possess a synergistic action, because both mediators are released in a cooperative manner. PGH_2 also serves as substrate for the recently cloned glutathione dependent microsomal prostaglandin E synthase (PGES ≈ 17.5 kDa). This enzyme represents an inducible member of the MAPEG superfamily (membrane-associated proteins in eicosanoid and glutathione metabolism). Other members are microsomal glutathione transferase 1 (MGST1), MGST2 and MGST3, that can conjugate glutathione to lipophilic substrates and are involved in cellular detoxification of several xenobiotics. MGST2 and MGST3 are both able to transfer GSH on leukotriene C_4 and possess, in addition, a peroxidase function. The family also includes 5-lipoxygenase activating protein (FLAP) and leukotriene C4 synthase, both of which are crucial for leukotriene biosynthesis. PGES is most closely related to MGST1, demonstrating 38% identity on the amino acid sequence level. Meanwhile, other enzymes with PGE_2 isomerase activity have been identified, which also exhibit a GSH dependent activity. One of them was identified as a 180 kDa protein, distributed in the cytosol. Researchers believe, because of its high molecular mass, that the enzyme contains several control elements for targeting and activity regulation. Our laboratory has identified the cytosolic 180kDa protein to be present in bovine smooth muscle cells of the aorta and the coronary arteries by Western blotting, but we have not been able to detect the small microsomal isoform (17.5 kDa) by molecular biological or biochemical methods.

Type	Subtype	Isoform	G Protein	Second Messenger
DP			G_s	cAMP ↑
EP	EP_1		Unidentified	Ca^{2+} ↑
	EP_2		G_s	cAMP ↑
	EP_4		G_s	cAMP ↑
	EP_3	EP_{3A}	G_i	cAMP ↓
		EP_{3B}	G_s	cAMP ↑
		EP_{3C}	G_s	cAMP ↑
		EP_{3D}	G_i, G_s, G_q	cAMP ↓, cAMP ↑, PI response
FP			G_q	PI response
IP			G_s, G_q	cAMP ↑, PI response
TP		TPα	G_q, G_i	PI response, cAMP ↓
		TPβ	G_q, G_s	PI response, cAMP ↑

Data obtained from receptors of various species are summarized, and representative signal transduction of each receptor is shown. TP receptor isoforms were from humans, EP_3 receptor isoforms were from bovine, and other receptors were from mice. PI, phosphatidylinositol; ↑, increase; ↓, decrease.

Figure 1.6 After Narumiya et al., 1999.

PGE_2 has four different receptors (EP_1-EP_4), and their distribution varies from tissue to tissue. This explains the manifold effects of the molecule since PGE_2 can increase cAMP via the EP_2/EP_4 receptor, but it also can increase Ca^{++} via the EP_1 receptor (fig. 1.6).

PGE_2 is involved in the regulation of the gastrointestinal peristaltic, mucous secretion, in the development of pain and fever under inflammation and in the regulation of vascular function. In particular Hailer and coworkers (2000) demonstrated, that PGE_2 leads to remodeling of the Weibel-Palade bodies and to expression of P-selectin on the endothelial surface. The receptor types involved in this process are unclear, but it is known to be Ca^{++} independent. On endothelial cells usually EP_2 and EP_4 receptors are expressed which increase cAMP and lead to relaxation of the vessel, but various stimuli can also desensitize or regulate the expression of the receptor, e.g. the EP_2 receptor is induced by inflammatory stimuli. Interestingly, PGE_2 leads to the stabilization of COX-2 mRNA via the EP_4 receptor (interaction with the p38 MAPK pathway) (Faour et al, 2001).

It is therefore difficult to give a general prognosis for the action of prostaglandins on endothelial cell function, since it depends on the vessel type, the species and the preexposure to other mediators.

1.3 Nitric Oxide

1.3.1 Chemical Properties and Reactions

Nitric oxide is a relative stable gaseous free radical and, earlier, had simply been regarded as a toxic molecule of air pollution. In the presence of oxygen, NO generates a variety of reactive nitrogen oxide species (RNS). The autoxidation of NO with oxygen is of third order, since two molecules of NO react with one molecule of oxygen to form nitrogen dioxide, a brown gas. In the aqueous phase at a physiological pH of 7.4, several laboratories confirmed that the rate constant is also of third order, but the reaction product is nitrite, which is often determined in biological systems (Griess-reaction) to measure NO release. This is of critical importance, because it explains why NO at low concentrations within the nM range can serve as a signaling molecule instead of leading to toxic effects. For example at a concentration of ~1µM the $t_{1/2}$ is ≈ 800s, whereas at 1 mM the half live time is less than 1s and also toxic reactions like nitrosations are reduced. At higher concentrations (>10µM), as found in activated macrophages, autoxidation and formation of RNOS increases dramatically.

$$\text{In the gaseous phase} \quad 2^{\bullet}NO + O_2 \rightarrow 2NO_2 \; k = 7.1x10^3 \; M^{-2}s^{-1} \quad (1.1)$$

$$\text{In the aqueous phase} \quad 4^{\bullet}NO + O_2 + 2H_2O \rightarrow 4HNO_2 \quad k = 8x10^6 \; M^{-2}s^{-1} \quad (1.2)$$

Generally NO has high reactivity towards paramagnetic metals, especially to ferrous iron. This is important for downstream effector molecules like guanylyl cyclase, which is believed to be activated by the $Fe^{II}NO$ adduct at the active site. Also oxyhemoglobin (ferrous) reacts very efficiently with NO to form methemoglobin (ferric), since NO in the vessel system should be trapped by the molecule. But under physiological conditions, hemoglobin is packed in the erythrocyte and trapping plays only a minor role for an excess formation of NOS. Nevertheless, the change to the oxidative state of the heme can be simply followed analytically by UV/VIS spectroscopy and serves as a very sensitive method for detecting free NO.

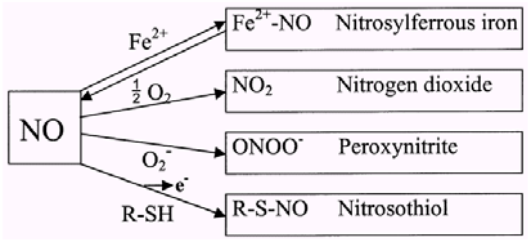

Figure 1.7

Main reactions of NO. NO may reversible bind to ferrous iron within haemproteins, such as guanylate cyclase, haemoglobin and cytochrome oxidase. At high concentrations NO may react with oxygen to produce NO_2 and N_2O_3. NO reacts at the diffusion limited rate with superoxide to produce peroxynitrite. NO, after oxidation to NO^+ or peroxynitrite, can react with thiols to produce nitrosothiols. After Brown, 2001.

Gaston et al. (Gaston, 1999) have demonstrated that NO_x also react specifically with biological thiols such as cysteine or GSH to form nitosothiols. This reaction is chemically termed S-nitrosation (R-SNO), sometimes the wrong term S-nitrosylation is in use.

$$^{\bullet}NO + R\text{-}S^- \rightarrow R\text{-}SNO + e^- \quad (1.3)$$

Stamler (Stamler et al., 1992a; 1992b) was the first to demonstrate that S-nitrosation serves as a biological posttranslational modification of enzymes and can also function as a storage and transport system for NO. For example, a subset of caspase 3 and 9 zymogens in resting cells is exclusively located in the mitochondria (Mannick et al., 2001). These inactive enzymes are S-nitrosated at the active site cysteine. Upon stimulation with FAS, the caspases are released from mitochondria and activated by cleavage and denitrosation. But there is still controversy about the nitrosating radical species, since Stamler postulated that NO directly reacts with the thiols whereas other researchers had difficulties with the above stoichiometry. He recently published a “hydrophobic motive”, for S-nitrosylation, revealed in the primary sequence, i.e., the cysteine, is flanked on either side by lysine, arginine, histidine, aspartate, or glutamate

and, in the prototype case, is followed by an acidic amino acid residue at the +1 position (also "Acid-Base Motif") (Sun et al., 2001).

1.3.2 NO and Vascular Physiology

Initially, NO was discovered in the mouth and stomach, were nitrites in the acidic milieu form NO and NO_2 and serve as cytotoxic agent against pathogens. Later, Furchgott (1984) was one of the first investigators to recognize that, upon stimulation of the endothelium, a factor with vasorelaxing properties was formed. When the endothelium was removed no reaction was observed but supernatants of stimulated culture endothelial cells immediately transferred to the denuded vessel promoted the same effect. This unidentified metabolite was then simply termed "endothelium-derived relaxation factor" (EDRF). Later, this metabolite was identified as NO, the smallest signaling molecule known to date.

ISOFORM	nNOS = NOS I	iNOS = NOS II	eNOS = NOS III
MW	2x 160 kDa	2x 130 kDa	2x 134 kDa
Activation	requires Ca^{++}		requires Ca^{++} phosphorylation
	constitutively	induced by cytokines	constitutively
Distribution	neuronal cells, skeletal muscle	Macrophages, hepatocytes, smooth muscle and a variety of other tissues	endothelial cells, cardiac myocytes, epithelial cells
Function	neurotransmission	host defence, pathologic vasodilatation, tissue damage	regulation of vasotonus
NO-Signal	small Ca^{++} triggered NO bursts	sustained large quantities of NO	small Ca^{++} triggered NO bursts
Km-Value	Km	Km (1-10μM)	-3 μM
Localisation	cytosolic	cytosolic	membrane associated

Table 1.2

NO in the cell is synthesized by three isoforms of NO-synthases (NOS), which belong to the P450- protein family. They use L-arginine as substrate and release NO and L-citrulline, via formation of L-hydroxy arginin, according to the equation (1.4).

$$2\text{L-Arginine} + 4O_2 + 3\ \text{NADPH} + 3H^+ \rightarrow 2\text{L-Citrulline} + 2^{\bullet}\text{NO} + 4H_2O + 3\text{NADP}^+ \quad (1.4)$$

The neuronal (Type I) and the endothelial isoforms of NO synthase (Type III) are constitutively expressed and activated via increased levels of intracellular Ca_i^{++}. In contrast inducible NOS (Type II) is induced by cytokines and is constitutively active. Often, literature describes iNOS as Ca^{++}/Calmodulin independent which is incorrect, since Ca^{++}/CaM are tightly bound to the enzyme even under resting Ca^{++} levels and therefore cannot be further activated by an increase of Ca_i^{++}. The NOS isoforms and their properties are summarized in table 1.2.

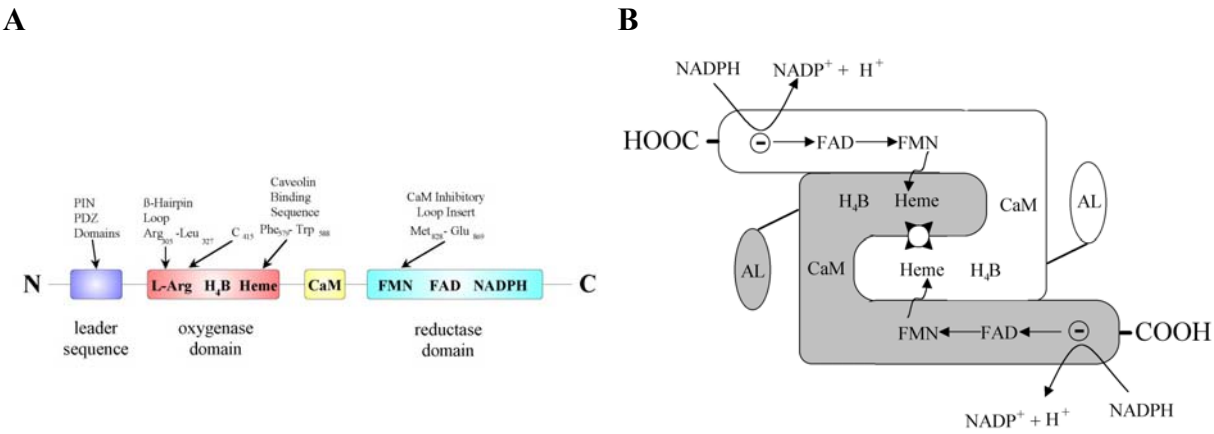

Figure 1.8 After Siddhanta et al., 1998

All NOSs consist of an oxidase and reductase domain (fig. 1.8 A). The reductase transfers the electrons from NADPH via flavins to the heme-center of the monooxygenase. Ca^{++}/CaM controls the electron flux. Usually, the enzyme forms homodimers and the electrons are transferred from the reductase domain of subunit I to the oxidase of subunit two. This model is termed swapping (fig. 1.8 B) and explains that monomerization can lead to superoxide production, since the reductase domain has no acceptor molecule and transfers the electrons onto dioxygen. As indicated by the cartoon eNOS is the biggest isoform and the only one which is membrane-associated by myristoylation. eNOS also contains several binding motifs for associated proteins, that are important for its function and localisation (HSP 90, Caveolin 1, eNOS associated protein-1 (ENAP-1)). It remains still unclear how these associated proteins influence the function of the enzyme, but several diseases where nNOS is thought to

be involved have been described. For example, mutations in two linker proteins of nNOS (α1-syntrophin and dystrophin), which couples the enzyme to the sarcolemmal membrane and to F-actin, leads to Duchenne and Becker muscular dystrophy (the skeletal muscle contains a splice variant of nNOS = μNOS). nNOS and eNOS (in the myocard) seem to be important for maintaining Ca^{++} homeostasis, since NO stimulates Ca^{++}-uptake into its storage systems and inhibits calcium channels. In the myocard it was demonstrated that NO also controls respiration, thus limiting ATP synthesis and protecting the heart from overwork (caused by a calcium overload). Beside these effects, NO has also antiapoptotic properties and leads to growth inhibition. Disturbances can therefore lead to myocardial remodelling and vascular structural changes (hypertrophy, fibrosis, medial thickening). NO in the vascular system has also synergistic effects with prostacyclin, thus inhibiting adhesion and thrombus formation, and leading to vasorelaxation. These effects are mediated via cGMP, which is synthesized upon activation of soluble guanylyl cyclase by NO. A newer promising attempt in treating endothelial dysfunction, caused by a loss of bioavailable NO, is to inhibit the phosphodiesterases metabolizing cGMP. Treatment of penile erectile dysfunction exemplifies one of such therapeutic strategies.

1.4 Peroxynitrite & Nitration

After the discovery of NO as a messenger, several adverse effects have been reported, although the radical itself is neither very reactive nor toxic under physiological conditions and concentrations. However NO forms secondary oxidants which are responsible for tissue injury. One major pathway that enhances the toxicity of nitric oxide is the very fast and near diffusion limited reaction with superoxide to form peroxynitrite (PN).

$$^{\bullet}NO + {}^{\bullet}O_2^- \rightarrow {}^-OONO \quad k = 6.7x10^9\ M^{-1}s^{-1} \quad (1.5)$$

Some authors described the reactivity and the adverse effects by a very simple scheme: NO in physiology maintains homeostasis and can function as a potent antioxidant (“The good”), $^{\bullet}O_2^-$ (“The bad”) neutralizes the NO effects by trapping the radical and forming a new very reactive species, PN (“The ugly”) (Beckman and Koppenol, 1996) which reacts with nearly every biomolecule.

Under physiological conditions ($t_{1/2} \approx 1s$) PN is protonated to peroxynitrous acid which decomposes rapidly without transition metal catalysis to an $^{\bullet}OH$ and $^{\bullet}NO_2$ like radical species $[HO\text{-}NOO]^*$. This intermediate is very reactive, and therefore, PN leads to single and double strand breaks of DNA (activating poly(ADP)ribosyl-transferase (PARS)), lipid oxidation, oxidation of thiols, mixed disulphides and NAD(P)H (oxidised NAD(P)H is suggested to contribute to permeability transition and depolarisation of mitochondrial membrane), protein modifications (fig. 1.9; PGI_2 synthase, MnSOD, neurofilament L, type II SERCA, aconitase).

$$ONOO^- + H^+ \rightarrow ONOOH \quad (1.6)$$

$$ONOOH \rightarrow [HO\text{-}NO_2]^* \quad (1.7)$$

$$[HO\text{-}NO_2]^* \rightarrow NO_3^- + H^+ \quad (1.8)$$

Our group has observed that PN caused inhibition of purified PGI_2 synthase already at very low levels. Also under physiological conditions, segments of coronary arteries revealed impaired release of PGI_2 after PN treatment. The underlying reaction has been identified as nitration of an active site-located tyrosine residue (Y430 by P. Schmidt et al., submitted) and model investigations demonstrated that hemoproteins in general and other P450 (Daiber et al., 2000b; 2000c) enzymes specially can cause such nitrations by the following mechanism.

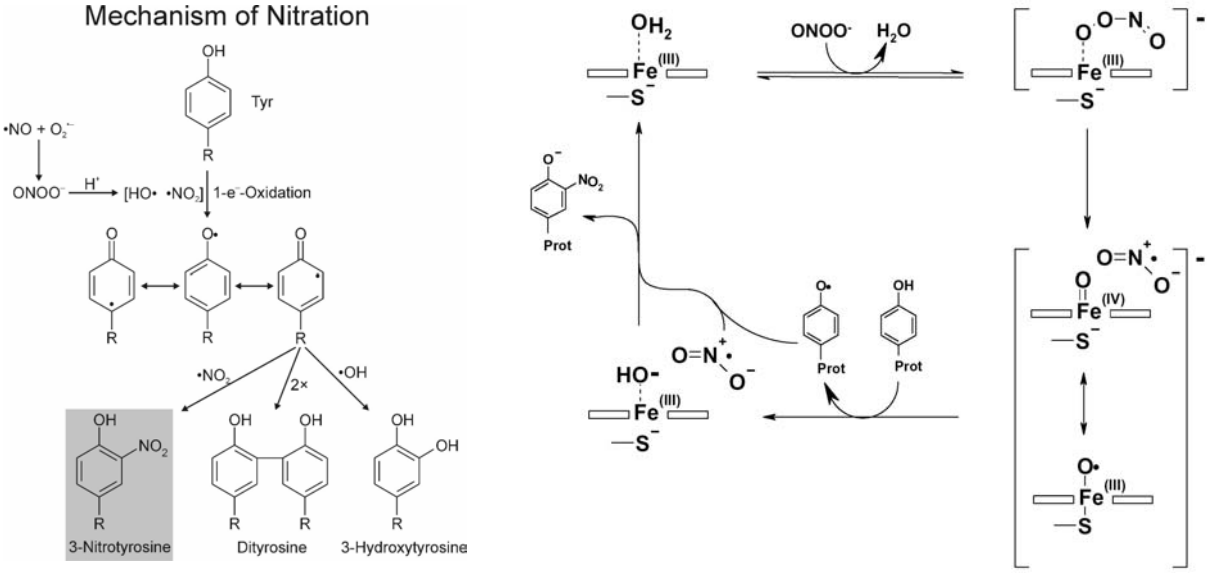

Figure 1.9 After Ullrich et al., 2001.

Besides nitration, also dityrosine formation of vicinal tyrosines, as it is the case for MnSOD, can be observed, which also leads to inactivation of the enzyme.

Another mechanism for nitration is the oxidation of NO_2^- by peroxidases (horseradish peroxidase, myeloperoxidase etc.) in the presence of hydrogen peroxide leading to $^{\bullet}NO_2$ as a nitrating species. But this pathway needs higher concentrations of either molecule within the µM range, that can be achieved under inflammatory conditions. Newer investigations in our lab pointed out that cyclooxygenase, containing its own peroxidatic function, is autocatalytically nitrated via this mechanism (Heinz et al., unpublished data).

1.5 Superoxide

The fast reaction of NO with $^{\bullet}O_2^-$ allowed the conclusion that $^{\bullet}O_2^-$ should possess an antagonistic messenger function since it would eliminate the effects of NO. This concept has found to be true, but recently has been expanded by results from our group, showing that $^{\bullet}O_2^-$ not only can trap NO but also can vary the activity of metalloenzymes like calcineurin (Namgalazde et al., 2002). The resulting PN exerts new messenger functions. We therefore have put forward the concept that $^{\bullet}O_2^-$ is not a simple byproduct of the oxidative metabolism, but serves as a distinct messenger for cell activation by various pathways. Hence the role of superoxide dismutases and the potential sources of $^{\bullet}O_2^-$ require a new definition and investigation. This became especially important since the discovery of $^{\bullet}O_2^-$ as a main causative agent in neurodegenerative disorders (ALS, Parkinson, Alzheimer-disease) or inflammatory events.

1.5.1 Chemical Properties and Reactions

It is a surprising chemical fact, that the formation of $^{\bullet}O_2^-$ from dioxygen ($^3O_2$) requires a strong one electron reducing agent although the four electron reduction to water is highly exergonic. The reason is the diradical nature of oxygen and its relative stability. Very often the further disproportionation of $^{\bullet}O_2^-$ to H_2O_2 and the further reduction of H_2O_2 to OH-radical generate a mix of “reactive oxygen species” (ROS), which has given the impression of $^{\bullet}O_2^-$ as a very reactive and toxic agent. This is incorrect, since isolated $^{\bullet}O_2^-$ is rather a reductant than an oxidant and reduces oxidized cytochrome c which can be used for quantification of $^{\bullet}O_2^-$.

A **B**

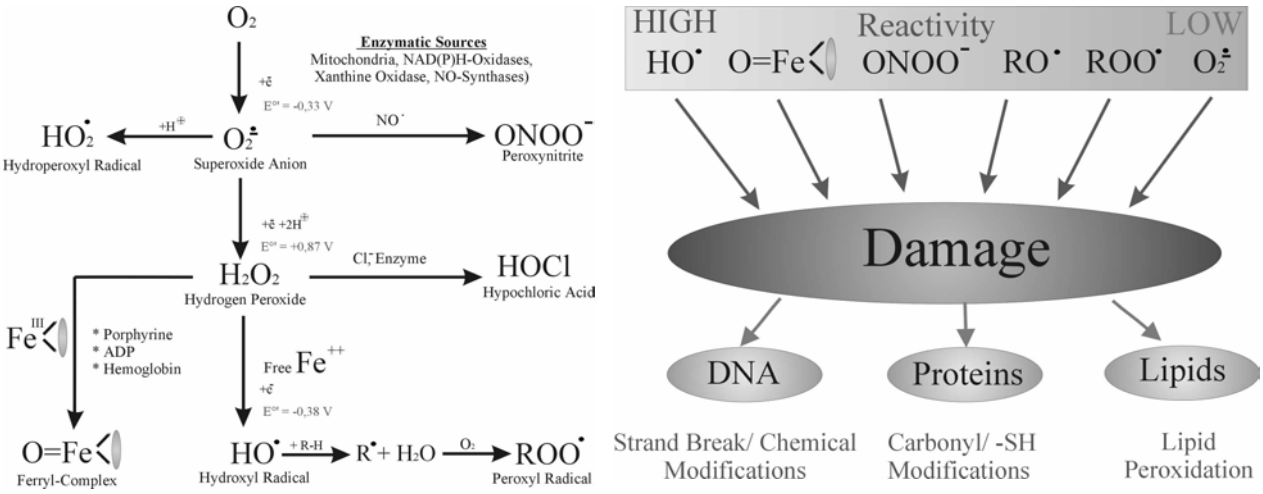

Figure 1.10

The reaction with NO as a radical itself has already been mentioned and its inactivation of calcineurin is based on its reaction with the ferrous center attached to a zinc site, which allows formation of a peroxo species with charge stabilization by the zinc. Similarly, $^{\bullet}O_2^-$ can oxidize iron-sulfur centers as in cytosolic aconitase. This releases the ferric iron and thus causes further oxidative stress, since $^{\bullet}O_2^-$ with this ferric ions forms Fe^{2+}, which then in the Haber-Weiss reaction leads to $^{\bullet}OH$:

$$HO^{\bullet}_2 + {}^{\bullet}O_2^- + H^+ \rightarrow H_2O_2 + O_2 \quad k=7.3x10^5\ M^{-1}s^{-1} \quad (1.9)$$

$$\text{Fenton-Reaction} \quad H_2O_2 + Fe^{2+} + H^+ \rightarrow {}^{\bullet}OH + Fe^{3+} + H_2O \quad (1.10)$$

$$\text{Haber-Weiss-Reaction} \quad H_2O_2 + {}^{\bullet}O_2^- + H^+ \rightarrow {}^{\bullet}OH + O_2 + H_2O \quad (1.11)$$

As a consequence of oxidative stress an influence on several signaling cascades such as the p38MAP kinase, of NFκ B, Ras-Erk pathway, JNK has been observed.

Several of such activating or inhibiting processes have been attributed to direct modification of cysteine residues by $^{\bullet}O_2^-$. This chemical reactivity of $^{\bullet}O_2^-$ with thiols has been proved, but it plays only a minor role in physiology since the pK_a of the superoxide conjugated acid, hydroperoxyl radical, is 4.8 (equ. 1.9). Therefore, direct interactions with metal centers of proteins are essential (like Zn-fingers) to explain $^{\bullet}O_2^-$ mediated alterations of enzymatic processes.

$$HO_2 + RSH \rightarrow H_2O_2 + RS^{\bullet} \quad (1.12)$$

$$2RS^{\bullet} \rightarrow RSSR \quad (1.13)$$

Furthermore, $^{\bullet}O_2^-$ can also react with low molecular weight compounds, including ascorbate, catecholamines, polyphenols and tetrahydrobiopterin (BH_4), which, in case of BH_4, may affect the function of the NO-synthases (see next chapter).

To eliminate the superoxide radical and to maintain a low steady state, mammalian cells contain three isoenzymes:

1.) **SOD1** cytosolic CuZn superoxide dismutase ($k=2x10^9\ M^{-1}s^{-1}$)
2.) **SOD2** mitochondrial manganese superoxide dismutase ($k=10^8\ M^{-1}s^{-1}$)
3.) **SOD3** extracellular CuZn superoxide dismutase

These enzymes are highly effective since researchers have demonstrated that E. coli without SOD 2 generates ~10^{-7} M of $^{\bullet}O_2^-$, whereas the SOD2-repleted bacteria had only levels of ~10^{-10} M. The critical role of SOD enzymes was revealed by Mn-SOD knockout mice, since they died within the first 10 days with a dilated cardiomyopathy and different metabolic abnormalties (Li et al., 1995). Cu/Zn deficient mice are viable, but highly sensitive to oxidative stress (Reaume et al., 1996). Several mutations of SOD are associated with familial amyotrophic lateral sclerosis (ALS). H_2O_2 released after the $^{\bullet}O_2^-$dismutation process is mainly removed by two enzymes, catalase and glutathione peroxidase (GPx). Catalase eliminates very rapidly high concentrations of hydrogen peroxide but works inefficiently at low concentrations. Therefore, the cell has an additional system, glutathione peroxidase, that catalyzes the decomposition of low amounts of hydrogen peroxide using GSH (γ-L-glutamyl-L-cysteinylglycine) as a co-substrate. The regeneration process of GSH requires cellular energy in form of NADPH as a redox-equivalent.

On the other hand, the cell has also enzyme systems which do not directly function as scavengers or antioxidants, but are involved in the anti-oxidant defence system. Glucose-6-phosphate dehydrogenase is important to regenerate NADPH, which maintains the reductive state of the cell. Ferritin chelates set free iron to prevent Fenton chemistry. Finally, some chaperons contribute to reduction of superoxide formation by prevention and repair of malfunctioning enzymes, e.g. heat shock protein 90 (HSP 90) and endothelial NO-synthase (Pritchard et al., 2001; Song et al., 2002 [for nNOS]).

Several investigators have demonstrated that enhanced $^{\bullet}O_2^-$ production in the circulatory system has adverse effects on the regulation of vascular function (aggregation, tone, adhesion), but the causal interaction between the radical and autacoids remained insufficiently explained. Many diseases have been associated with the enhanced production of ROS:

Diabetes, atherosclerosis, hypoxia/ reoxygenation, aging, inflammation, hypertension, homocystemia etc.

It is self evident that trapping of NO and the reduction of free bioavailable NO is one possible and simple explanation for some of these models. Brune et al. (1990; Mülsch et al., 1997) published in vitro data showing that soluble guanylyl cyclase is efficiently inhibited by $^{\bullet}O_2^-$. Concomitantly in many model systems a relation between $^{\bullet}O_2^-$ and the prostanoid pathway was observed. Cyclooxygenase inhibitors and TxA_2/ PGH_2 receptor antagonists improved or even restored vessel function. (Vanhoutte, 2002)

As a summary of these molecular effects, $^{\bullet}O_2^-$ acts as a signaling molecule at low concentrations since it alters the function of some enzymes involved in intracellular signal transduction. It also seems to play an important function in changing vascular homeostasis. At high concentrations, $^{\bullet}O_2^-$,in parallel with NO, exerts cytotoxic effects via e.g. Fenton chemistry, myeloperoxidase etc..

1.5.2 Enzymatic Sources of $^{\bullet}O_2^-$

1.5.2.1 Xanthine Dehydrogenase/ Xanthine Oxidase

A well known $^{\bullet}O_2^-$ generating system consists of xanthine dehydrogenase/xanthine oxidase, which is found membrane-associated on endothelial and other cells and has been found to be responsible for vascular oxidative reactions leading to endothelial dysfunction. The problem arises from the fact that $^{\bullet}O_2^-$ formation via this enzyme requires a conversion of xanthine dehydrogenase to its oxidase form by either thiol oxidation or proteolytic (fig 1.11) cleavage. Also the substrates xanthine or hypoxanthine may only become available in sufficient amounts after ATP or GTP degradation, i.e. under conditions of mitochondrial damage or dysfunction.

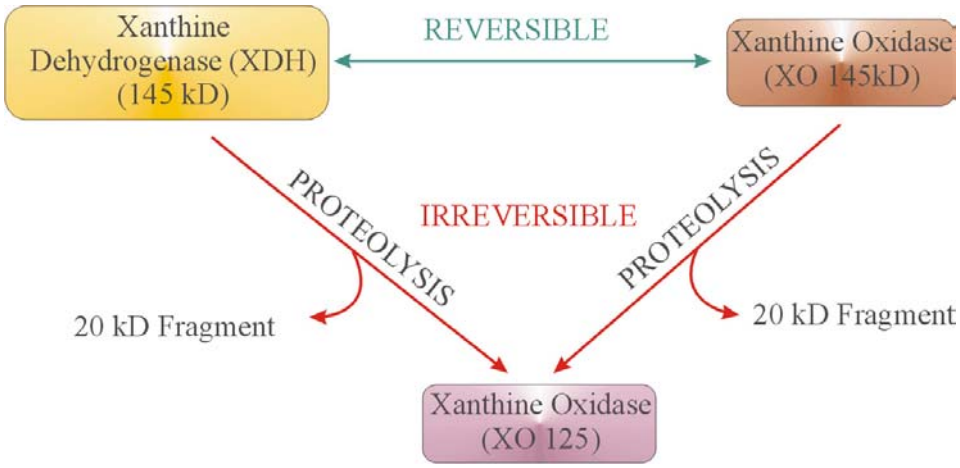

Figure 1.11

Therefore, it is likely that $^{\bullet}O_2^-$ formation by a proteolytically derived xanthine oxidase occurs as a rather late event in vascular damage in contrast to fast and reversible oxidative conversion.

1.5.2.2 NAD(P)H – Oxidases

The first and most prominent member of this superoxide producing enzyme family was discovered as the cause for the severe human immune disorder chronic granulomatous disease (CGD) (Segal, 1996). The symptoms are recurrent and include life threatening bacterial and fungal infections. This may occur due to the inability of phagocytosing cells to generate an $^{\bullet}O_2^-$ burst. Furthermore, $^{\bullet}O_2^-$ may serve as important precursor for bactericidal species like hypochloride, hydrogenperoxide etc. The accumulation of big phagosomes with granula can be observed microscopically. This enzyme was earlier termed as the respiratory burst or phagocyte oxidase (phox), with the catalytically active transmembrane subunit $gp91^{phox}$, newly termed as NOX 2 (NAD(P)H Oxidase).

$$NAD(P)H + 2O_2 \rightarrow NAD(P)^+ + H^+ + 2^{\bullet}O_2^- \quad (1.14)$$

This subunit couples the oxidation of intracellular NAD(P)H (equ. 1.14), directing the electron flux via an FAD-containing flavoprotein (FAD-FP) over two molecules of heme with different redox potentials (cytochrome b558, Cyt b), with the reduction of molecular oxygen for generation of extracellular or phagosomal superoxide. For activation of $gp91^{phox}$, the assembly of further subunits ($p22^{phox}$, $p47^{phox}$, $p67^{phox}$ and rac 1 or 2) is essential (Griendling et al., 2000). Myeloperoxidase is secreted extracellularly or into the phagosome, permitting

hypochlorous acid generation in the extracellular/ phagosomal compartment. Associated with the enzyme, a proton channel guides NAD(P)H-derived protons to the phagosome resulting in a shift of the pH. This is an important step in the activation of phagosomal proteases. The main function of NOX-2 is participation in cellular host defence. Meanwhile, four new isoforms of gp91^{phox} have been identified, but their exact functions and the dependence on activating cytosolic subunits remains a matter of intense research.

All isoforms consist of a C-terminal flavoprotein domain, which is homologous to flavoprotein dehydrogenases, five transmembrane alpha helices and the putative N-terminal secretion signal peptide motif that is cleaved off. NOX-5 is an exception, that contains one further transmembrane alpha helix, which could serve as a "built-in p22^{phox}" (Cheng et al., 2001). The proline/ argenine rich sequence could function as a putative Src-Homology 3 (SH3) binding sequence for the interaction with p47^{phox}.

NOX-1, also termed as mitogenic oxidase (MOX-1/ p65^{MOX}), is important for the regulation of cell growth, cell differentiation and tumor progression (anchorage independent growth). A splicing variant of this enzyme (NOH-1) interestingly codes for a voltage gated proton channel. NOX-3 has been mainly identified in fetal tissue and seems to be important in developmental processes. NOX-4 also named as renal oxidase or kidney oxidase (Renox/ Kox) is mainly distributed in the kidney cortex and colocalizes with erythropoetin synthesis.

A

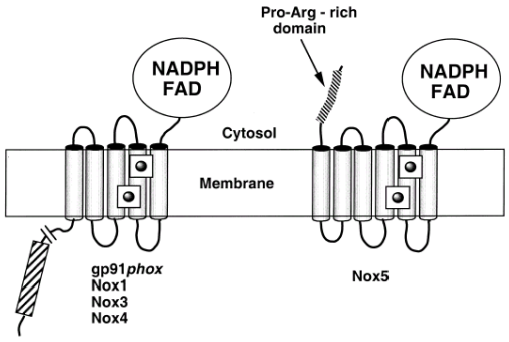

B

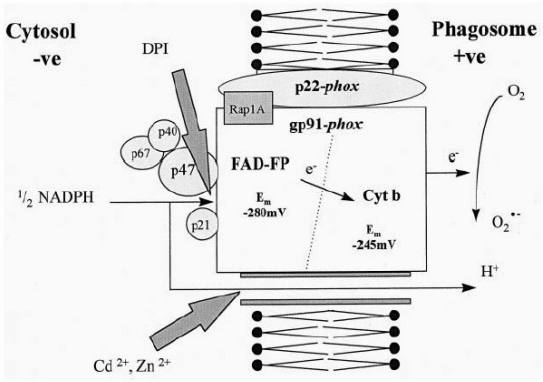

C

Figure 1.12

A. Transmembrane model for NOX proteins. The indicated models for a gp91^{phox}-like group of Nox proteins and for NOX-5 were constructed based upon the presence and predicted orientations of transmembrane alpha helices in the Nox proteins, as well as the presence of putative secretion signal peptide motifs (hashed box). The double bar in the gp91^{phox} group indicates the predicted cleavage sites following the signal peptide. Also indicated are the Flavoprotein

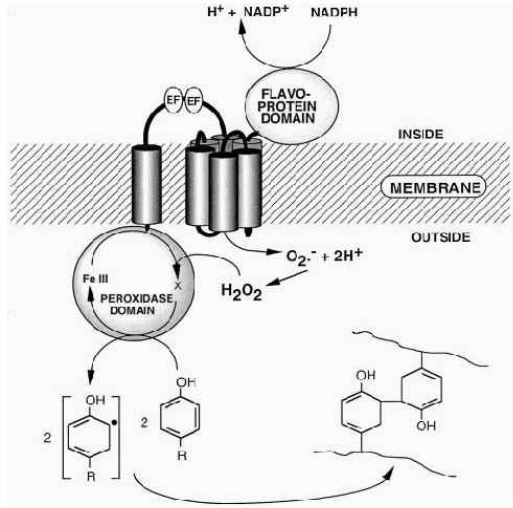

domain containing putative binding sites for NADPH and FAD, bound hemes (shaded balls in white square) and a proline-arginine-rich sequence at the C-terminus of NOX-5. According to Cheng et al Gene 2001

B. Diagrammatic representation of NOX-2 showing the route of passage for the protons (H1) and electrons (e2) generated from the oxidation of NADPH. The enzyme consists of an a and b subunit ($p22^{phox}$ and $gp91phox$ respectively), the latter being a FAD-containing flavoprotein (FAD-FP), two molecules of heme (cytochrome b558, Cyt b), and an associated proton channel. Full activity of the enzyme requires the translocation of polypeptide activating factors $p67^{phox}$ (p67), $p47^{phox}$ (p47) and possibly $p40^{phox}$ (p40), and the G proteins $p21^{rac1/2}$ (p21) and possibly Rap1A. Inhibitors of the enzyme complex include diphenyleneiodonium (DPI), which competes with NADPH for binding at the flavoprotein-FAD complex, and cadmium and zinc ions (Cd21/Zn21), which reversibly block the proton channel. According to Jones et al Free Rad Biol Med 00

C. Ecto peroxidase function for the cross linkage of tyrosine residues to stabilise the cuticular extracellular matrix
According to Edens et al JCB 2001

These investigators assume that NOX-4 functions as an oxygen-sensor. New data indicate a relation of NOX-4 to angiotensin II-induced hypertension. NOX-5 is badly characterized and is mainly expressed in fetal tissue or adult reproductive tracts (Cheng et al., 2001).
The characterization of the exact function, regulation, distribution and enzyme complex formation in the vascular wall still remains a matter of debate and is a very fascinating topic for the future.

1.5.2.3 NO-Synthases

NO synthases, like most cytochrome P450 dependent monooxygenases, have an oxidase activity leading to the release of $^{\bullet}O_2^-$. Loss or deficiency of the tetrahydrobiopterin (BH_4), lack of the substrate L-arginine or even monomerisation associated with zinc release can induce the oxidase function of NOS and generate $^{\bullet}O_2^-$ instead of NO. If NOS becomes a functional oxidase, it is immediately apparent that the enzyme itself could antagonize NO synthesis by trapping NO partially or completely dependent on the degree of conversion to the oxidase form.

1.5.2.4 Mitochondrial Respiration Chain

Mitochondrial respiration involves a complicated network of enzymes for coordinated electron transport. Four electrons being donated by either NADH to complex I (NADH dehydrogenase) or by succinate to complex II (succinate dehydrogenase), respectively, are required for the reduction of oxygen to water. Ubiquinone (coenzyme Q) accepts the electrons from both complexes , undergoes two sequential one-electron reductions to semiquinone and ubiquinol (Q cycle) and transfers them to complex III (UQ-cytochrome c reductase). Via cytochrome C and complex IV (cytochrome c oxidase), the electrons are finally accepted by oxygen. However, electron leaks in the transport chain lead to $^{\bullet}O_2^-$ formation(~0.1 to 1% of total electron flux) but are detoxified by the mitochondrial manganese superoxide dismutase (Mn-SOD) and cytochrome c itself, thus leading to the by-product of hydrogen peroxide. On the other hand, there are disorders like hypoxia/reoxygenation, inflammation and hyperglycemia which are associated with enhanced $^{\bullet}O_2^-$ production. A nonenzymatic mechanism is the autoxidation of ubisemiquinone (UQ_{10}) as shown in equ. 1.15.

$$UQ_{10}^- + O_2 \rightarrow {}^{\bullet}O_2^- + UQ_{10} \quad (1.15)$$

Complex I and III have also been identified as enzymatic sources of $^{\bullet}O_2^-$ generation, including the determination of formation sites within these multiple protein complexes (comp. I is assembled of 34 subunits) via inhibitor studies (I: rotenone, piericidin; III: myxathiazol, antimycin A).

1.6 Nitration and Inhibition of Prostacyclin Synthase

The work presented in this thesis was initiated by the finding of Zou et al. (1996), that PN was able to inhibit PGIS already at submicromolar levels, which can be generated under physiological conditions. An IC_{50}-value for the isolated enzyme of about 0.1 µM was calculated (Zou et al., 1997), but with a microsomal fraction, which contained the enzyme in about 0.1 %, the half-inhibition required more than 10 µM. This was obviously dependent on the presence of other targets for PN, like sulfhydryl groups, since blocking such groups with Ellman's reagent improved the sensitivity. Also enzymes catalyzing the decomposition of PN such as the $P450_{CAM}$ protects PGIS from nitration and inactivation (Zou et al., 2000). However, when intact vessels were used (Zou et al., 1999a), the inhibition was as sensitive as

with the isolated enzyme. A physiological explanation was offered later by the finding that PGIS was located to the caveolae (Spisni et al., 2001), implicating that PN did not have to penetrate through the cytosolic compartment. Interestingly, eNOS is also localized to the same compartment, so that a close neighborhood between the NO generation and PGIS must exist. Furthermore two potential $^{\bullet}O_2^-$ sources are located in close vicinity, since the catalytic subunit of NAD(P)H oxidase ($gp91^{phox}$ and homologs) is a transmembrane protein and extracellular xanthine oxidase is membrane-associated. At the beginning of this thesis work, the process of tyrosine nitration of PGIS was only postulated from a positive Western blot staining with a commercial anti-nitrotyrosine antibody. The inhibition of the staining by active site blockers of PGIS suggested an active site located tyrosine residue, but no direct evidence for 3-nitrotyrosine was yet available.

1.7 The Working Hypothesis

Under physiological conditions, released arachidonic acid upon agonist stimulation like Ang II, is converted by constitutive COX-1 to the prostaglandine endoperoxide H_2. Since this enzyme is rate limiting in the prostanoid pathway and transfer of intermediates is highly coordinated, terminal enzymes like PGI_2-synthase immediately isomerise PGH_2 into the corresponding prostanoid. Therefore, no accumulation of PGH_2 can be observed. PGI_2 diffuses into the subendothelial and luminal space, acts on the smooth muscle IP receptor and increases cytosolic cAMP levels via stimulation of adenylyl cyclase. This activates PKA, resulting in the relaxation of the vessel. (fig. 1.13 “Physiology”). Zou et al. (1999a) have demonstrated that, after treatment of bovine coronary arteries with authentic PN, PGI_2 synthase was nitrated. This was paralleled by a reduced synthesis of PGI_2. In addition strong alterations in vascular tone had been observed. The normal stimulation with Ang II resulted in a biphasic reaction of the vessel, composed of a vasoconstriction and -relaxation phase. In contrast, after PN treatment and stimulation with Ang II, the vessel contracted normally, followed by either a short relaxation phase or at least a tension plateau. This continuously devolves into a second sustained vasoconstriction. Pharmacological studies implicated that the constriction does neither result from an increase in TxA_2 or isoprostanes, nor from an affection of the cGMP pathway. Furthermore, a selective receptor antagonist of the TxA_2/PGH_2 receptor indicates that the vasoconstriction results from increased levels of PGH_2. In conclusion, inhibition of PGIS causes accumulation of PGH_2, which acts on the TxA_2/PGH_2 receptor, thus provoking vasoconstriction. This can simply be regarded as an

imbalance of "endothelium-derived relaxing"- and "endothelium-derived contracting factors" (EDCF) towards constriction. This thesis work demonstrates that $^{\bullet}O_2^-$, PN, and PGH_2 belong to the group of EDCFs and are physiological relevant.

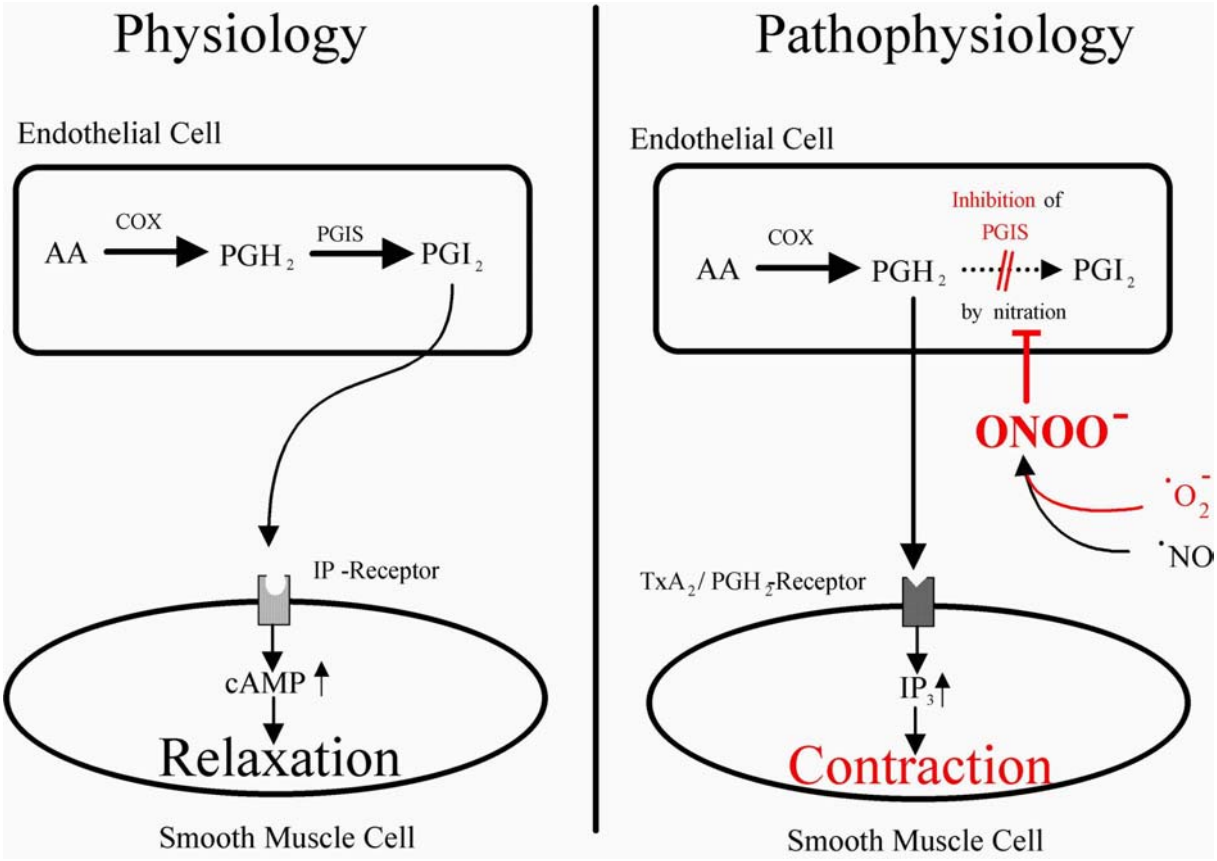

Figure 1.13
Concept of changes in vascular physiology leading to vasoconstriction under pathophysiological situations like hypoxia/ reoxygenation injury, inflammation, diabetes, aging, atherosclerosis, hypertension etc. The vasoconstriction is caused by an imbalance of endothelium derived mediators: Reduction of prostacyclin, and free NO, and increase of PGH_2 levels.
cAMP = cyclic adenosine monophosphate; cGMP = cyclic guanosine monophosphate; IP_3 = inositol tris phosphate; PGH_2 = prodstaglandin endoperoxide H_2; PGI_2 = prostacyclin; AA = arachidonic acid; COX = cyclooxygenase; PGIS = prostacyclin synthase; $ONOO^-$ = peroxynitrite; IP-Receptor = prostacyclin receptor.

2 Aims of this Study

The discovery of a tyrosine nitration at prostacyclin synthase in our laboratory had been discussed controversially in literature and on international meetings since the analytical proof as well as the physiological significance could not be definitely established. It therefore seemed necessary to concentrate on several aspects of this unusual reaction on order to obtain general acceptance of this reaction as a new regulatory mechanism:

1. The presence of 3-nitrotyrosine in the enzyme had to be shown by direct HPLC-identification.

2. The position of 3-nitrotyrosine in the sequence of prostacyclin had to be established by MS-analysis.

3. Physiological or pathophysiological conditions of a regulation by peroxynitrite should be found besides the already published occurrence of nitrated enzyme in atherosclerotic plaques (Zou et al., 1999a). The following diseased states seemed relevant:
   a) ischemia/reperfusion
   b) diabetes or hyperglycemia
   c) inflammation
   d) aging

   In these diseased states the formation of oxygen radicals had been suggested and even demonstrated. Since NO is almost ubiquitous the formation of peroxynitrite in small amounts seemed possible and hence the nitration of PGI_2 -synthase.

4. In case of a verification of prostacyclin synthase nitration the further interest had to be turned to superoxide as the primary messenger, which would combine with NO as the mediator of its message. Reliable analytics were necessary for the assessment of its role.

3 Material & Methods

3.1 Synthesis

3.1.1 Peroxynitrite Synthesis

PN was prepared using a quench-flow reaction as described by Reed et al., 1974. Briefly, an aqueous solution of 0.6 M sodium nitrite (Riedel-de Haen) was rapidly mixed with an equal volume of 0.7 M hydrogen peroxide (Merck) containing 0.6 M HCl (Merck) and immediately quenched with the same volume of 1.5 M NaOH (Merck). All reactions were performed on ice. To remove residual hydrogen peroxide, the solution was mixed with Mn(IV)-oxide (Merck) and filtrated. The concentration of PN was determined spectrally in 0.7 M NaOH (ε_{302}=1670 M^{-1} cm^{-1}). PN was stored at -20°C and diluted in NaOH to adjust the working concentration.

3.1.2 Biosynthesis of PGH_2

Microsomes from sheep seminal vesicles were prepared according to the method described by Hammarström, 1980. ^{14}C-PGH_2 was prepared by incubation of ^{14}C-AA (BioTrend) with sheep seminal microsomes (Graff, 1982) followed by normal phase HPLC separations (Hecker et al., 1987) as briefly described. 1 mg [650µM] ^{14}C-AA (labeled with 2000 dpm/nmol) were incubated with sheep seminal vesicle microsomes (30 mg of protein) for 1 min at 30°C under supply of oxygen gas. Microsomes were preincubated in 5 ml of 100 mM potassium phosphate buffer, 1 mM p-hydroxymercuribenzoate (Sigma), 5 mM L-tryptophan (Sigma), 1 µM hemin (Sigma), pH 8.0 for 2 min at 30°C. The incubation was terminated by addition of 1.2 ml 2 M citric acid and prostaglandins were immediately extracted from the incubation mixture with 20 ml of diethyl ether (Roth)/ hexane (Roth) 5:1 (v/v) in two sequential steps. The extracts were dried over 1 g $MgSO_4$ (Merck), filtered and the solvent evaporated to dryness. The residue was dissolved in 2 ml of HPLC solvent and separated on an semi preparative LiChrosorb® Si60 5 µM (Merck) column (10mm x 250mm) (HPLC pump 2150, LKB; UV/VIS detector Spectra Focus, SpectraPhysics; Scintillation detector Ramona D, RayTest). Elution was performed isocratically (hexane/isopropanol (Merck)/acetonitrile (Merck)/glacial acetic acid (Roth) 95:25:0.05:0.05) at a flow rate of 4 ml/min, continuously

recording absorbance (200 nm) and radioactivity. The average elution time for PGH_2 was about 12 min (see fig. 3.1). Collected fractions were concentrated by evaporation under a continuous stream of nitrogen and store at –70°C.

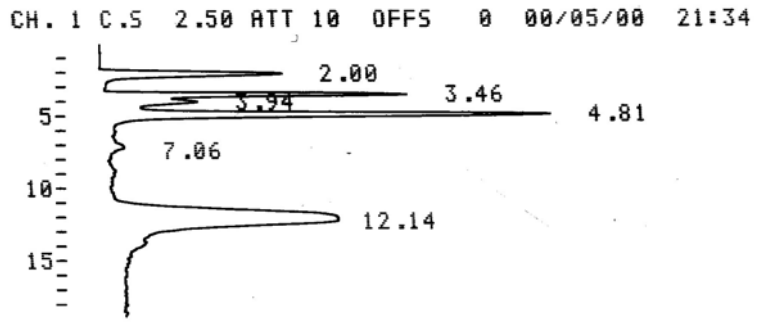

Retention Time [min]	Relative Amount	Metabolite
02.00	09.8 %	Arachidonic acid
03.46	16.2 %	unknown
03.94	01.5 %	unknown
04.81	23.3 %	unknown
07.06	00.7 %	Prostaglandin Endoperoxide G_2
14.14	48.5 %	Prostaglandin Endoperoxide H_2

Figure 3.1
Representative chromatogram of ^{14}C labeled reaction products, subjected to HPLC straight phase separation with the corresponding retention times.

3.1.3 Regeneration of Silica HPLC Columns (Straight Phase)

Problems have frequently occurred during the separation of PGH_2 by straight phase HPLC, due to changes in the water content of the silica phase. This leads to decomposition of the labile PGH_2, reduced separation and shift in retention times. Therefore the liquid phase is substituted with 2,2-dimethoxypropane (DMP; Acros) which reacts in the presence of an acid catalyst with water to form acetone (Bredeweg et al., 1979). The water content can be reduced down to 0.2%. The following two procedures were used:

1.) After every run:

50 ml of hexane/ glacial acid/ DMP 90:10:2.5 (v/v/v) followed by reequilibration with the normal phase

2.) Regeneration of heavily contaminated columns:

Chloroform (Riedel de Häen) → methanol (Merck) → methanol / water 1:1→ methanol → chloroform → chloroform → chloroform / DMP / glacial acetic acid 96:2:2 (each step with 50 ml)

3.2 Preparation of Bovine Aortic Microsomes

Endothelial and smooth muscle layers from 8-10 freshly received bovine aortae were isolated by dissection at 4°C, rapidly frozen in liquid nitrogen and stored at

-70°C. Frozen strips were homogenized at 4 °C in a Waring blender in 100 mM K-phosphate buffer, pH 7.5, containing 1 mM EDTA, 0.1 mM dithiothreitol (DTT), 0.1 mM butylated hydroxytoluene (BHT) and 44 mg/l phenylmethylsulfonyl fluoride (PMSF). The microsomal fraction was obtained by centrifugation as described and made up to a final volume of 75-100 ml, with a protein concentration of 10-20 mg/ml. The homogenization buffer contained 50 mM K_2HPO_4, pH 7.5, without additional protease inhibitors.

3.3 PGIS Activity Assay in Microsomes

PGI_2-synthase activity of bovine aortic microsomes, purified PGIS and bovine coronary arteries after the treatments indicated were assayed as follows: 100 µM ^{14}C-PGH_2 was added and the samples were incubated for additional 3 min. The reaction was stopped by acidification with 1 N HCl to pH 3.5. The incubation media were extracted with 3 volumes of ethyl acetate and after centrifugation, the organic phases were evaporated to dryness under nitrogen. Samples were then resuspended in 60 µl of ethyl acetate and lipids were subsequently separated by TLC (ethyl acetate/water/isooctane/acetic acid 90:100:50:20) (Salmon and Flower, 1982). Prostanoids were quantified with a phosphor imager system (Image Quant, Molecular Dynamics).

3.4 Pronase Digestion of Nitrated PGIS and HPLC Analysis of 3-Nitrotyrosine

3.4.1 Pronase Digestion

Samples of 100 µl of electroeluted PGI_2-synthase were treated with different concentrations of PN (0, 10, 50, 100 and 250 µM), were heated for 10 min to 95°C, then mixed with 10 mM $CaCl_2$ to stabilize proteases. After addition of pronase (1 mg/ml) the samples were incubated for 24 h at 40°C, then another 1 mg/ml pronase was added and incubated again for 24 h at 50°C. Digestion was repeated with a third and fourth portion (0.5 mg/ml) for 12 h at 50°C.

3.4.2 Basic Hydrolysis

Homogenates were hydrolyzed under argon atmosphere in 4 N NaOH for 16 h at 120°C. Samples were neutralised and subjected to HPLC analysis.

3.4.3 HPLC Detection

Prior to HPLC separation the samples were filtered with the 10 kDa MICROCON Centrifugal Filter Devices (Millipore Corporation, Bedford, MA, USA) by centrifuging for 30 min at 10,000 x g. Products were analysed on a Jasco HPLC system consisting of a PU-980 pump, a Jasco UV-1575, Spectra Physics spectra focus UV/Vis detector, ESA electrochemical detector (Coulochem II) and a LG-980-02 low pressure mixing unit. A C_{18} Nucleosil-100-5 250 x 4.6 column from Macherey & Nagel (Düren, Germany) was used with a mobile phase gradient (0-15 min, 0 % (v/v) B; 15-30 min, 0-90 % (v/v) B; 30-40 min, 90 % (v/v) B (A: 0.1 % (v/v) TFA, pH 2, B: 80 % (v/v) acetonitrile with 0.08 % (v/v) TFA)). The flow rate was 1 ml/min and sample aliquots of 100 µl were injected. Tyrosine, phenylalanine, tryptophan and 3-NT were identified and quantified at 270 and 360 nm or +850 mV, respectively by internal and external standards. The retention time of 3-NT was 13 min. for optical detection and ~11 min. for the ECD system. As a control 3-NT was reduced with sodium dithionite to 3-aminotyrosine or spiked with 50 nM of authentic NT.
For ECD detection an isocratic elution was required with the same column and HPLC system (mobile phase: 50 mM potassium phosphate buffer pH 6.0; 10% methanol).

3.5 Analysis of Prostaglandins

Assayed media were acidified with 1 M citric acid (Merck) to a pH between 3.5 and 4 and extracted with 3 sample volumes of ethyl acetate (Merck). The samples were vigorously mixed on an vortex device for 1 min and stored for 1 h. After that samples were again vortexed for 1min, centrifuged at 3000g for 5 min (Varifuge, Heraeus) and the upper phase was transferred to fresh tubes. The samples were stored at –20°C, and the frozen water crystals were again centrifuged and separated from the supernatant. The supernatant was then evaporated under a continuous nitrogen stream to dryness. The residue is redissolved in EIA assay buffer, provided by the manufacturer. Enzyme immunoassay kits were performed according to the instructions of the manufacturer (Cayman Chemical, USA).

3.6 MALDI-TOF Peptide Mapping

MALDI-time-of-flight mass spectrometry was performed with a Bruker BiFlex-DE mass spectrometer equipped with a Scout MALDI source and video system, a nitrogen UV laser (337 nm), and a dual channel plate detector. Sample preparation was performed with 1 µl of a freshly prepared saturated solution of 4-HCCA in acetonitrile/0.1 % TFA (2:1), which was mixed with 0.5 µl of the peptide solution (Bauer et al., 2001). Spectra were recorded at an accelerating voltage of 25 kV and were averaged over forty single laser shots.

3.7 Trypsin Digestion of Nitrated PGIS

Immunoprecipitates were incubated in Laemmli buffer for 5 min at 95°C and separated by SDS-PAGE on a „Novex“ 8 %-Tris-glycine gel (10 wells, Invitrogen Corporation; 30 mA, 1 h). Protein bands were visualized by reverse staining with imidazole-zinc as described above. Proteolytic digestion in the gel matrix was carried out according to the procedure of Shevchenko et al. (1996). The protein bands were excised from the gel, cut into pieces and washed with 2 % citric acid, then with water to remove staining dye, gel buffers and SDS, and dried at room temperature in a vacuum centrifuge. The washing step was repeated by dehydration of the gel pieces and discarding the solution. After shrinking by vacuum centrifugation the gel pieces were reswollen in 200 µl digest solution containing 50 mM ammonium hydrogencarbonate, pH 8.5, 1 mM $CaCl_2$, 10% (v/v) acetonitrile, and 12.5 ng/µl trypsin, and the supernatant was removed. Proteolytic digestion was carried out for 24 h at 37°C under gentle shaking. Peptides were extracted several times with 0.1 % TFA/acetonitrile for 12 h, lyophilized to dryness and analyzed on the above described HPLC system. A C_{18} Nucleosil-100-3 125 x 4.6 column from Macherey & Nagel (Düren, Germany) was used with a mobile phase gradient (0-5 min, 0 % (v/v) B; 5-50 min, 0-60 % (v/v) B; (A: 0.1 % (v/v) TFA in water, pH 2, B: 80 % (v/v) acetonitrile with 0.08 % (v/v) TFA)), at a flow rate of 0.8 ml/min. Peptide fragments were detected at 220 and 365 nm; peaks showing a strong absorption at 365 nm were collected and lyophilized for further analysis.

3.8 Isolation and Isometric Tension Measurement

3.8.1 Tension Measurements in Rat Aorta (Aging)

On the day of the experiment, rats were anesthetized with ketamine (1 ml/kg body wt) and xylazine (0.5 ml/kg body weight; E. Gräub AG). To avoid intravascular clotting, a bolus of 5,000 IU heparin was given before surgery. The chest and abdomen were opened with a medial sternotomy, and the entire aorta from the heart to the iliac bifurcation was excised and placed in cold (4°C) Krebs-Ringer bicarbonate solution. The isolated aorta was cleaned of adhering tissue under a dissection microscope (model M3C; Wild AG). All studies were performed on corresponding anatomical sites of the aorta from each animal (unless otherwise stated, n=8 for young and old rats, n=7 for middle-aged rats). All of the procedures and experimental protocols were approved by the local authorities for animal research (Commission for Animal Research of the Canton of Zurich, Switzerland).

Rings of aorta 4–5 mm long were horizontally mounted between two stirrups in organ chambers filled with Krebs-Ringer bicarbonate solution (pH 7.4, 37 °C, 95% O_2; 5% CO_2) of the following composition: NaCl (118.6×10^{-3} M), KCl (4.7×10^{-3} M), $CaCl_2$ (2.5×10^{-3} M), KH_2PO_4 (1.2×10^{-3} M), $MgSO_4$ (1.2×10^{-3} M), $NaHCO_3$ (25.1×10^{-3} M), glucose (11.1×10^{-3} M), calcium EDTA (0.026×10^{-3} M). Isometric tension was recorded continuously. After a 30 min equilibration period, rings were gradually stretched (2 *g*) until the optimal tension –length relationship was reached as determined by the contraction to KCl (100×10^{-3} M). Before the start of the experiments, rings were allowed to equilibrate for another 30 min. Vessels were preconstricted with $2–5 \times 10^{-7}$ M norepinephrine (Sigma) until a stable plateau of ~70% of the contractile response to KCl was reached. For endothelium-dependent relaxation, vessels were then relaxed with acetylcholine (10^{-10}-10^{-4} M, Sigma) or calcium ionophore A23187 (10^{-10}-10^{-6} M, Sigma). SNP (10^{-10}-10^{-5} M, Cayman) was used as an endothelium-independent agonist.

3.8.2 Isolation and Isometric Tension Measurement Bovine Coronary Arteries (BCA) (Hypoxia-Reoxygenation)

Bovine coronary arteries (BCA) of the left ventricle were isolated and resuspended in a tissue bath with 15 ml of Krebs buffer, gassed with 95% O_2/5% CO_2 (37 C; pH 7.4), and attached to a force–displacement TFT6V5 transducer coupled to a polygraph for the measurement of isometric tension. Passive tension was adjusted to 1 g over a 30 min equilibrating period, and

then coronary arteries were preconstricted by addition of the thromboxane mimetic U46619 ($0.001–0.01x10^{-3}$ M; Cayman). The vasorelaxation after acetylcholine ($0.01–1x10^{-3}$ M) was used to demonstrate the presence of endothelium-dependent relaxation. Throughout the experiment, care was taken to avoid any injury to the endothelium. Experiments were started by obtaining from each spiral a reference response of vasoconstriction–relaxation with Ang II ($5 x10^{-8}$ M) for 30 min. After removal of the agonist from the chambers and return of tone to basal levels, the oxygen tension was then reduced abruptly from 95% O_2 (hypoxia, PO mmHg) and was maintained for 10, 30, or 40 min hypoxia. After this phase of hypoxia, 95% was resumed (reoxygenation), and the tension was allowed to stabilize for 40 min before addition of agonists. If required, pharmacological agents were added in the organ chamber 40 min before hypoxia and kept during hypoxia–reoxygenation and the second stimulation with the agonists. Tissues were kept for immunohistochemistry or immunoprecipitation and Western blots. The media from the first and second stimulations with Ang II were collected and stored at –20°C for prostanoid analysis, as previously described (see 3.5), using ELISA kits according to the manufacturer's instructions.

3.8.3 Isometric Tension Measurement BCA (Endotoxin)

Briefly, experiments were started by obtaining from each vascular strip a reference response of vasoconstriction-relaxation and prostanoid release after addition of Ang-II ($1x10^{-7}$ M, Sigma) over a time period of 30 min. Subsequently, the strip was rinsed several times with Krebs-Ringer bicarbonate solution (composition as described previously) and supplemented with LPS (1-100 µg/ml, E. coli serotype 0127:B8, Sigma). At times indicated, the incubation was stopped by removing the LPS-containing medium. The vessel was rinsed several times and 15 ml fresh Krebs buffer without LPS was added. After the tension returned to the baseline, the vessel was stimulated with the same concentration of Ang-II. Indomethacin (10^{-5} M, Sigma) or N^{ω}-mono-methyl-L-arginine (L-NMMA, Tocris) (10^{-4} M) or SOD-PEG (300 U/ml, Sigma), where required, were added during LPS incubation and also supplemented immediately to the organ bath after removing the LPS containing medium as well as during the second stimulation with Ang-II. The media from the first and the second stimulation with Ang-II were collected and stored at -20^{o} C for prostanoid analysis by using enzyme-linked immunoassay kits (Cayman; See chapter 3.5), according to the instructions provided by the supplier. In some experiments, the endothelial layer was deliberately removed after dissection by intraluminal perfusion with 0.5% 3-[(3-cholamidopropyl)-dimethyl-ammonio]-1 propane

sulfonate (CHAPS, Sigma) in Krebs-Ringer buffer for 40 s followed by repeated washings with Krebs-Ringer buffer.

3.9 PKC Activity Measurement (Hyperglycemia, Aging)

Frozen aortic segments (5mm length) were pulverized and homogenized in a buffer (pH 7.40) containing 250 mM Tris-HCl, 10 mM EDTA, and 10 mM EGTA. Homogenates of animals belonging to one age group (young: n=6, middle-aged: n=6, or old: n=6) were pooled according to protein content. After centrifugation at 21,000 g and 4 ^{0}C for 5 min, the supernatant was transferred to fresh microcentrifuge tubes. PKC in soluble and membrane-associated fractions was separated by further centrifuging at 100,000 g for 60 min. PKC activity was measured using a PKC enzyme assay system (Amersham, U. K.).

3.10 Measurement of Superoxide (Aging, LPS)

$^{\bullet}O_2^-$ concentration in aortic tissue was determined using a lucigenin enhanced chemiluminescence method (Brandes et al.,). Each tissue sample (5 mm length) was placed into 500 µl modified Krebs-Ringer bicarbonate solution, pH 7.40, and prewarmed to 37 °C for 1h. Immediately before measurement, rings were transferred into scintillation vials filled with 500 µl Krebs-Hepes solution, pH 7.40, at room temperature with the following composition: Hepes acid ($10x10^{-3}$ M), NaCl ($135.3x10^{-3}$ M), KCl ($4.7x10^{-3}$ M), $CaCl_2$ ($1.8x10^{-3}$ M), $MgSO_4$ ($1.2x10^{-3}$ M), KH_2PO_4 ($1.2x10^{-3}$ M), Na-EDTA ($0.026x10^{-3}$ M), glucose ($11.1x10^{-3}$ M). 12.5 µl lucigenin (bis-*N*-methylacridinium nitrate; Sigma-Aldrich) was added to give a final concentration of $25x10^{-5}$ M. $^{\bullet}O_2^-$-generated chemiluminescence of lucigenin was detected with a scintillation counter (Raytest PW 4700; Philips) connected to a Philips personal computer system. The computer was programmed to measure $^{\bullet}O_2^-$ in defined time intervals. $^{\bullet}O_2^-$ production by the tissue was calculated as the mean of those last five values that did not differ by > 5% from each other and was expressed as counts/(min x mg tissue). For maximal stimulation, rings were incubated with 10^{-6} M calcium ionophore A23187 (Sigma). In some vessels, the endothelium was mechanically removed 30min before the experiment. All measurements were performed on two or three aortic rings for each animal, and the mean was calculated.

3.11 Porphyrinic NO Microsensor (Aging, Hyperglycemia)

Direct in situ measurements of NO were carried out using a three-electrode system: a porphyrinic NO microsensor as the working electrode (anode), a platinum wire auxiliary electrode (cathode), and a standard calomel reference electrode (Azhar et al., 1995; Tschudi et al., 1996). Amperometric mode detection was used at a constant potential, equal to the peak potential for NO oxidation of the working electrode. The signal was detected in a current range of 10 μA with a pulse height of 50 mV and a drop time of 0.5 s. The amperometric signal was recorded with a Kipp & Zonen chart recorder (Recom Electronic AG). Standard NO solutions ($1.8x10^{-3}$ M) were prepared from an aqueous solution saturated with pure NO gas (Garbagas), and NO concentrations were calculated using a calibration curve with an NO standard. Immediately before NO measurements, aortic rings of 3–4 mm length were cut longitudinally and pinned on the bottom of an organ chamber filled with fresh, phenol red–free, HBSS buffer (37°C, pH 7.4). Then the active tip of the L-shaped porphyrinic NO microsensor was placed on the endothelial surface using a precision stereo zoom microscope and a micromanipulator M3301
(World Precision Instruments). For maximal stimulation of eNOS, calcium ionophore A23187 (Sigma) was injected into the organ bath to yield a final concentration of 10^{-6} M. A mean of at least two independent determinations on two adjacent sections were calculated for each animal.

3.12 Cell Culture (Hyperglycemia)

Human aortic endothelial cells were obtained from Clonetics (San Diego, Ca) and grown in gelatin-coated flasks in optimized endothelial growth medium (EGM, Clonetics) supplemented with 10% fetal calf serum (Biochrom). The cells were detached by exposure to trypsin/EDTA for about 120 sec in HEPES buffered saline and reseeded in collagen-coated 6 cm cell-culture dishes for Western blotting, PKC activity determination and ROS measurement. Cells were first grown ton confluence in humidified air- 5% CO_2 at 37°C. Confluent cells were maintained in EGM containing 2% fetal calf serum, essential and nonessential amino acids and antibiotics. They were incubated up to 24h with control ($5.5x10^{-3}$ M) and elevated glucose concentration ($22.2x10^{-3}$ M) in the absence and in the presence of vitamin C, N-acetylcysteine (NAC), calphostin C, diphenylene iodonium, indomethacin. To rule out an hyperosmolar effect of high concentrations of glucose we also performed

experiments in human aortic endothelial cells after treatment with similar concentrations of mannitol (22.2 mM). Cells between the third and the sixth subpassages were used for the experiments.

3.13 Western Blot

3.13.1 SDS PAGE and Western Blot Analysis (Hyperglycemia)

ENOS and $p22^{phox}$ proteins were analyzed by Western blotting using anti-human eNOS (Transduction Laboratories, USA) and anti- $p22^{phox}$ (kindly provided by Dr. Imajoh-Ohmi, Dpt. Of Bacterial Infection, University of Tokio, Japan) antibodies. The antibodies were used at 250, 200, 100, and 500 times dilution, respectively. After treatment, cells were washed with PBS and lysed (10% glycerol, 2.3% SDS, 62.5 mM Tris-HCl pH6.8, and 5% mercaptoethanol). The lysate was then heated at 95-100 °C for 5 min. Whole cell lysates which contained 20 µg of protein were subjected to SDS-PAGE (8 or 15%). The separated proteins were blotted onto Immunobilon-P (Millipore Corporation, USA) by a semi-dry procedure and then incubated with the prim. antibodies for 60 min. Finally the protein bands were visualized by using a sec. horseradish peroxidase conjugated antibody and the ECL detection kit (Amersham Life Science, England). Densitometric measurements were performed by Fotodyne, visualization and documentation system (Fotodyne, Bio Cell Consulting Research, Switzerland) with MacIntosh Classic II, NIH imaging 1.4 software.

3.13.2 Probing with Anti –Nitrotyrosine Antibody

Complete unfolding of proteins is essential for the presentation of the nitrotyrosine (NT) epitope, therefore the following buffer composition for probing was used: antibody dilution 1: 1000 [final concentration 1µg/ml] in PBS pH 7.4, 0.1% SDS; 0.5% Nonidet P-40; 0.5% Tween 20. This will keep the proteins on the blot denatured. Also only a moderate blocking solution should be used like 1-2% milk powder or BSA. Artificial blocking solutions like Roti-Block lead to a complete loss of the signal. Striping of the membrane at 70 °C for 30 min (62 mM Tris pH 6.8, 2% SDS, 0.007% mercaptoethanol) will further increase the signal.

3.14 Affinity Purification of Anti-NT and Antibodies Against PGIS

For the production of antibodies the following peptides were used:

Nitrated peptides (yellow)

PGIS (485-500; bovine)	LMQPEHDVPVRYRIRP (BioTrend)
PGIS (478-493; bovine)	DLSRYGFGLMQPEH (Prof. Dr. Tanabe/ Osaka)
PGIS (416-428; bovine)	SEKKDFYKDGKRL (Nastainczyk, Hanover)
PGIS (427-440; bovine)	LKNYSLPWGAGHNQ (Kohlmann/ Prof. Dr. Przybylski)

All peptides were either covalently linked to keyhole limpet hemocyanin (KLH) or bovine serum albumin. Immunisations were performed in the local animal house by Dr. med. Schopper and H. Henseleit, according to the actual animal protection law. The antibody titer in the plasma was controlled once every two weeks.

Peptides were coupled to Affi-Gel 10 (Bio-Rad) by the anhydrous coupling procedure according to the manufacturers protocol. The column material was transferred into 1 ml Mobicol's (Mo Bi Tec/ Göttingen) and equilibrated with PBS pH 7.4 or stored in 20% ethanol at 4°C. PBS equilibrated columns were loaded with either 1 ml of ascites fluid or serum and incubated with shaking at 4 °C for at least 2h. Columns were connected to a BioLogic HR Workstation (BioRad), rinsed with PBS and eluted with 50 mM glycine-HCL pH 2.7. The following gradient-program was used: Flow 1ml/min; 15min rinsing with PBS; 15min linear gradient to 100% glycine-HCl buffer; requilibration with PBS until pH is neutral. 2 ml fractions were collected and immediately neutralized with 1M Tris-HCl pH 9.0. Fractions were then concentrated with Ultrafree-4 Biomax 30k (Millipore) centrifugal filters and the protein concentration was adjusted to 2mg/ml. Antibody solutions were mixed with glycerol (1:1 v/v) and protease inhibitors (Complete™/ Roche). Aliquots were stored at –20°C for later use.

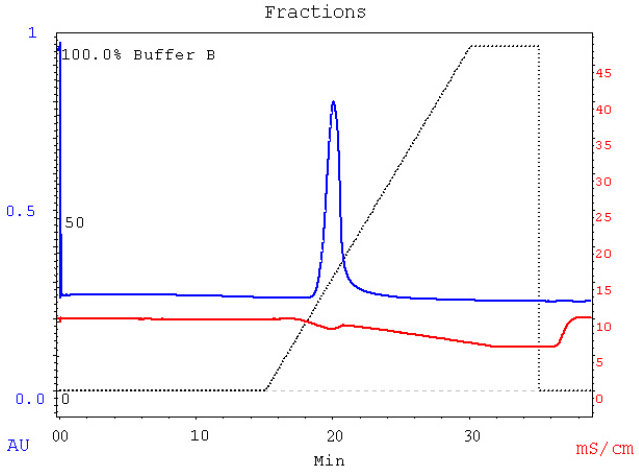

Figure 3.2
Representative elution profile of anti NT monoclonal antibody from ascites fluid, affinity purified against nitrated bovine PGIS peptide (427-440).
Blue line = absorbance at 280nm [AU]; Red line = conductivity [mS/cm]; Black line = gradient profile

3.15 NOS Activity Assay (Aging)

3.15.1 Column Chromatography

Frozen aortic rings (5 mm length) were homogenized in 400 µl of a buffer containing 20 $x10^{-3}$ M Hepes, 200 $x10^{-3}$ M sucrose, 1 $x10^{-3}$ M dithiothreitol, 10 mg/ml soybean trypsin inhibitor, 10 mg/ml leupeptin, and 2 mg/ml aprotinin. Before sonication, PMSF at 0.1 $x10^{-3}$ M final concentration and [(3-cholamidopropyl)-dimethyl-ammonio]-1-propanesulfonate (CHAPS; 20 mM) were added to homogenized samples. Tissue homogenates of each age group of animals were pooled according to protein content, and samples were measured in triplicates. Samples were then centrifuged at 45,000 rpm and 4°C for 20 min. The supernatants were depleted of endogenous arginine by passage over activated resin, and the protein concentration was adjusted to 2.4 mg/ml. NOS activity was measured by the conversion of l-[^{14}C]arginine to l-[^{14}C]citrulline and expressed as pmol per mg protein per min. Cytosols from homogenized samples (18 ml) were incubated at 37°C for 20 min with 100 ml of the optimized assay buffer for citrulline formation consisting of: l-citrulline (1.2 mM), l-arginine ($2x10^{-2}$ mM), NADPH (0.12 mM), tetrahydrobiopterin (10^{-2} mM), $MgCl_2$ (1.2 mM), $CaCl_2$ (0.24 mM), calmodulin (40 U/ml), FAD (10^{-3} mM), FMN (10^{-3} mM), and l-U[^{14}C]arginine ($1.2x10^{-4}$ mmol/liter; 18.5 kBq/ml).

A

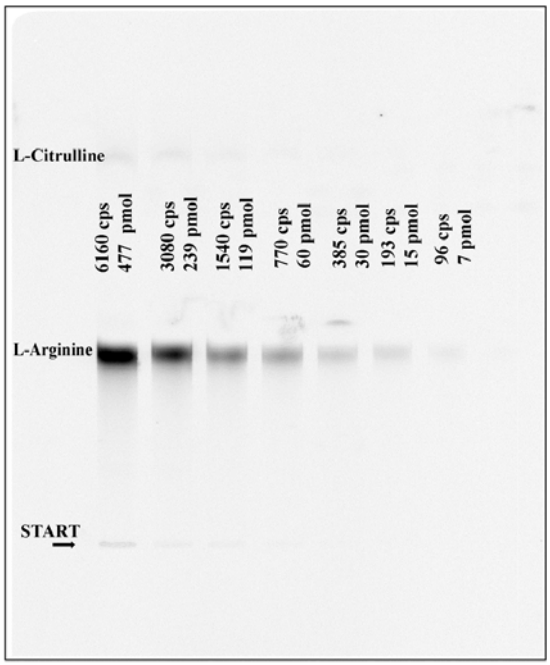

B

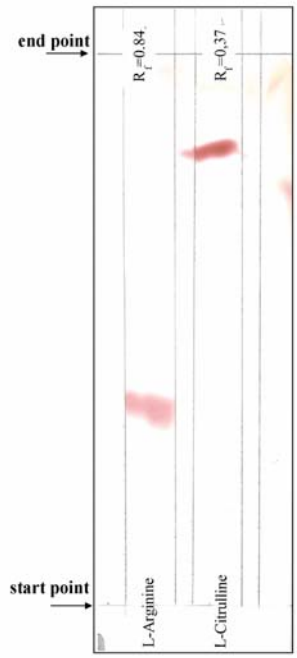

C

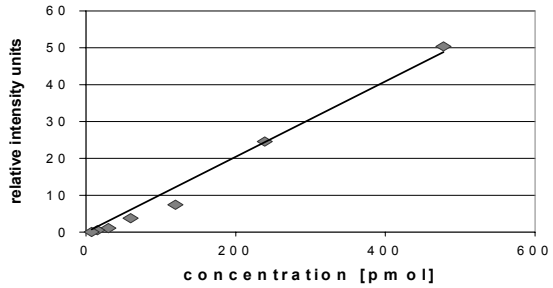

D

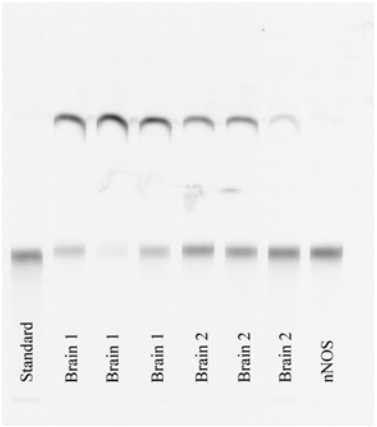

Figure 3.3
A) Separated standards of (^{14}C)-L-arginine by TLC and visualization and quantification (**C**) with the Phosphor-Imager (Molecular Dynamics) and Image Quant software. B) Determination of R_f-values for non-radioactive L-arginine and L-citrulline visualized with ninhydrine. **D**) Activity measurements in brain homogenates to establish the method.

Incubations were performed for each sample in the presence or absence of 1 mmol/liter EGTA to determine the amount of Ca^{2+}-dependent and Ca^{2+}-independent formation of citrulline. The NOS-specific and NOS-unspecific formation of citrulline was determined in samples containing 1 mM L-NMMA. The reaction was terminated by removal of substrate and addition of 1 ml (1:1, vol/vol) H_2O/Dowex 50x8-400 cationic resin, pH 7.20, and 5 ml of water. After centrifugation of the incubation mix for 3 min at 1,500 rpm, 4 ml supernatant in 10 ml scintillant was examined for [^{14}C]citrulline formation using a scintillation counter.

3.15.2TLC Assay

Samples were homogenized using a “Polytron” homogenizer (Polytron PT3100; Kinematica; Switzerland) in PBS pH 7.4containing the following supplements: 1% NP40 (Sigma), $2x10^{-3}$ M PMSF (Sigma), $1x10^{-6}$ M pepstatin (Sigma), $20x10^{-3}$ M EDTA and 3.7 mg/ml iodoacetamide(Serva). The samples were left for 30min on ice and centrifuged for 20 min at 10 000g in a cooled microcentrifuge. The mixture (20 µl) essentially consisted of 30 mM Hepes, pH 7.0, $2.0x10^{-3}$ M NADPH (BioMol), $1.0x10^{-3}$ M $CaCl_2$ (Riedel de Häen), $1x10^{-4}$ M FAD (Sigma), 0.83 µg/ml of calmodulin (BioMol), 100 µM tetrahydrobiopterin (Alexis), and 0.5 µl of L-[^{14}C] arginine (Amersham). The incubation was carried out at 37 °C for 30 min. The NOS reaction was terminated by adding 2.5 volumes of cold methanol. The samples were left on ice for 20 min and centrifuged a 4 °C. 20µl of the supernatant were directly applicated by glass capillaries onto a silica gel TLC plate (Silica 60, Merck), dried under a hot stream of air, and subjected to chromatography. The solvent was composed of a ammonium hydroxide,

chloroform, methanol and water (2:0.5:4.5:1) mixture. The products were identified by exposing the plates 24-48 to a phosphor imager screen. The screens were read with an phosphor imager (Molecular Dynamics, USA) and quantified by using the "ImageQuant" software.

Advantage of the assay is the chromatographic purification and identification of all metabolites, including L-arginine (R_f = 0.37), L-citrulline (R_f = 0.84), and L-ornithine, which excludes interferences from nuclei acids or proteins. Also the assay is rapid, highly reproducible and can be carried out in large numbers.

3.16 Immunoprecipitation

3.16.1 Preparation of Antibody Agarose

Lyophilized protein G-agarose(Sigma, Pharamcia) was reconstituted overnight at 4°C with PBS. After several washes a 1:1 slurry was prepared and 200 µl were incubated with 100 µg of monoclonal antibody against nitrotyrosine (Clone 1A6, Upstate) for 1 h. The mixture was rinsed several times with PBS. The antibody was covalently cross-linked by addition of fresh 6 mg/ml DMP (dimethylpimelimidate, Pierce) dissolved in 0.1 M triethanolamine (Merck), pH 8.2 for 1 h at room temperature. Remaining unreacted groups were blocked by washing and incubation with 0.1 M ethanolamine, pH 8.2 for 10 min at RT. Unfixed antibodies were removed by rinsing the material several times with 0.1 M glycine buffer pH 2.8. The antibody-agarose was washed several times with PBS and stored in PBS + 0.05% sodium azide.

3.16.2 Immunoprecipation of Nitrotyrosine-Containing Proteins

BCA homogenates were prepared in RIPA buffer (Santa Cruz) and adjusted to a protein concentration of 5 mg/ml. Denaturation was achieved by heating the solution for 20 min at 95°C in screw cap tubes. The solution was precleared by addition of 40 µl of protein G agarose (Sigma) and the supernatant was incubated (18 h, 4°C) with 20 µl of a 1:2 antibody agarose slurry. Immune complexes were precipitated by centrifugation (14000 g, 1 min) and washed with 0.5 ml SNNTE (0.5 % sucrose (Merck), 1 % NP-40, 0.5 M NaCl, $50x10^{-3}$ M Tris, $5x10^{-3}$ M EDTA, pH 7.4). Protein pellets were then resuspended in 40 µl Laemmli sample buffer (5:1) without any reducing agents and heated at 95°C for 5 min.

3.16.3 Western Blots

Protein precipitates were separated by 8% SDS-PAGE and blotted onto a nitrocellulose membrane in a semidry blot procedure (48 mM Tris/ 39 mM glycine/ 20% methanol/ 0.037 % SDS). Proteins were visualized with a 0.1% Ponceau S(Sigma) solution in 5% acetic acid to check transfer efficiency. After destaining, the membrane was blocked with 5% milk powder in PBS/ 0.1% Tween 20 for 2 h at room temperature and incubated with a polyclonal antibody directed against PGIS overnight at 4°C. After washing several times with PBS / 0.1% Tween 20, the membrane was further incubated with a goat anti-mouse antibody (Pierce) at a dilution of 1:7500 for 45 min. Antibody binding was visualized by the ECL technique (Amersham), according to the instructions of the supplier.

3.17 Immunohistochemistry

3.17.1 Immunohistochemistry of BCA (Hypoxia/ Reoxygenation, LPS)

Coronary arteries were fixed in PBS buffered 4% paraformaldehyde for 3 h followed by cryoprotection at 1 h incubations in 10, 20 and 30% sucrose in 0.1M sodium cacodylate buffer. Tissues were then embedded in pre-cooled, OCT-containing cups and frozen in liquid nitrogen-cooled isopentane (Ridel de Häen). Samples were stored at –80°C. Ten µm sections were mounted on poly-L-lysine (Sigma) coated glass slides, air-dried and blocked for 45 min in a blocking solution consisting of 4% BSA (Serva), either 10% goat serum (Vector) or 10% horse serum (Vector) and 3% Triton X-100 (Sigma) in PBS (Gibco), pH 7.4. Sections intended for double staining and the appropriate controls were coincidently blocked by coincubation with the monoclonal anti-NT antibody (15 µg/ml, Upstate) and the polyclonal PGIS antibody (5 µg/ml) overnight at 4°C. Control sections were stained with the nitrotyrosine antibody prepared in 10 mM 3-nitrotyrosine in 0.1 M PBS with a controlled pH of 7.4. Antibody binding was then visualized by coincubation of fluorescein isothiocyanate (FITC)-conjugated anti-mouse IgG (1:50 dilution) with anti-rabbit IgG conjugated to Texas Red (1:100 dilution) for 1 h. Sections were washed and examined under a Leica microscope (Leica DMIRB, Wetzlar, Germany) fitted with an digital imaging system (RT Spot Camera, Diagnostic Instr. USA , Visitron Systems, Puchheim, Germany). Negative controls were performed by either eliminating one or the other or both primary antibodies, or by incubating

sections with a nonspecific primary antibody. All pictures were obtained under the magnification as indicated with identical camera and print settings.

3.17.2 Immunohistochemistry of Human Aortic Endothelial Cells (Diabetes)

To visualize 3-nitrotyrosine formation and PGIS, endothelial cells were grown on culture slides (Falcon) under the same conditions as described before. After incubation cells were fixed in –20 °C cold pure methanol (Merck) for 5 min. and transferred into –20°C cold pure acetone (Merck) for 10 sec. Thereafter, slides were 3 times gently rinsed with PBS and blocked for 2 hours at room temperature with PBS containing 5 % of BSA. The 3-nitrotyrosine antibody (dilution 1:30) and the prostacyclin synthase antibody (dilution 1:300) were diluted in PBS containing 1% BSA and incubated overnight at 4 °C in an humidified atmosphere. After rinsing the slides gently for 3 times with PBS, fluorescence labeled secondary antibodies with the Alexa™ dye 568 or 488 (Molecular Probes) were applied in a dilution of 1:200 for 1h at room temperature under humidified atmosphere. Then slides were again rinsed three times with PBS and embedded in Immuo-Mount for fluorescence microscopy with an Leica DMIRB equipped with an digital spot camera from Visitron-Systems.

4 Biochemical Analysis of PGIS Nitration

Contribution of coworkers to this work:

Prof. Dr. Przybylski (Coordination of Mass spectroscopy)
Nick Svinovscky (MALDI-TOF MS analysis)

Prof. Dr. Ullrich (Supervisor)
Patrick Schmidt (Trypsin digestion, PGIS purification, HPLC –peptide analysis, PGIS activity assay)

Own contribution (Immunoprecipitation, PGIS activity assay (data not shown), total hydrolysis and ECD-nitrotyrosine detection)

Parts are published in:
Schmidt P, Youhnovski N, Daiber A, Balan A, Arsic M, Bachschmid M, Przybylski M, Ullrich V. Specific nitration at tyrosine-430 revealed by high resolution mass spectrometry as basis for redox regulation of bovine prostacyclin synthase. Submitted to Journal of Biological Chemistry.

4.1 Introduction

The nitration of tyrosine residues in proteins has become a well recognized reaction, but has been severely disputed with regard to the mechanisms involved and its physiological and/or pathophysiological significance. PN generated from NO and $^{\bullet}O_2^-$ can react with Tyr or Tyr-containing proteins to form 3-nitrotyrosine (3-NT) (Crow and Beckman, 1995; Beckman and Kopppenol, 1996; Viner et al., 1999) but in general the required concentrations are higher than expected to occur *in vivo*. Pfeiffer and Mayer (Pfeiffer et al., 1998; 2000; 2001a; 2001b) have even questioned the significance of PN as a cellular nitrating agent and have proposed nitrite / hydrogen peroxide as an alternative pathway with myeloperoxidase as a catalyst (Brennan et al.,

2002; van Dalen et al., 2000). The nitrating species under these conditions is supposed to be N_2O_3, which may account for nitration of some proteins in severe inflammation. Only under these conditions the required amounts of peroxide and NO_2^- by the decomposition of iNOS-derived NO were reached (van Dalen et al., 2000).

In case of PN it has not been considered that PN can be activated by transition metal ions, which may then catalyze the self-nitration of metalloproteins at low PN levels. Daiber and coworkers (2000b; 2000c) provided evidence for this reaction when studying several heme-thiolate (P450) proteins catalysing nitration and PN decomposition. P450 enzymes with an vicinal tyrosine residue at the active site were clearly nitrated, in contrast, non-tyrosine containing enzymes just catalyzed PN decomposition. Thus PGIS is significantly protected from nitration and inactivation by PN in the presence of other P450 enzymes, as demonstrated for bacterial NO reductase (P450 NOR). In addition, substrate analogs of prostaglandin-endoperoxide have been recently shown to inhibit nitration, (Zou et al., 1996) a fact which suggested a proximity of the tyrosine to the active site.

Further, variations among different anti-NT antibodies in immunostaining procedures with different P450's were evaluated and showed a clear dependence on the amino acid sequence. Some antibodies did not recognize the nitrated epitope, although HPLC analysis of hydrolyzed samples revealed a clear NT peak or vice versa. Hence one may argue that interpretations of such immunostainings could be deceitful.

PGI_2-synthase was inactivated by micromolar PN bolus concentrations (Zou et al.; 1996; 1997) or by a continuous equimolar generation of NO and $^{\bullet}O_2^-$. In cellular systems the inhibition of nitration by an NO-synthase inhibitor and polyethylene glycolated (PEG) superoxide dismutase (SOD) provided evidence for the involvement of PN, whereas nitrite was ineffective (Zou et al., 1998). Since NO and PGI_2 are important for the endothelial barrier function, the formation of PN and the nitration of PGI_2-synthase could play a role in the process of endothelial cell activation for adhesion and emigration of white blood cells into the tissue (Ullrich et al., 2001).

Beyond this physiological background no proof for the molecular basis of enzyme inhibition has hitherto been obtained, neither by identification of nitrated tyrosine nor by immunostaining using modern proteomic tools. Previous attempts have been unsuccessful to detect and identify the nitrated tyrosine. This study presents molecular evidence for the specific nitration of bovine PGIS by immunoprecipitation (IP) of

nitrated PGIS followed by MALDI-TOF MS (matrix assisted laser-desorption ionisation time of flight mass spectroscopy) analysis of the trypsin digested precipitates. These methods confere the validity of NT immunostaining for PGIS and serve as a powerful tool for the investigation of the physiological and pathophysiological significance of PGIS nitration.

4.2 Results and Discussion

4.2.1 Pitfalls in the IP Method

The best method to detect semi-quantitatively nitration is the immunoprecipitation of nitrated proteins using the monoclonal NT-antibody clone 1A6 (MacMillan-Crow and Thompson, 1999). According to commonly used protocols several severe interferences at the required range around 50 kDa with Western blot procedures had been observed. These disturbances made the detection of nitrated PGIS impossible. The following three major points accounted for these problems.

Protein A sepharose or agarose is commonly used, but spontaneous cleavage ("bleeding") generated a protein band at 50kDa. The protein incidentally interfered with the primary antibody against PGIS and raised a nonspecific signal on Western blot membranes (data not shown).

The second problem was related to the vast amounts of IgG molecules, causing distortions in the SDS-PAGE. Further, for the elution of the antigen, Laemmli buffer was applied and included reducing agents, such as DTT or ß-mercaptoethanol which cleaved the disulfide bounds of the IgG molecule. Thus two more bands were visible on the gel, the light chain at ~25 kDa and the interfering heavy chain at ~50 kDa (fig. 4.1).

The third point is related to the PGIS molecule itself in view of its high stability towards denaturation. Sensitivity and specificity of immunostainings were increased when stringent buffers and heat denaturation were used. For blot membranes we observed that the stripping procedure always reduced the background and improved staining, since PGIS seems to be able to refold on blot membranes. According to our concept of specific tyrosine nitration near the active site, antibody binding should be hampered by the geometry of the molecule. Complete denaturation of the molecule deallocates the epitope to interact with the antibody.

4.2.2 Principals of the Adapted Immunoprecipitation Method

Several adaptations of the protocol were made to guarantee a reliable and reproducible IP procedure.

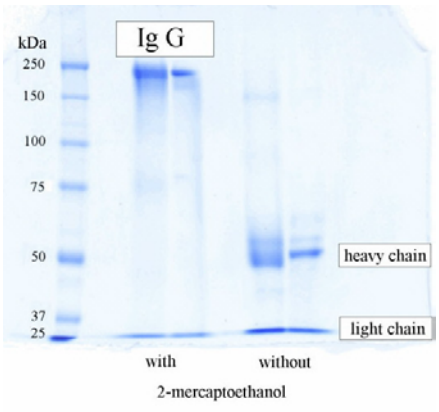

Figure 4.1
Coomassie stained gel (8%) to demonstrate the differences in the separation of the primary antibody after boiling the sample in buffer with or without 2-mercaptoethanol.

First protein A sepharose was substituted by the more expensive protein G sepharose, which has a molecular weight of ~20 kDa. Next, reducing agents could be excluded from the Laemmli buffer, since PGIS contains no disulfide bonds. The IgG molecule remained intact and appeared as a single band at ~240 kDa on the SDS-gel (fig. 4.1). This was of further advantage in the later applied mass spectroscopy, since PGIS peptides were not masked by the excessive Ig G fragments. The use of high stringent buffers such as RIPA and heat denaturation of the homogenates before IP improved antigenicity of nitrated PGIS.

The amount of IgG was reduced by orientated covalent cross-linkage of the antibody at its constant region (Fc) to the matrix. This is performed by binding the antibody first to protein G sepharose and then establishing a covalent coupling via the free amino groups of both proteins with chemical cross-linkers like DMP or DSS. These remedial measures reduced the interference of Ig G molecules and delivered a clear PGIS signal depending on nitration and protein amount.

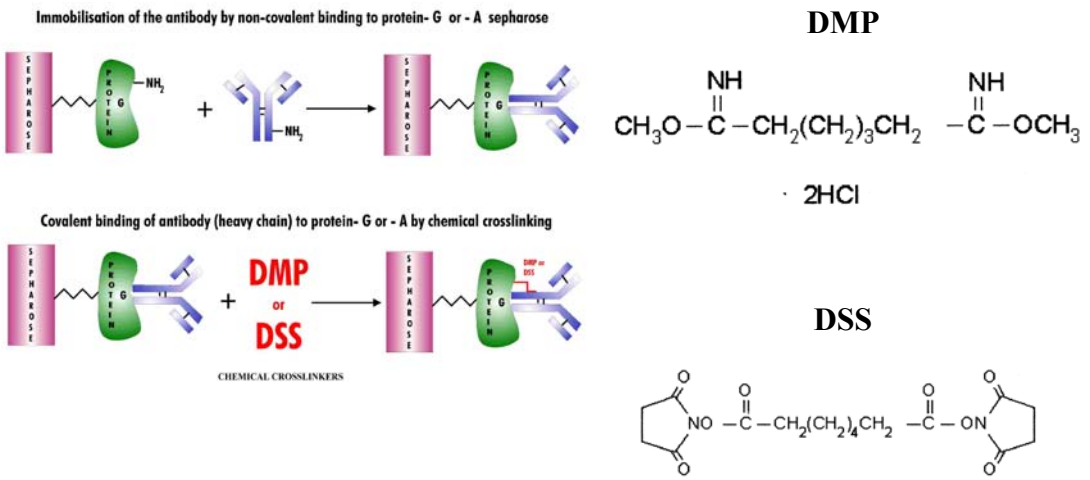

Figure 4.2
Principle of the orientated cross-linkage of antibodies and examples of chemical cross-linkers like DMP = dimethyl pimelimidate or DSS = Disuccinimidyl suberate.

4.2.3 Immunoprecipitaion of Nitrated PGIS

The accuracy of the adapted IP procedure was controlled with homogenates prepared from bovine coronary arteries treated with PN, SIN-1, xanthine oxidase and/ or NO-donors. In figure 4.3 A intact arteries were treated with either PN or decomposed PN, homogenized, and subjected to IP. The signal of PGIS was consistently dependent on PN mediated nitration and protein concentration. Always low amounts of nitrated PGIS were found in controls, which could be derived from slaughter procedure or atherosclerotic plaques. Treatment with SIN-1, a substance releasing equimolar concentrations of NO and $^{\bullet}O_2^-$, demonstrated a clear concentration-dependent signal of nitrated PGIS. Also the combination of an enzymatic $^{\bullet}O_2^-$ source (xanthine oxidase) together with an NO donor (DEA-NONOate), resulted in a nitrated PGIS band, whereas NO or xanthine oxidase alone had no effect.

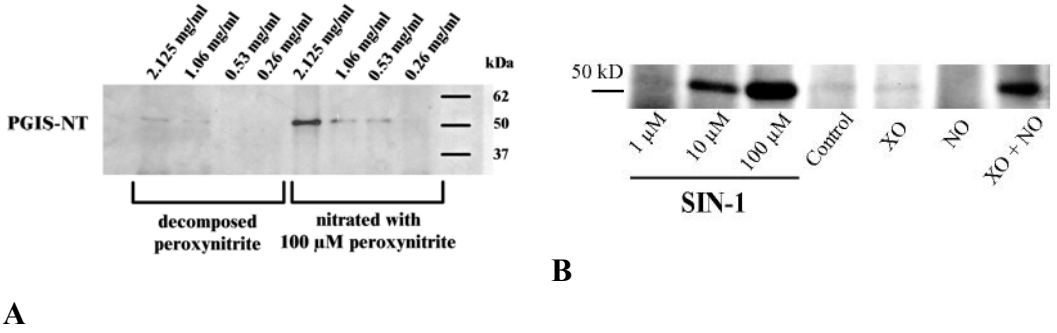

Figure 4.3
Immnuoprecipitation of nitrated proteins from BCA with the anti-NT antibody 1A6 and immunostaining against PGI. A) Dependence on protein content and peroxynitrite of the precipitation of NT-PGIS. B) Nitration of PGIS by exogenous sources of PN. XO = xanthine oxidase [(10 mU/ml in presence of 100 µM hypoxanthine] for 45 min; NO = DEA-NONOate [20 µM] for 45min; SIN-1 [1-100 µM] for 2h or the combination of xanthine oxidase)

4.2.4 HPLC Detection of NT

Classically applied acid hydrolysis was ambiguous in its specificity since traces of nitrite may yield artefacts and false-positive results (Frost et al., 2000). Therefore, basic hydrolysis (fig. 4.4) and pronase digestion were used and compared with each other. Similar recovery rates of protein bound NT in microsomes for both methods were obtained.

The digestion process with pronase was controlled by detection of free NT from either nitrated bovine serum albumin or microsomes. Obviously maximal yields of NT for

BSA were already obtained after six hours, in contrast optimal digestion of microsomes required several additions of pronase and a minimum of five days incubation (fig. 4.5 A).

We assume that the proteolytic degradation of the Tyr-nitrated domain was hampered by the high stability in the microenvironment of the nitration site, whereas the basic hydrolysis was unaffected. Representative ECD chromatograms of the basic hydrolysis protocol were shown in fig. 4.4.

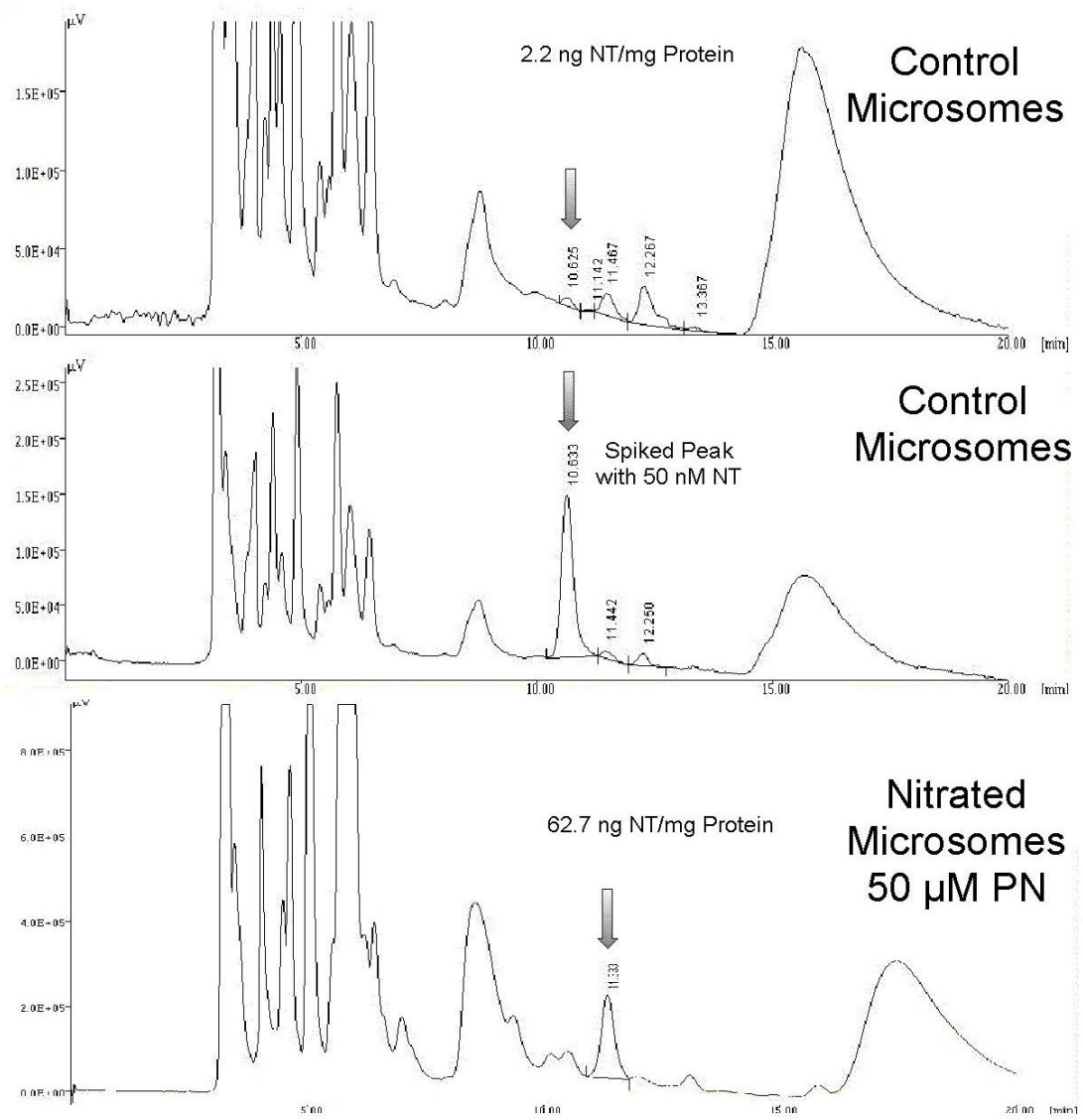

Figure 4.4
Basic hydrolyzed (6N NaOH for 12h at 95 °C) microsomes were neutralized and analyzed by reversed phase HPLC (125 mm x4 mm Column C18 100 A° 3µ from Machery-Nagel) connected to an optical and ECD detector. Representative ECD chromatograms (+825 mV) of control microsomes, control spiked with 50 nM NT and with 50 µM PN nitrated microsomes. Retention times can shift due to temperature changes, high amounts of other amino acids and byproducts caused by the total hydrolysis or by variations in mobile phase. NT peak was confirmed by spiking the sample with authentic NT. The arrow indicates the NT peak.

In contrast to the pronase digestion protocol, the method was more sensitive, since "self-digestion" of the protease lead to the accumulation of amino acids and higher dilutions for HPLC analysis were required to prevent column overcharge. The NT retention time was always controlled by spiking the samples with the NT standard. Shifts in retention time were due to variations in the buffer composition, ambient temperature and column performance (typically around 11 min).

Using the prolonged pronase digestion, a PN-concentration -dependent increase of the 3-NT formation providing qualitative and quantitative evidence for the nitration reaction was established (fig. 4.5 B). With only 25 µM of authentic PN specific nitration at Y430 was demonstrated, which was important in view of the possibility that the heme-catalyzed formation of a ferryl complex and the $^{\bullet}NO_2$ radical may lead to additional modifications of other Tyr residues in PGI_2-synthase. These results confirmed the immunostaining of former Western blots, where only a single NT positive band at ~52 kDa was observed, which increased parallel with the PN concentration. Increasing the PN concentration to over 250 µM, nonspecific nitration reactions were observed on blot membranes.

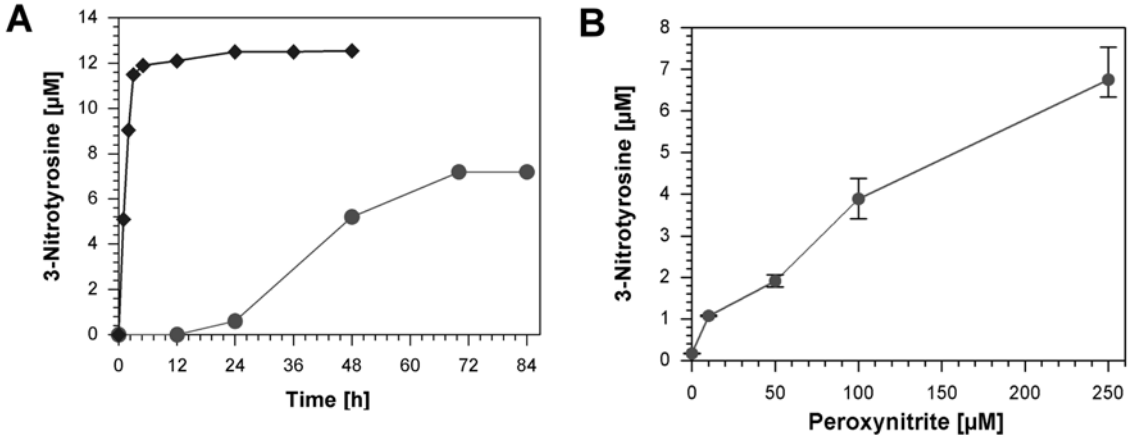

Figure 4.5
Time- and PN-concentration-dependent 3-NT yield from nitrated BSA or PGI_2-synthase after digestion by pronase. (A) BSA (20 µM) and PGI_2-synthase (~5 µM, isolated from bovine microsomes after nitration), both nitrated by 250 µM of PN, were treated with equal concentrations of pronase (0.5 mg/ml every 12 h). 3-NT was detected and quantified by HPLC. Squares represent values for BSA, circles for PGI_2-synthase. (B) PGI_2-synthase (5 µM final concentration) was isolated from microsomes after treatment with different concentrations of PN. All samples were digested by pronase for five days.

4.2.5 Peptide Mapping with MALDI-TOF Mass Spectroscopy

Several aliquots of bovine aortic microsomes were treated with PN [final concentration 25 µM] and the nitrated proteins were immunoprecipitated after the

new modified protocol. The precipitates were then separated by SDS-PAGE, obtaining a single band at 52 kDa and the intact Ig G molecule band at approximately 240 kDa (fig. 4.1). Gel bands at 52 kDa were excised, collected and in-gel-digested with trypsin (Shevchenko et al., 1996). The cleaved peptides fragments were extracted and analyzed by MALDI-TOF MS. The typical sequence recovery was about 40%, although the obtained peptide yield was low due to the high proteolytic stability of protein. Peptide Nr. 11 covered the region around Y430, located near the active site of PGIS. This peptide exhibited an altered mass (fig. 4.7). Additional experiments with synthesized nitrated peptides, revealed that MALDI ionization yields extensive fragmentation by cleavage of the nitro group with elimination of NO and O, since the resulting ions may obscure the assignment of nitration sites in complex proteolytic peptide mixtures. In his thesis work P. Schmidt developed a method to purify nitrated PGIS and improved analysis of nitrated PGIS. A better protocol was developed to achieve higher yields and a more efficient cleavage, hence tryptic digestion was not well suited. Therefore, the protease thermolysin working even under high denaturating conditions cleaved the protein efficiently which eventually led to a higher yield, but to smaller peptide fragments. Thus the cleaved peptides were separated on an HPLC system, allowing the identification of nitrated peptides by their absorption at 362 nm. A single NT positive peptide was detected and isolated. Sequencing and high resolution electrospray-FTICR-MS (Fourier transform ion cyclotron resonance) analysis confirmed the exact location of NT at the residue 430. Schmidt further confirmed that, at low concentrations of PN, no additional tyrosine residues were nitrated, thus proving the specificity of the nitration mechanism and confirming the proximity of the residue to the active site. C441 binds the heme domain at its fifth coordination site and Y430 to C441 is expected to form a loop around the heme and this structure may be embedded in a tightly folded conformation. Such a concept was further supported by inhibitors of the active site, which abolished

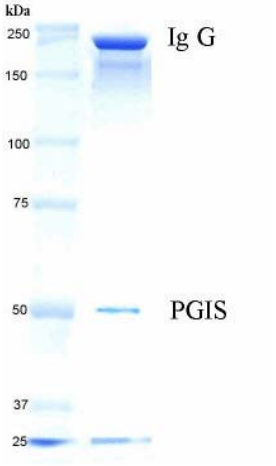

Figure 4.6
Immunoprecipitation of nitrated microsomes with the monoclonal antibody 1A6. A single band at 50 kDa was detected and the intact Ig G molecule at about 240 kDa. Several IP's according to modified protocol were performed, the bands at 50 kDa were excised, collected and subjected to proteomic analysis.

nitration. The lack of a crystal structure allows only assumptions based on indirect approaches such as active site blockers or computed sequence analysis.

A

Mass spectrometric identification of immunoprecipitated PGIS

Peptide	From-To	$(M+H)^+_{CALC.}$	$(M+H)^+_{EXP.}$	Sequence
1	198-208	1315.65	1315.3	VHSADVFHTFR
2	132-145	1638.82	1638.7	ELQALTDAMYTNLR
3	481-495	1744.85	1744.3	YGFGLMQPEHDVPVR
4	334-350	1858.97	1858.4	VLDSMPVLDSSVLSESLR
5	73-91	2233.14	2233.1	HVTVLLDPHSYDAVVWEPR
6	423-444	2487.23	2486.0	DGKRLKNYSLPWGAGHNQCLGK
7	175-197	2546.91	2547.8	AGYLTQYGVEAPPHTQESQAQDR
8	383-404	2736.45	2737.5	LLLFPFLSPQKDPEIYTDPEVFK
9	383-408	3170.66	3171.2	LLLFPFLSPQKDPEIYTDPEVFKYNR
10	146-174	3197.60	3199.4	TVLLGDTVEAGSGWHEMGLLEFSYGFLLR
11	423-452	2219.68	3318.3	DGKRLKNYSLPWGAGHNQCLGKGYAVNNSIK
12	198-232	3847.11	3846.3	VHSADVFHTFRQLDLLLPKLARGSLSAGDKDRVGK
13	22-58	4146.23	4147.4	RRTRRPGEPPLDLGSIPWLGHALEFGKDAAGFLTRMK

B

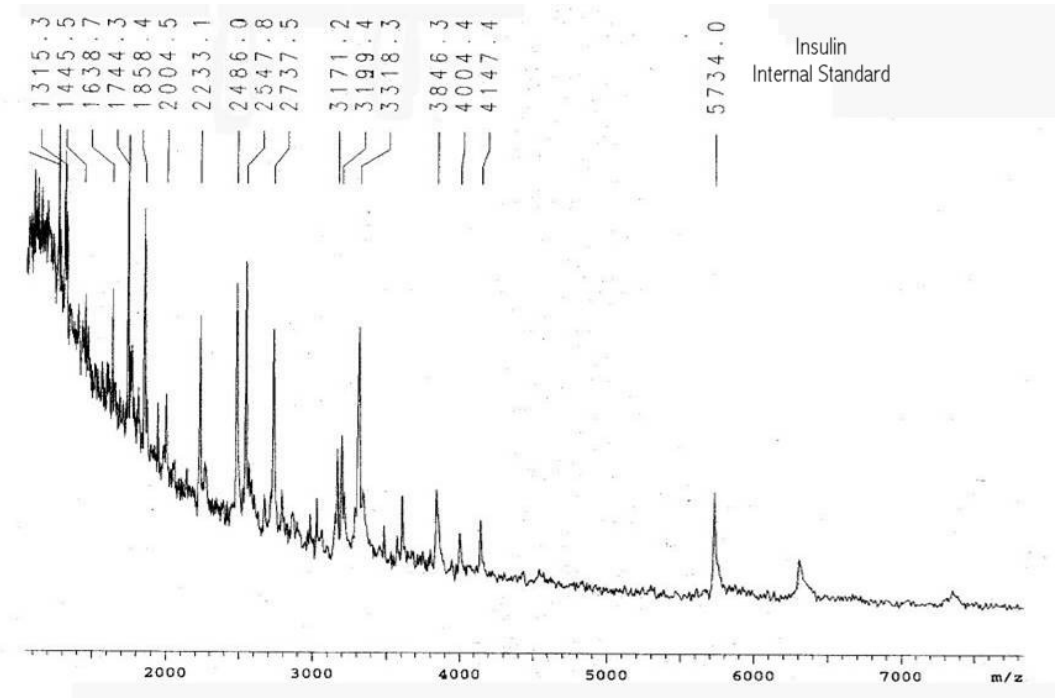

Figure 4.7
(A) Recovered and identified peptides of immunoprecipitated PGIS after tryptic digestion. The mass of peptide 11 was altered.
(B) Representative TOF mass spectra averaged form 10 scannings.

5 Hypoxia-Reoxygenation

Contribution of coworkers to this work:
Prof. Dr. Ullrich (Coordination)
Ming Hui Zou (Coordination, immunoprecipitation, PGIS activity assay)

Own contribution: (BCA isometric tension measurements, EIA prostaglandin analysis, PGH_2 synthesis and PGIS activity assay)

Published in:
Zou MH, Bachschmid M. Hypoxia-reoxygenation triggers coronary vasospasm in isolated bovine coronary arteries via tyrosine nitration of prostacyclin synthase. J. Exp. Med. 1999 Jul 5;190(1):135-9.

5.1 Introduction

Under physiological conditions, the endothelium provides vasodilatory and antiaggregatory properties to the cardiovascular system and also prevents growth of the underlying vascular smooth muscle cells by releasing nitric oxide (NO), endothelium-derived hyperpolarizing factor, and PGI_2 (Vane et al., 1990; Moncada et al., 1991). Each of these mediators acts by a different mechanism, NO by the stimulation of guanylyl cyclase and PGI_2 by activating adenylyl cyclase, so that these mediators can act synergistically and also serve as backup systems for each other (Vane et al., 1990; Moncada et al., 1991). It was interesting to study this interdependence after a selective inhibition of PGIS by PN had been described (Zou and Ullrich, 1996). As PN is generated in vivo by a rapid combination of NO and $^{\bullet}O_2^-$ (Beckman et al., 1990 and 1996), it seemed that $^{\bullet}O_2^-$ not only can neutralize NO but subsequently, through its product PN, could suppress PGI_2 formation. The underlying mechanism for PGIS blockade has been suggested as the nitration of a tyrosine residue at the active site through a reaction catalyzed by the ferric iron of this heme-thiolate (P450) protein (Zou et al., 1997). In spite of the cellular antioxidant potential, PN causes PGIS nitration in whole cells (Zou et al., 1998) as well as in intact coronary arteries (Zou et al., 1999a). Endothelial dysfunction (impaired vasorelaxation and/or increased vasoconstriction) is an important early-recurring phenomenon in virtually all forms of ischemia/ reperfusion diseases, including a variety of

shock states (Lefer and Lefer, 1993). This dysfunction appears to be triggered simultaneously with the endothelial generation of $^{\bullet}O_2^-$. Therefore, the formation of PN during hypoxia–reoxygenation is likely because of a simultaneous generation of NO and $^{\bullet}O_2^-$ (Huie and Padmaja, 1993). In this study, we investigated a role of PN in hypoxia–reoxygenation-induced coronary vasospasm by monitoring the pattern of Ang II–triggered vasoconstriction/ vasorelaxation, PGI_2 release, and the nitration of PGIS. Our results suggest that hypoxia–reoxygenation elicits PN formation, leading to a subsequent nitration and inhibition of PGIS. Most importantly, the unmetabolized PGH_2 triggers vasospasm by acting upon the TxA_2 /PGH_2 receptor before being converted to PGE_2.

5.2 Results and Discussion

In BCA, Ang II elicited a biphasic response consisting of a primary vasoconstriction that was selectively blocked by Losartan, a selective Ang II receptor blocker, and a secondary vasorelaxation that was mainly PGI_2 dependent (Zou et al., 1999a). Abrupt decrease of oxygen tension from 95% O_2/ 5% CO_2 to 95% N_2/ 5% CO_2 caused a slight decrease in tension after a transient rise. Reoxygenation (from 95% N_2/ 5% CO_2 to 95% O_2/ 5% CO_2) did not alter the tension of unstimulated arteries. Although hypoxia–reoxygenation did not affect the initial constriction of Ang II, it selectively blunted the Ang II–triggered relaxation phase after 30 min of hypoxia. Along with this suppression of the relaxation phase, a second constriction phase developed in parallel, with a decrease of 6-keto-$PGF_{1\alpha}$ (fig. 5.1) that closely resembled the pattern seen previously after PN pretreatment (Zou et al., 1999a).

Both the unspecific COX inhibitor indomethacin and the TxA_2/PGH_2 receptor blocker SQ29548 restored hypoxia–reoxygenation-impaired relaxation without affecting 6-keto-$PGF_{1\alpha}$ release (fig. 5.1). This suggests that a COX-derived product, TxA_2 or PGH_2, caused vasoconstriction via the TxA_2 /PGH_2 receptor (fig. 5.1). A role of TxA_2 was excluded, as CGS13080, a TxS inhibitor, did not affect hypoxia–reoxygenation-triggered vasospasm (fig. 5.1), and the levels of TxB_2 remained low and unaffected after hypoxia–reoxygenation treatment (97±11 vs. 99±15 pg/30 min). The level of 8-iso-$PGF_{2\alpha}$, which also could act on the TxA_2/PGH_2 receptor (Takahashi et al., 1992), was low and remained unchanged after hypoxia–reoxygenation (43±12 vs. 47±17 pg/30 min). PGH_2 is known to cause vasoconstriction via the TxA_2/PGH_2 receptor (Mais et al., 1985). In arterial vessels, PGH_2 is metabolized primarily by PGIS to yield PGI_2. Therefore, we postulated that an inhibition on PGIS could be the primary cause for the accumulation of PGH_2, which then caused

vasoconstriction by stimulating the TxA_2/PGH_2 receptor. Parallel measurements of prostaglandins in the incubation medium further supported this hypothesis.

Hypoxia –reoxygenation lowered 6-keto-$PGF_{1\alpha}$ formation but raised the level of PGE_2, an enzymatic or nonenzymatic metabolite of PGH_2 (fig. 5.1). As COX activity was slightly decreased after hypoxia–reoxygenation, an excess formation of PGH_2 after hypoxia–reoxygenation could be excluded.

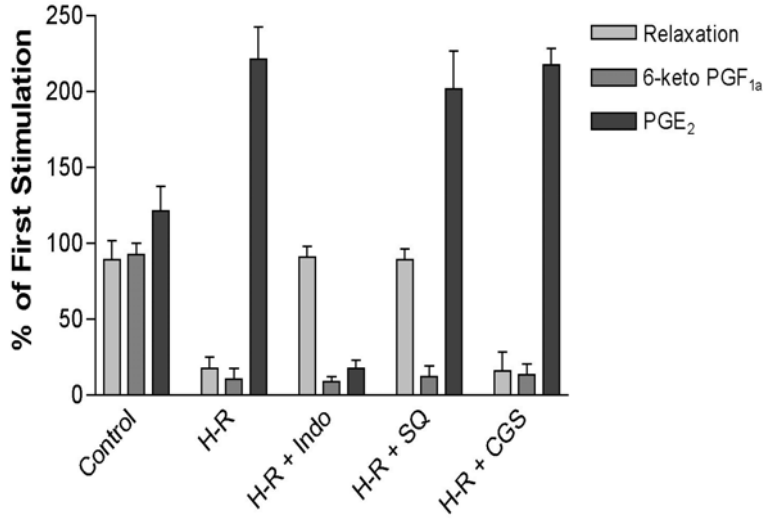

Figure 5.1

Hypoxia–reoxygenation on Ang II–triggered relaxation and eicosanoid metabolism in BCA. Effects of SOD, L-NMMA, and L-NAME on Ang II–triggered relaxation (light grey bars) and the release of 6-keto-$PGF_{1\alpha}$ (grey bars) and PGE_2 (black bars) in hypoxia–reoxygenated BCA. After having obtained a reference response to Ang II, the coronary strip was exposed to hypoxia for 40 min after 40 min reoxygenation in presence of indomethacin (10^{-5} M), CGS13080 (10^{-5} M), SQ-29548 (10^{-5} M), PGE^2 and 6-keto-PGF_{1a} in the media were analyzed by EIA. Data represent means ± SEM from 10 experiments.

Conclusive evidence for an inactivation of PGIS came from the experiments with ^{14}C-PGH_2 as a substrate for PGIS. A significant inhibition on the conversion of ^{14}C-PGH_2 into 6-keto-$PGF_{1\alpha}$ (289±8%) with a concomitant increase of PGE_2 (135±21%) was observed, confirming the selective inhibition of PGIS and the reorientation of PGH_2 metabolism toward PGE_2 after hypoxia –reoxygenation. The sustained vasoconstriction after hypoxia–reoxygenation could also have been the consequence of a decreased sensitivity of vascular smooth muscle to NO. However, NO generated from DEA-NO in arteries with or without hypoxia–reoxygenation resulted in a similar potency to induce vasorelaxation. Similarly, an increased sensitivity of the TxA_2/PGH_2 receptor was excluded, as pD2 (the negative logarithm of the molar concentration of agonist that elicits a half- maximal response) of U46619, an agonist for the TxA_2/PGH_2 receptor, was identical before and after exposure to hypoxia–reoxygenation (7.7±0.5 vs. 7.8±0.5). A correspondent dose of PGE_2 (20 ng/ml) applied to the bath solution did not cause vasoconstriction (data not shown), indicating that the higher levels of PGE_2 after hypoxia –reoxygenation were not responsible for the second constriction phase. According to our working hypothesis, hypoxia–reoxygenation could induce PN formation, which inactivates PGIS.

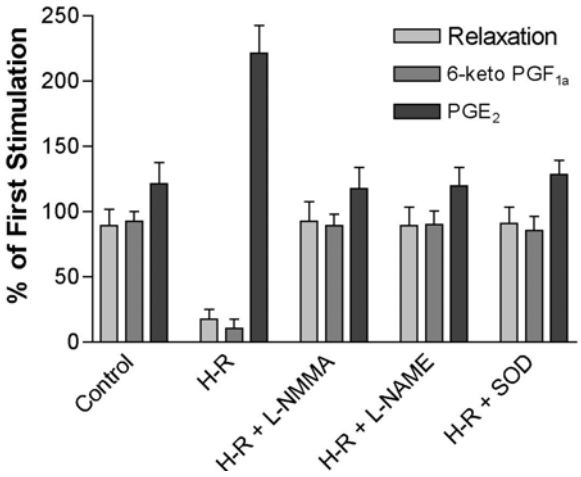

Figure 5.2

Hypoxia–reoxygenation on Ang II–triggered relaxation and eicosanoid metabolism in BCA. Effects of indomethacin, SOD, L-NMMA, and L-NAME on Ang II– triggered relaxation (light grey bars) and the release of 6-keto-$PGF_{1\alpha}$ (grey bars) and PGE_2 (black bars) in hypoxia–reoxygenated BCA. After having obtained a reference response to Ang II, the coronary strip was exposed to hypoxia for 40 min after 40 min reoxygenation in presence of indomethacin (10^{-5} M), CGS13080 (10^{-5} M), SQ-29548 (10^{-5} M), PGE2 and 6-keto-PGF_{1a} in the media were analyzed by EIA. Data represent means ± SEM from 10 experiments.

To test whether PN was indeed responsible for the hypoxia–reoxygenation-induced vasospasm, the NOS inhibitors, both L-NMMA (10^{-4} M) and L-NAME (10^{-4} M) were concurrently administered during hypoxia–reoxygenation. L-NMMA, which reduced the Ang II–induced relaxation phase by about 25% without affecting 6-keto-$PGF_{1\alpha}$ formation in normal vessels (data not shown), prevented hypoxia–reoxygenation-induced suppression of Ang II–induced vasorelaxation and 6-keto-$PGF_{1\alpha}$ release (fig. 5.2); L-NAME was as effective as L-NMMA (data not shown). Alternatively, concurrent administration of PEG-SOD (500 U/ml) abolished hypoxia–reoxygenation-induced secondary vasoconstriction and restored Ang II–stimulated vasorelaxation by blunting the hypoxia–reoxygenation mediated inhibition on 6-keto-PGF_{1a} formation (fig. 5.2). It was important to show that neither NO nor $^{\bullet}O_2^-$ alone could cause vascular dysfunction and inhibition on PGI_2 release.

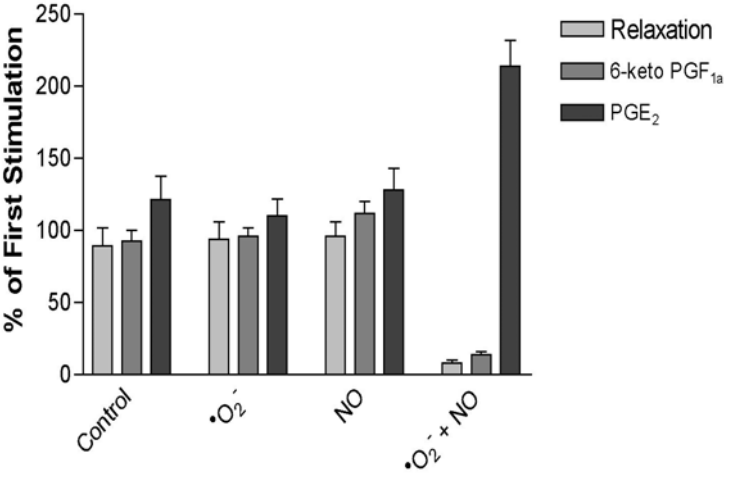

Figure 5.3

Effects of $^{\bullet}O_2^-$, NO, and concurrent administration of superoxide and NO on angiotensin II–induced vasorelaxation and prostaglandin release in BCA. After having obtained a reference response to angiotensin II, the coronary strip was exposed to superoxide generated from 10 mU/ml xanthine oxidase/10^{-4} M hypoxanthine or to NO generated from $2x10^{-5}$ M DEA-NO or superoxide plus NO. PGE_2 (black bars) and 6-keto-PGF_{1a} (grey bars) in the media were analyzed by EIA. Data represents means ± SEM from 12 experiments.

Therefore, preincubation of BCA with an $^{\bullet}O_2^-$-generating system (10 mU/ml xanthine oxidase/ $1x10^{-4}$ M hypoxanthine) did not significantly affect either Ang II–triggered

vasorelaxation or 6-keto-PGF_{1a} release (fig. 5.3). Alternatively, the incubation of BCA with DEA-NO ($2x10^{-5}$ M) as an NO-releasing system also failed to affect Ang II–induced relaxation and 6-keto-PGF_{1a} release (fig. 5.3). However, concomitant administration to the organ baths of both $^{\bullet}O_2^-$ and NO-generating agents for 40 min caused a loss of PGI_2-dependent vasorelaxation, an indomethacin- and SQ29548-sensitive vasospasm, and a nitration of PGH_2 synthase.

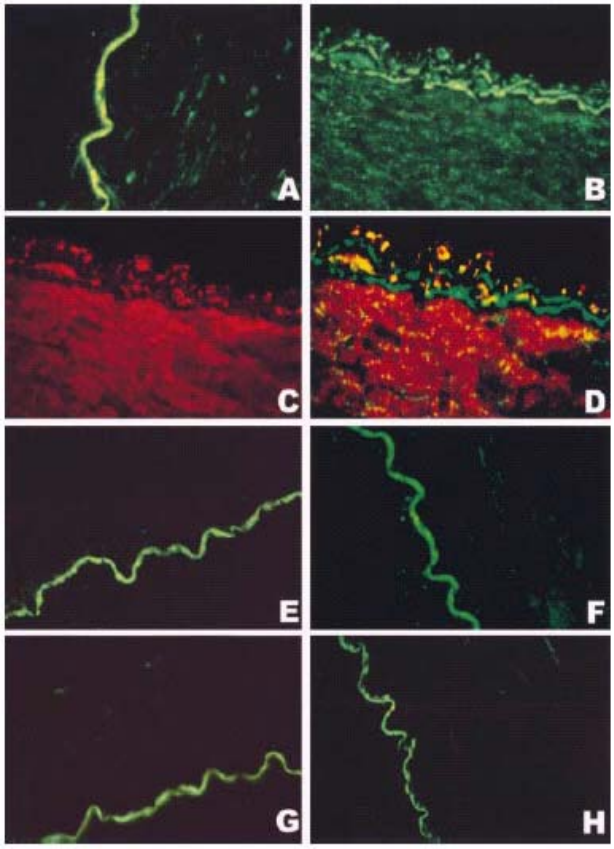

Figure 5.4

Immunohistochemical colocalization of a polyclonal anti–PGIS antibody and an monoclonal antibody against 3-nitrotyrosine in hypoxia-reoxygenated BCA. The yellow coloring resulting from a computer-generated overlay of green (3-nitrotyrosine) and red (PGIS) fluorescence indicates areas of the colocalization of anti-NT and anti–PGS antibodies in BCA with or without hypoxia–reoxygenation treatment. All pictures were obtained under 400-fold magnification with identical camera and print settings. (A) 3-nitrotyrosine staining in a sham-treated artery (green), where 3-nitrotyrosine staining is very weak and the endothelium is intact. The green wiggly line is due to endogenous fluorescence of the lamina and not specific immunostaining for 3-nitrotyrosine. (B) 3-nitrotyrosine staining in a hypoxia-reoxygenated artery; both endothelium and vascular smooth muscle cells are strongly immunopositive for 3-nitrotyrosine (green). (C) The staining of PGIS antibody in a hypoxia-reoxygenated artery. Dense staining with anti–PGIS antibody was visible in both endothelium and smooth muscle (red). (D) A computer-generated overlay of the staining with the antibodies against 3-NT (B) and PGIS (C) in a hypoxia-reoxygenated artery. Yellow indicates the colocalization of the binding with both antibodies. (E) An hypoxia-reoxygenated artery was stained for anti-NT antibody in the presence of 10 mM free 3-nitrotyrosine. Only the autofluorescence of the lamina is visible. (F) 3-nitrotyrosine staining in a hypoxia-reoxygenated artery in the presence of L-NMMA, where the staining for 3-nitrotyrosine is only weakly visible in both endothelium and vascular smooth muscle. (G) 3-nitrotyrosine staining in a hypoxia-reoxygenated artery in the presence of PEG-SOD, where 3-nitrotyrosine staining is weakly visible in vascular smooth muscle. (H) An hypoxia-reoxygenated artery was stained for 3-nitrotyrosine when the antibody against 3-nitrotyrosine was omitted, where only the autofluorescence of the lamina is visible.

As previously described, the exposure of BCA to PN produced a nitrated protein that colocalized with PGIS (Zou et al., 1999a). The same technique was applied to hypoxia–reoxygenation-exposed BCA segments after their mechanical responses had been established. Staining with anti-NT antibody was weakly visible in control tissue (fig. 5.4 A), but clearly enhanced staining emerged in endothelium and smooth muscle after hypoxia–reoxygenation (fig. 5.4 B), where the staining with antibody PGIS were intensively presented (fig. 5.4 C). A computer generated overlay of the staining with anti-NT (green) and anti–PGIS (red) resulted in the yellow colocalizing patches in vessels after hypoxia–reoxygenation (fig. 5.4 D). The presence of L-NMMA or PEG-SOD abolished the increased staining with anti-NT antibody (fig. 5.4, F and G) but not those with anti–PGIS antibody (data not shown). The specificity of the staining with anti-NT antibody was deduced from its suppression by 10 mM 3-NT (fig.

5.4 E) and the lack of staining when anti-NT antibody was omitted (fig. 5.4 H). 3-chloro- or 3-aminotyrosine or phosphotyrosine were ineffective in blocking the staining with anti-NT antibody (data not shown). Further evidence for hypoxia–reoxygenation-triggered tyrosine nitration of PGIS came from the immunoprecipitation with both antibodies against 3-NT and PGIS. Immunoprecipitation with anti–PGIS antibody yielded similar amounts of protein in both hypoxia–reoxygenation-treated arteries and control tissues (fig. 5.5 A). In Western blot analysis, a dense band was detected by anti-NT antibody in the immunoprecipitates with anti–PGIS antibody from hypoxia–reoxygenation-treated vessel homogenates against a weakly visible signal in those from the control tissues (fig. 5.5 A). In the same homogenates, 3-NT–containing proteins were precipitated with anti-NT antibody in parallel. Higher amounts of these proteins were recovered in hypoxia–reoxygenation-treated arteries than in those without hypoxia–reoxygenation. Moreover, when these precipitates were blotted and probed with anti–PGIS antibody, a dense staining appeared in arteries with hypoxia–reoxygenation (fig. 5.5 B). In agreement with the immunohistochemistry results, both PEG-SOD and L-NMMA effectively abolished the increased stainings with both antibodies in the immunoprecipitates with either anti-NT or anti–PGIS (fig. 5.5, A and B). In summary, our results indicate that hypoxia–reoxygenation elicits the formation of $^{\bullet}O_2^-$, which neutralize NO to form PN. Subsequently, PN nitrates and inactivates PGIS, leaving PGH_2 unmetabolized, which then causes vasospasm and platelet aggregation via the TxA_2/PGH_2 receptor. This finding might offer a new mechanism for coronary vasospasm during hypoxia–reoxygenation, especially in atherosclerotic arteries where PGIS is partially nitrated (Zou et al., 1999c).

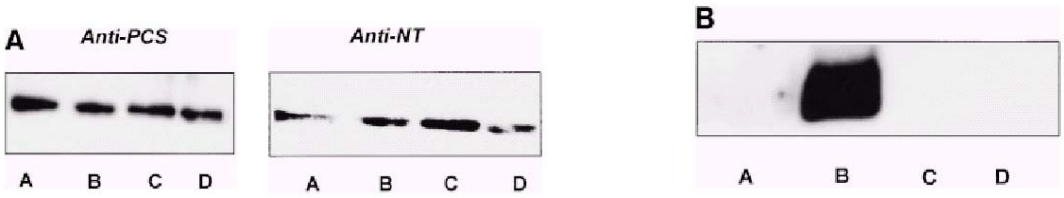

Figure 5.5

Immunoprecipitation of nitrated proteins and PGIS in hypoxia-reoxygenated BCA. (A) Proteins from normal or hypoxia-reoxygenated BCA were immunoprecipitated with a polyclonal antibody against PGIS (α-PGIS) after hypoxia–reoxygenation. As described in Materials and Methods, proteins precipitated by α-PGIS were separated electrophoretically and immunostained with a monoclonal α-PGIS (left) or a monoclonal α-NT (right). Lane A, hypoxia–reoxygenation + L-NMMA; lane B, hypoxia–reoxygenation + SOD; lane C, hypoxia–reoxygenation; lane D, control. (B) 3-NT–positive proteins were precipitated by an monoclonal antibody against 3-NT. Proteins were separated similarly and analyzed by immunoblots with polyclonal antibody against PGIS. Lane A, control; lane B, hypoxia–reoxygenation; lane C, hypoxia–reoxygenation + L-NMMA; lane D, hypoxia–reoxygenation + SOD.

6 The Early Inflammatory Response

Prof. Dr. Ullrich (Supervisor)
Ming-Hui Zou (Coordination)
Svenja Thurau (BCA isometric tension measurement and EIA prostaglandin analysis)

Own Contribution (BCA isometric tension measurement, EIA prostaglandin analysis, immunoprecipitation)

Published in:
Bachschmid M, Thurau S, Zou M, Ullrich V. Endothelial cell activation by endotoxin involves superoxide/NO mediated nitration of prostacyclin synthase and thromboxane receptor stimulation. Submitted to the FASEB Journal 2002.

6.1 Introduction

The vascular endothelium under physiological conditions exerts its anti-adhesive, anti-aggregatory and vasorelaxant properties mainly through a cooperative release of NO and PGI_2 (Vane et al., 1990). Both mediators act by different mechanisms: NO by stimulating soluble guanylyl cyclase and PGI_2 by activating adenylyl cyclase, allowing both pathways to act synergistically and also to serve as back-up systems for each other.

Pathophysiological conditions like ischemia/reperfusion, atherosclerosis or inflammatory events lead to a sequelae of opposing responses like endothelial barrier dysfunction, expression of adhesion molecules, change to a prothrombotic situation, cytokine production and impairment of agonist-induced relaxation in order to level the way for immune cells to the spot of injury. In literature this transition from a physiological to a pathophysiological state is either termed "endothelial cell activation" (ECA), "priming phase", "stunning" or even "endothelial dysfunction " (Cines et al., 1998; Pober, 1988; Bhagat et al., 1996 ;Bhagat and Vallance, 1997).

As a more mechanism-based definition we here prefer ECA Type I which characterises a first phase in which endothelial cells retract from each other, express P-selectins from their storage in Weibel-Palade bodies (Prescott et al., 2001; Hunt and

Jurd, 1997) and release the von Willebrand factor. Such events are independent of *de novo* protein synthesis and are essentially completed within 1 h.

A second stage (ECA Type II) becomes apparent after about one hour and involves induction and expression of early genes like the adhesion molecules ICAM or VCAM, proinflammatory cytokines and regulatory enzymes like NOS-2 and COX-2. As a consequence white cells can tightly adhere and emigrate into tissues, NO and prostaglandins are formed in excess and cytokines orchestra the further inflammatory response.

Our interest was focused on ECA Type I for which we had suggested an inhibition of NO and PGI_2 production by a novel mechanism involving PN formation from NO and a still unknown source of $^{\bullet}O_2^-$ radicals (Ullrich and Bachschmid, 2000). PN then caused tyrosine nitration and concomitant inhibition of PGIS (Zou and Ullrich, 1996; Zou et al., 1997). This again lead to accumulation of 15-hydroxy-prostaglandin 9,11-endoperoxide (PGH_2) which was able to activate the TxA_2/PGH_2 receptor mediating smooth muscle contraction and activation of platelets, white cells and the endothelium (Saussy et al., 1986). This series of events could be shown *in vitro* but also in anoxic/reperfused *ex vivo* experiments (Zou and Bachschmid, 1999d).

The present investigations aimed to understand ECA under inflammatory conditions which can be mimicked ex vivo by endotoxin action on bovine coronary artery (BCA) vessels. It was found that PGIS becomes nitrated after an incubation period of about 45 min resulting in a vasospasm which was completely prevented by a TxA_2/PGH_2 receptor blocker. Thus, for infections by gram-negative bacteria we postulate a signal transduction pathway leading to primed $^{\bullet}O_2^-$ production, PN formation, PGIS nitration/ inhibition, and TxA_2/PGH_2 receptor activation as essential events in ECA Type I preceding the fulminant inflammatory cascade.

This topic has been subject of intense research and not all relevant literature can be listed here. The reader is referred to excellent reviews for further information (Stevens et al., 2000; Lum and Roebuck, 2001; Goligorsky et al., 2000; Vanhoutte, 2002).

6.2 Results

6.2.1 LPS Effects on Vessel Tension and Prostaglandin Synthesis

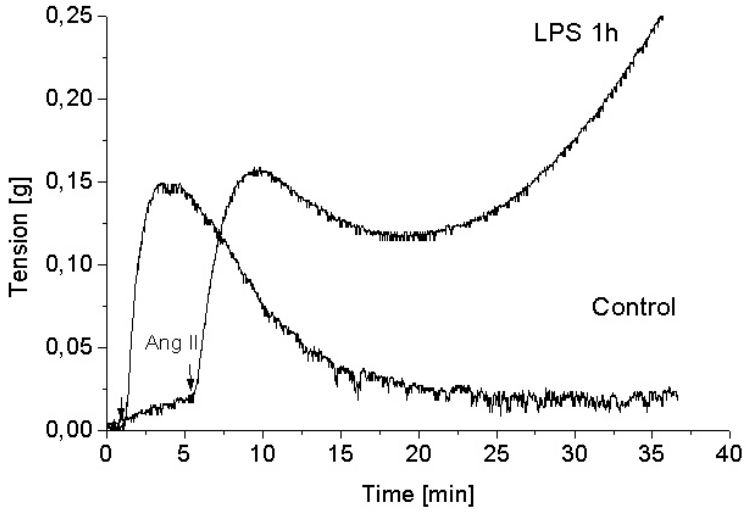

Figure 6.1

Representative recordings of Ang-II-triggered vasoconstriction and relaxation in bovine coronary artery segments. LPS effect [100 µg/ml] on vessel tension after 1h incubation. Arrows indicate the addition of 50 nM Ang-II.

The response of BCA segments to a bolus addition of 100 nM Ang-II was composed of a primary constriction phase followed by a relaxation process (fig. 6.1). LPS directly applied (100 µg/ml) did not affect the basal vasotone and the initial constriction triggered by Ang II. However, pre-exposure to LPS for 1h significantly diminished the Ang II-triggered vasorelaxation phase and even replaced the vasorelaxation response by a sustained vasoconstriction after a short delay (fig. 6.1). Varying the time intervals between LPS addition and Ang II stimulation revealed that about 45 min were required to observe the second vasoconstriction. After a 60 min preincubation the effects were optimal (fig. 6.2, dotted line). Since this time course of the response suggested involvement of protein synthesis cycloheximide and dexamethasone were coincubated with LPS but no effect was noticed (results not shown). The action of LPS was concentration dependent with 100 µg/ml resulting in about 80 % and 10 µg/ml in about 50 % inhibition (not shown). Therefore 100 µg/ml LPS incubated over 60 min were used as standard conditions.

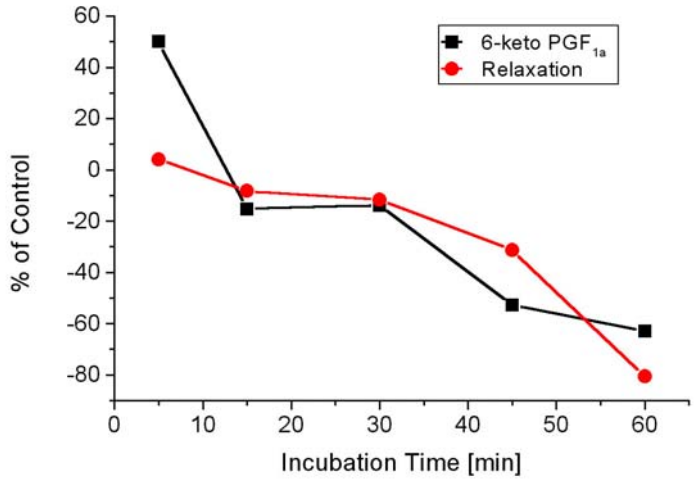

Figure 6.2

Time-dependent effects of LPS [100 µg/ml] on Ang-II-stimulated vasorelaxation (red line) and 6-keto-$PGF_{1\alpha}$ release (black line) expressed as percentage of the control procedure.

The response to Ang II in the BCA segments used after the control incubations was still 80 % compared with the tissue used directly after isolation.

The loss of relaxation was closely parallel to the decrease in PGIS activity as measured by 6-keto $PGF_{1\alpha}$ formation in the incubation medium (fig. 6.2 solid line). It is known that the relaxation response in BCA is mainly controlled by prostacyclin (Zou et al.; 1999a). An exception was the value at 5 min which always showed a significantly higher PGIS activity than the control. Since in intact endothelia the peroxide tonus for cyclooxygenase (COX) is limiting (Chen et al., 1999; Rhoden and Barnes, 1989), this may reflect the formation of some kind of peroxide (probably PN) leading to an initial activation of the PGI_2 synthesizing pathway.

The massive inhibition of 6-keto-$PGF_{1\alpha}$ formation after 60 min LPS incubation was compensated almost exclusively by a corresponding increase in PGE_2 (tab 6.1).

Table 6.1

	LPS		LPS+L-NMMA		LPS + SOD		LPS + denuded vessels	
	pre	post	pre	post	pre	post	pre	post
6-keto-$PGF_{1\alpha}$	1940±324	430±223$^{\#}$	2070±337	1780±425	2110±434	1980±337	180±37	160±41
PGE_2	550±162	2330±409$^{\#}$	590±161	600±363	570±211	670±137	290±56	310±75
$PGF_{2\alpha}$	330±103	400±78	290±38	380±59	410±117	410±109	70±36	40±21
TxB_2	180±56	210±78	200±56	220±66	160±43	200±78	40±11	50±21
8-iso-$PGF_{2\alpha}$	50±23	60±22	70±45	90±56	60±23	80±26	60±22	60±37

Effect of LPS, L-NMMA and SOD on angiotensin-II stimulated eicosanoid release in LPS treated bovine coronary arteries. Values are expressed as means ± S.E.M (pg/ml per 30 min). $^{\#}$indicates pretreatment is different from post-treatment ($p<0.001$) (n=12). pre-: pre-treatment to LPS; post-: post-treatment to LPS.

It was especially important that neither TxA_2, assayed by its stable TxB_2 derivative nor 8-iso-$PGF_{2\alpha}$, levels increased, since these eicosanoids possess strong vasoconstrictive properties (Kromer and Tippins, 1999; Yura et al., 1999). Only a small stimulation could be observed for $PGF_{2\alpha}$.

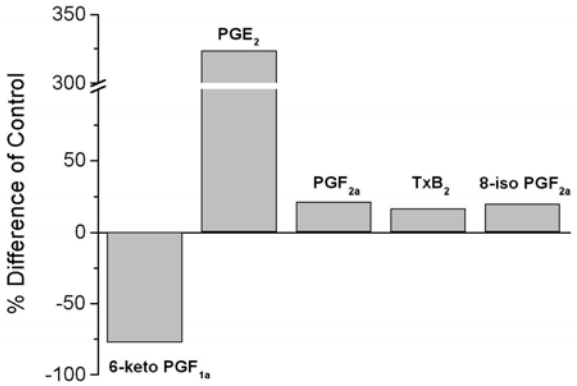

Figure 6.3

Effect of LPS on the eicosanoid metabolism of Ang II triggered BCA. After having obtained a reference response to Ang-II, bovine coronary arteries were exposed to LPS for 1h. The incubation was stopped by washings and the vessels were stimulated again, but in the absence of LPS. The amount of eicosanoids in supernatants from two stimulations were analyzed by enzyme-linked immunoassay. The results are expressed in percentile change of the second Ang II stimulation compared to the first. (n=10).

Denuded vessels are largely devoid of PGI_2 synthesis, even though smooth muscle cells contain sufficient amounts of PGIS (DeWitt et al., 1983; Smith et al.; 1983; Harold et al., 1985). LPS treatment for 1h left the SMC derived prostanoids unchanged and proved that the observed effects were endothelium dependent.

6.2.2 Participation of NO, $^{\bullet}O_2^-$ and Peroxynitrite in the LPS Effects

Growing evidence supports the concept that next to NO also other reactive oxygen species are involved in regulation of blood vessel function (Cosentino et al., 1998; Griendling and Harrison, 1999). Therefore we tested the effects of NO synthase inhibition and $^{\bullet}O_2^-$ scavenging by SOD on the vasoconstriction after LPS challenge. Almost no inhibition of PGI_2 synthesis nor vasoconstriction (fig. 6.4 a) took place in the presence of the non-specific NOS inhibitor L-NMMA [100 µM] as well as with polyethylene-glycolated (PEG)-Cu/ Zn-SOD [300 U/ml]. With native Cu/Zn-SOD the effect is much less indicating that a close attachment of the enzyme to the endothelial surface or on improved stability (Beckman et al., 1988) is required for an efficient scavenging of $^{\bullet}O_2^-$.

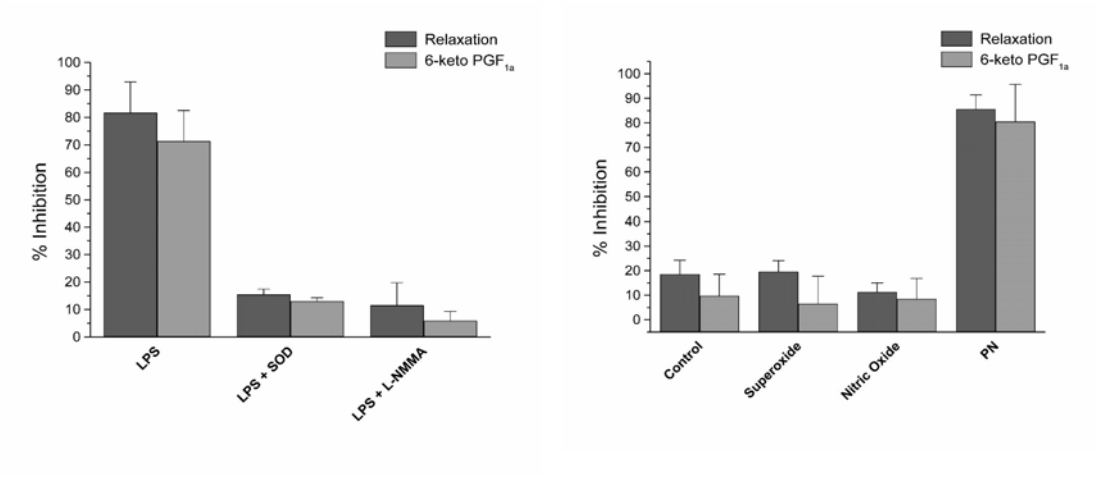

Figure 6.4

A) Effects of PEG-SOD [300 U/ml] and L-NMMA [100µM] on Ang-II-stimulated vasorelaxation and 6-keto-$PGF_{1\alpha}$ release in BCA after 1h exposure to LPS. **B**) Inhibitory effects of exogenously generated $^{\bullet}O_2^-$, NO and PN on vessel relaxation and 6-keto $PGF_{1\alpha}$ release. The organ bath was suplemented either with an $^{\bullet}O_2^-$ producing system (10 mU/ml xanthine oxidase in presence of 100 µM hypoxanthine) or alternatively with DEA-NONOate (20 µM) as an NO-generating system. Both $^{\bullet}O_2^-$ and NO-generating systems were added simultaneously to generated peroxynitrite. After 1h the medium was exchanged to normal buffer without additions and stimulated with Ang II. Values represent means±SD (n=8; PN vs control P<0.0001).

It was then tested whether exogenous sources of $^{\bullet}O_2^-$ and NO could also evoke vasoconstrictions. Therefore, BCA incubations were supplemented with either an $^{\bullet}O_2^-$ producing system (10 mU/ml xanthine oxidase (Houston et al., 1999) in the presence of 100 µM hypoxanthine) or alternatively with DEA-NONOate [20-100 µM] as an NO-liberating system. None of the radicals alone were able to change 6-keto $PGF_{1\alpha}$ nor the relaxation response upon Ang II stimulation, but the concomitant addition of both systems to generate PN clearly gave rise to a strong impairment of relaxation and 6-keto $PGF_{1\alpha}$ production (fig. 6.4 b).

6.2.3 LPS Causes Inhibition of PGIS by Nitration

According to our previous work (Zou and Ullrich, 1996; Zou et al., 1997) such data could be explained by the formation of PN from NO and $^{\bullet}O_2^-$. PN could then nitrate a tyrosine residue of PGIS and block the enzyme. Further support for this mechanism was obtained by immunoprecipitation of tyrosine-nitrated proteins by a monoclonal α-NT, separation by SDS-PAGE and western blotting with a polyclonal α-NT. Only one main band at 52 kDa was detected. After stripping the membrane, a second immunostaining with anti-PGIS-antiserum (α-PGIS) identified this band as PGIS (fig.

6.5 a). A densitometric evaluation confirmed that PEG-CuZn-SOD and L-NMMA reduced the nitration process to almost control levels (fig. 6.5 b).

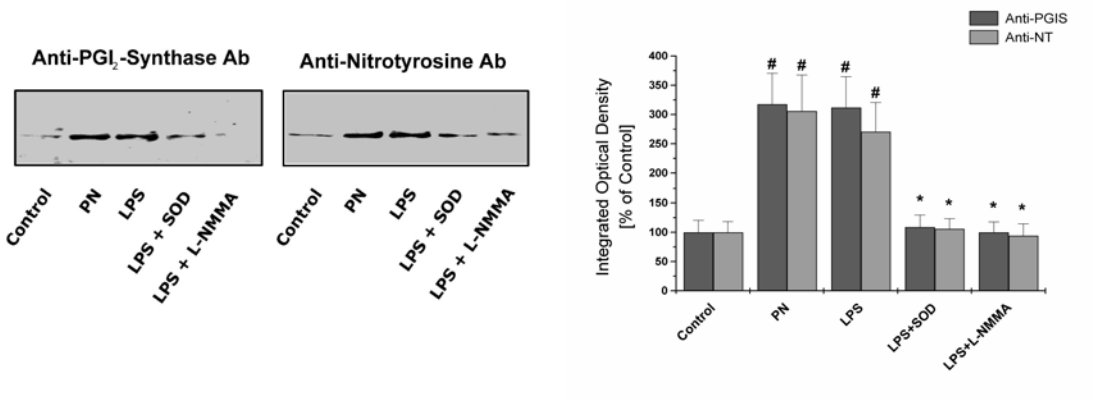

Figures 6.5

Immunoprecipitation of nitrated PGIS A) 3-Nitrotyrosine-containing proteins in the vessel homogenates of 6 samples after the treatments indicated were precipitated by a monoclonal antibody against 3-nitrotyrosine. Proteins were separated by 8% SDS-PAGE and examined by Western blot with a polyclonal antibody against PGI2-synthase and a polyclonal antibody against 3-nitrotyrosine. B) Quantitative densitometric analysis of nitrated PGIS by using SigmaGelTM software. Results are expressed as means±SD (#p<0.05 vs control; *p<0.05 vs LPS).

It should be noted that also the control is weakly positive in agreement with earlier findings that the process of nitration is extremely sensitive for PN and seems to occur already during death of the animal (Zou and Bachschmid, 1999). A relative comparison between the various intensities of NT staining in Western blots can be taken from fig. 6.5 b.

In Fig. 6.6 the blot contains tissue treated with two different sources of NO/$^{\bullet}O_2^-$. Neither $^{\bullet}O_2^-$ nor NO alone could cause nitration of any protein. SIN-1 [1-100μM] generates both radicals at about equal rates (Darley-Usmar et al., 1992) and the generation of $^{\bullet}O_2^-$ from xanthine oxidase and of NO from NONOate was adjusted to equal rates. By showing the full range of protein separation and α-NT staining on the blot the specificity of the nitration process for PGIS becomes apparent. Only higher concentrations of SIN-1 [0.5–1mM] or of authentic PN [0.2-1mM] produced further bands of nitrated proteins (data not shown).

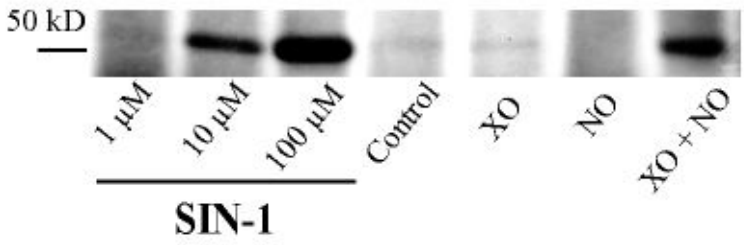

Figure 6.6

Immunoprecipitation of nitrated prostacyclin synthase after incubation with PN generating systems. PN was produced by simultaneous generation of NO and $\cdot O_2^-$ either by incubation of BCA with SIN-1 [1-100 μM] for 2h or the combination of xanthine oxidase (10 mU/ml in presence of 100 μM hypoxanthine) and DEA-NONOate [20 μM] for 45 min..

Having documented this specificity for PGIS nitration the immunohistochemical staining with the α-NT clearly located nitrated PGIS to smooth muscle and endothelial cells. The basal lamina gives a bright unspecific auto-fluorescence (fig. 6.7). Although smooth muscle cells and endothelial cells contain comparable densities of PGIS (DeWitt et al., 1983) most of the staining after LPS appeared in the endothelium. Nitrations with PN or SIN-1 showed much higher densities also in the smooth muscle layer (not shown) (Zou et al., 1999a), indicating that LPS more selectively exerts its action on the endothelium.

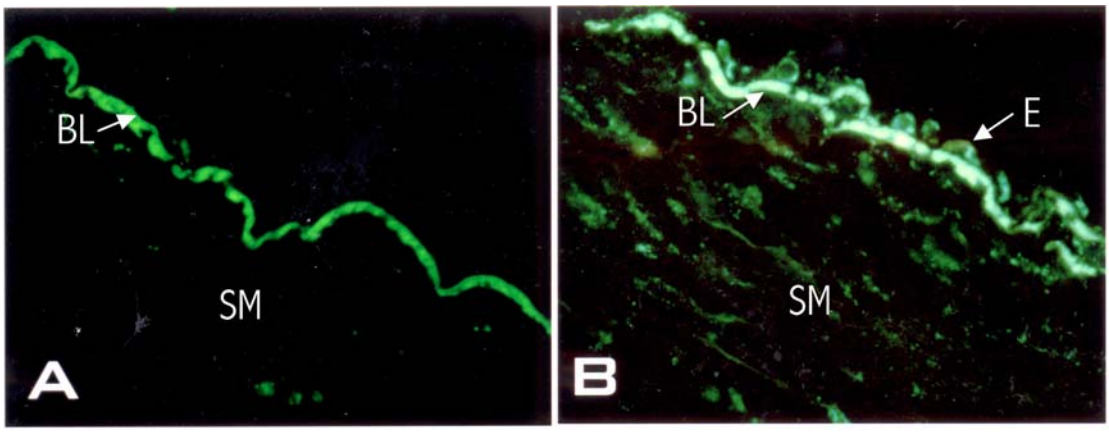

Figure 6.7

Immunohistochemical stainings with an antibody against 3-nitrotyrosine in isolated bovine coronary arteries. **A**. anti-nitrotyrosine staining in a sham-treated artery; **B**. anti-nitrotyrosine staining in a LPS-exposed bovine coronary artery. Reduction of the nitrotyrosine to aminotyrosine with sodium dithionite as well as blockage of the antibody with 10 mM nitrotyrosine completely abolished the staining. The visible green line in all pictures indicates the autofluorescence of the basal lamina. All pictures were obtained under 400-fold magnification with identical camera and print settings. SM= smooth muscle cell layer; E= endothelial cell layer; BL= basal lamina.

6.2.4 Ang II is Required for the Generation of Peroxynitrite after LPS

It has been demonstrated that Ang II can stimulate $^{\bullet}O_2^-$ (Zhang et al., 1999; Sohn et al., 2000) and NO (Thorup et al., 1998) formation in parallel to generate PN (Pueyo et al., 1998). From fig. 6.8 it is evident that the nitration requires stimulation by Ang II. Compared to the maximum of nitration seen with 10 μM PN the LPS/ Ang II spot is somewhat weaker, which according to our recent data may be due to an overnitration by PN. In organ bath studies the relaxation phase is blocked under both conditions. PEG-SOD and allopurinol could be omitted from the 1h preincubation period with LPS, which did not affect the outcome of nitration and vasospasm.

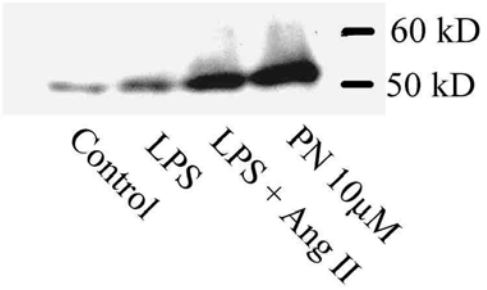

Figure 6.8

Immunoprecipitation of nitrated PGIS after 1h challenge with LPS. Stimulation with Ang II [50 nM] significantly increased tyrosine nitration compared to unstimulated LPS-treated tissue, indicating that Ang II triggers PN formation.

Therefore, both inhibitors were added after the preincubation period during the 30 min recovery time of the tissue before Ang II stimulation. These results are in accordance with ECA Type I, demonstrating that PN formation, nitration of PGIS and development of vasospasm depend upon the stimulation by an agonist, represented here by Ang II.

6.2.5 LPS Induced Vasospasm is Caused by PGH_2

The vasospasm in segments treated with LPS could be fully blocked with SQ 29548, a selective antagonist of the TxA_2/PGH_2 receptor (Dogne et al, 2000), whereas the TxA_2 synthase inhibitor CGS 1380 was without effect (fig. 6.9). The denuded endothelium incubated with LPS showed no vasospasm with Ang II. CGS1380 also blocks PGIS but this enzyme was already inhibited by the nitration process. An interesting observation concerns the action of indomethacin when given together with Ang II. The absence of a vasospasm is in agreement with the abolishment of any prostaglandin biosynthesis by indomethacin. However, the vessel showed normal relaxation which indicates that the relaxation must be due to a process different from PGI_2, probably NO or more likely EDHF.

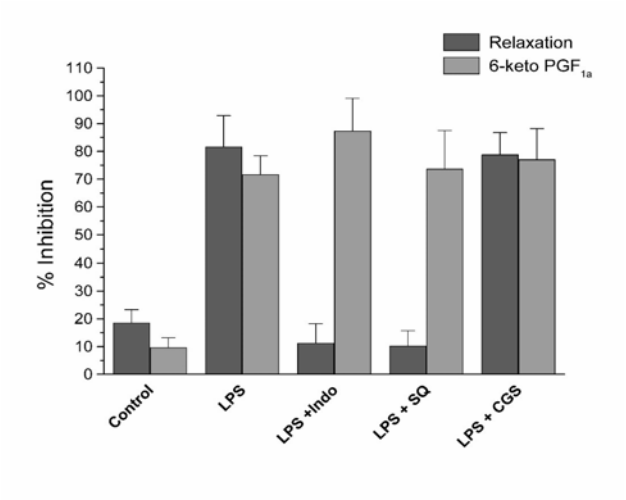

Figure 6.9

Effects of indomethacin [10 µM] a cyclooxygenase inhibitor, SQ 29548 [10 µM] a TxA_2/PGH_2-receptor blocker and CGS 13080 [10 µM] a thromboxane synthase inhibitor on Ang-II-stimulated vasorelaxation and 6-keto-$PGF_{1\alpha}$ release in BCA after exposure to LPS. The results are expressed as means±SD (n=12, $^{\#}p$<0.01 vs controls; *p<0.01 vs LPS).

6.2.6 Xanthine Oxidase is a Possible O_2^- Source After LPS Challenge

The major remaining question concerns the signal transduction pathway leading to superoxide formation. All effects by LPS could be blocked by diphenylene iodonium (DPI) but the four potential sources of $^{\bullet}O_2^-$, xanthine oxidase, NADPH oxidase, mitochondria and uncoupled NO synthase, will be inhibited by this unspecific flavoprotein inhibitor (Li and Trush, 1998; Rand and Li, 1993). L-NMMA as a blocker for NO-synthase oxidase would also block NO synthesis and specific inhibitors for its oxidase function do not exist to our knowledge. We then used allopurinol as a selective competitive xanthine oxidase antagonist and indeed found a significant inhibition of the vasospasm and of 6-keto-$PGF_{1\alpha}$ formation. Oxypurinol was also effective and allopurinol given 15 min before the second stimulation with Ang II was still effective (fig. 6.10).

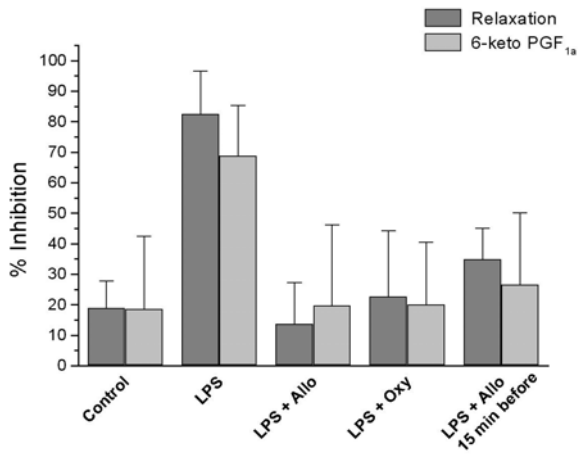

Figure 6.10

Effects of xanthine oxidase inhibitors [100 µM allopurinol, 100µM oxypurinol] on Ang-II-stimulated vasorelaxation and 6-keto-$PGF_{1\alpha}$ release in BCA after exposure to LPS. The results are expressed as means±SD (n=8, , $^{\#}p$<0.01 vs control; *p<0.01 vs LPS).

There was an enhancement of lucigenin-induced chemiluminescence after LPS treatment (not shown), but the relative unspecificity of this reaction does not allow to discriminate between different radical species. Still this test confirmed that LPS triggers reactive oxygen formation.

6.3 Discussion

Our results help to clarify the biochemical events that lead to endothelial cell activation in the early phase of an inflammatory stimulus. Endotoxin (LPS) can be considered as a model for gram-negative bacteria although in the serum-free media used higher concentrations than in vivo have to be employed. A preincubation for at least 45 min with LPS has a profound effect on the response of BCA's to Ang II. The normal contraction-relaxation curve is dramatically altered and instead of leading to complete relaxation a preincubation-time dependent vasoconstriction was observed which corresponds to a vasospasm. The underlying mechanisms were found in complete analogy to the vasospasm that develops as a consequence of PN action on BCA's Tyrosine-nitration of PGIS with inhibition of the enzyme, accumulation of PGH_2 which activates the TxA_2/PGH_2 receptor, followed by smooth muscle contraction. The fall in 6-keto-$PGF_{1\alpha}$ production and the corresponding rise in PGE_2 levels provide clear experimental proof for a switch in PG metabolism. One has to assume that PGH_2 first acts at its receptor before it reaches PGE_2 synthase. This enzyme, however, is located in VSMC and not in the endothelium which requires a transcellular process of PGH_2 transfer from the endothelium to VSMC. Whether PGE_2 serves a new function in the system was not directly followed but a recent report correlates P-selectin expression on endothelial cells with PGE_2 (Hailer et al., 2000) action and this would indeed complete the sequence of events postulated for ECA Type I with the adhesion of white blood cells to the endothelium after release of P-selectin from Weibel-Palade bodies (Prescott et al., 2001; Hunt and Jurd, 1997). The transcellular signaling therefore includes the PGE_2 feedback signal from smooth muscle to the endothelium.

Thus the action of LPS reveals sophisticated mechanisms of time-dependent changes in the signaling components one of which generates superoxide if an agonist like Ang

II is present. We also found bradykinin causing the same effect and suggest that the generation of PN requires the Ang II or bradykinin receptor pathway for activating NO and $^{\bullet}O_2^-$ production (Pueyo et al., 1998; Shimizu et al., 1994). LPS alone had no major direct influence on the nitration but exerts a priming role for the subsequent receptor-stimulated PN formation. Since we observed the same pattern of events under hypoxia/reperfusion conditions (Zou and Bachschmid, 1999) the terminal signaling pathways for both situations should involve the same crucial components for PN formation. It remains to be investigated which priming mechanism by 60 min LPS exposure causes $^{\bullet}O_2^-$ formation after Ang II addition.

For the first time our experiments allow to conclude that a major source for $^{\bullet}O_2^-$ is xanthine oxidase, at least for LPS action. However, it is unclear whether xanthine oxidase originated from serum and remained attached to the endothelial surface (Houston et al., 1999) or was formed from endothelial xanthine dehydrogenase by proteolytic cleavage or oxidation at its thiols (Ryan et al., 1997; Harrison, 1997). Support for a serum-derived attached xanthine oxidase stems from observations that passaged bovine endothelial cells can be stimulated by LPS but show little depression of 6-keto $PGF_{1\alpha}$ formation. The latter cause of conversion of endogenous xanthine dehydrogenase to its oxidase form could have been triggered by NAD(P)H-oxidase (Zhang et al., 1999; Brandes et al., 1999; Lassegue et al., 2001).

For the resulting xanthine oxidase its substrate xanthine and hypoxanthine were detected by HPLC analysis of the supernatant (M. Bachschmid, unpublished).

Interestingly, NOS III is located to the caveolae as also is PGIS (Spisni et al., 2001). Hence, if $^{\bullet}O_2^-$ formation also takes place at the plasma membrane a close neighbourhood of all enzymatic components will generate high local concentrations of NO and $^{\bullet}O_2^-$. This would also solve the question why there was no trapping of PN by cellular reductants or the high serum levels of hemoglobin and uric acid as excellent quenchers for PN (Scott and Hooper, 2001; Minetti et al., 2000).

Another factor governing the specificity for PGIS nitration in comparison to all other enzymes is the presence of a heme-thiolate catalytic site which reacts extremely fast with PN. Earlier findings and data from heme-thiolate models (Zou et al., 2000) indicate a close-by tyrosine at the heme and therefore also a rapid transfer of the nitrating species to the tyrosine residue. The position of the 3-nitrotyrosine in the polypeptide chain was found not accessible to trypsin digestion but using different

approaches a pentapeptide could recently be isolated which allowed its location at the active site (P. Schmidt et al., to be published).

The early phase of ECA Type I therefore seems to critically depend on the priming for a superoxide source and it is understood that the onset of this event must be carefully regulated. A time interval of 45 min would guarantee that this process cannot be started accidentally, but that some sort of assembly or posttranslational modification is occuring. It will be interesting to unravel the mechanisms that are controlling this process and wether this process can be reversed.

A final consideration concerns ECA Type II. Whereas Type I is independent of protein synthesis the second phase heavily relies on the induction of early immediate genes. By the new synthesis of NOS-2 and COX-2 in VSCM the function of the endothelium will be restored and even overcompensated. We recently have shown that NO is an excellent scavenger for PN (Daiber et al., 2002) and therefore any PN will be removed as long there is a more than twofold molar excess of NO. ECA Type II therefore will be governed by very different events than ECA Type I and may also include the restoration of the endothelium under resting conditions.

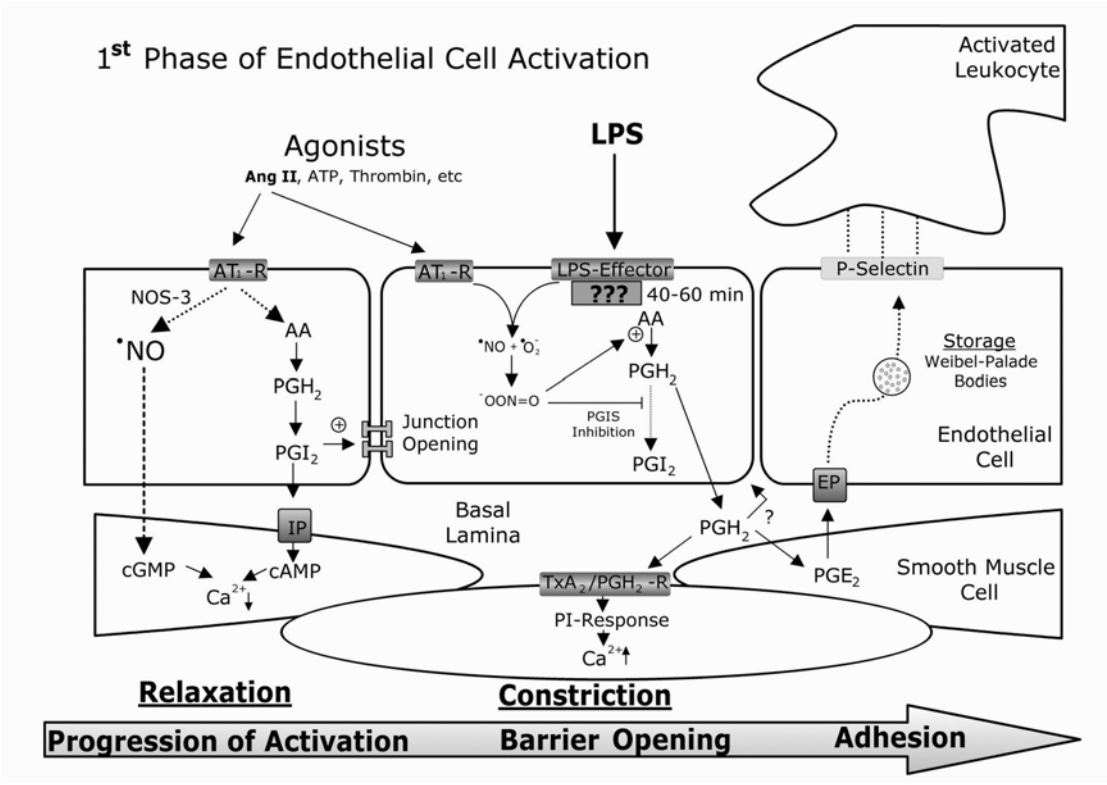

Scheme 6.1

AA = arachidonic acid; EP = PGE_2 receptor; AT_1-R = angiotensin II receptor; IP = PGI_2 receptor

7 Hyperglycemia - Diabetes

Contribution of coworkers to this work:

Prof. Dr. Lüscher (Coordination)
Dr. Francesco Cosentino (Coordination)
Dr. Bernd van der Loo (NO-measurements)
Masato Eto (PKC Activity)
Paola De Paolis (Western Blotting)

Prof. Dr. Ullrich (Supervisor)
Own contribution (Immunohistochemistry, ROS measurements)

Cosentino F, Eto M, DePaolis P, Van der Loo, Bachschmid M, Ullrich V, Luscher T. Protein kinase C and reactive oxygen species link glucose-induced paradoxical upregulation of NO pathway and endothelial dysfunction. Submitted to Circulation

7.1 Introduction

The relation between diabetes and premature cardiovascular disease is well established. Macro- and microvascular diseases are currently the major cause of morbidity and mortality in patients with diabetes mellitus. Loss of the modulatory and homeostatic function of the endothelium is a critical initiating factor in the development of diabetic vascular disease (Zou et al., 2002b; Ruderman et al., 1992; Cosentino and Luscher, 1998). Several signaling pathways had been found to account for these effects, like alterations in the polyol pathway activity (Williamson et al., 1993), formation of advanced glycation end products (AGEs) (Mullarkey et al., 1990) and reactive oxygen species (ROS) (Baynes, 1991).
Vasodilation mediated by NO is impaired in animal models and in patients with insulin dependent and independent diabetes mellitus (Cosentino and Luscher, 1998). Hyperglycemia, which is clearly the primary culprit in the pathogenesis of diabetic complications, may initiate the reduction of bioavailable endothelium-derived NO. Although the exact molecular mechanisms responsible for hyperglycemia induced endothelial dysfunction remain poorly understood, it may result from 1) decreased NO synthesis, 2) inactivation of NO by $^{\bullet}O_2^-$ to

form PN, and /or 3) increased production of endothelium-derived contracting factors. However, Cosentino et al. (1998) recently observed that human aortic endothelial cells exposed to high concentrations of glucose paradoxically increased endothelial NO synthase (eNOS) gene and protein expression, suggesting that the inactivation of NO by $^{\bullet}O_2^-$ is an important pathogenic element in diabetic endothelial dysfunction. Enhanced $^{\bullet}O_2^-$ has been observed and confirmed by several investigators (Inoguchi et al., 2000; Sano et al., 1998; Oberley, 1988). This leads to the formation of PN with an array of biological actions contributing to impairment of endothelial function. Vice versa, supplementation of SOD prevents the impaired endothelium-dependent relaxations caused by elevated glucose.

One possible signaling pathway involved in $^{\bullet}O_2^-$ production is the activation of protein kinase C (PKC), leading to the assembly of the vascular NAD(P)H-oxidase via a complex phosphorylation cascade. Several intermediary steps of this process are still unclear. Nevertheless hyperglycemia increases diacylglycerol, a strong activator of PKC (Lee et al., 1989, Ishii et al. 1998) chronically activated in diabetic tissues (Inoguchi et al., 1992; deRubertis and Craven, 1994). The promoter region of human eNOS gene contains a phorbol ester responsive element (Marsden et al., 1993), suggesting that PKC activation induces eNOS mRNA expression. In normal blood vessels, activation of PKC by phorbol ester reduces endothelium-dependent relaxations as occurs in diabetes via release of $^{\bullet}O_2^-$ induction and activation of NAD(P)H-oxidase and vasoconstrictor prostanoids (Tesfamariam et al., 1991; Zou et al., 2002b).

In addition, oxidative stress and PKC activation are among the most potent stimuli for activation of transcription factor nuclear factor-kappa B (NF-κB) (Ogata et al., 2000; Boyle et al., 1991), which is regarded as a key event for gene expression of a variety of adhesion proteins and inflammatory products. Hence, activation of the PKC system may represent an important common pathway by which endothelial dysfunction, oxidative injury and vascular inflammation are initiated in diabetes. Nevertheless, the effect of high glucose on these events has not been thoroughly examined. This prompted us to investigate whether activation of the PKC pathway by high glucose may link together the paradoxical upregulation of eNOS, increased formation of reactive oxygen species (ROS) and endothelial dysfunction in cultured human aortic endothelial cells.

7.2 Results

7.2.1 Glucose and Phorbol Ester Enhance eNOS Protein Expression

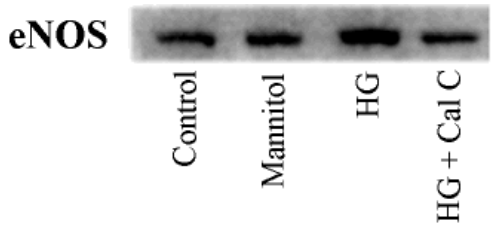

Figure 7.1

Western blot analysis of human aortic endothelial cells. A) Endothelial NO-synthase expression of cells exposed to control conditions [5.5 mM], high levels of glucose [22.2 mM] or mannitol [22.2 mM]. Calphostin C [$3x10^{-7}$ M] prevents high glucose induced eNOS expression.
HG = high glucose; Cal C = calphostin C; eNOS = endothelial NO-synthase

High glucose concentrations (22.2 mM) significantly increased the expression of eNOS. Densitometric analysis showed an almost twofold increase of eNOS expression by glucose, whereas mannitol (22.2 mM), which was used as a hyperosmotic control, did not affect expression of the enzyme (fig. 7.1). Comparing the effects of high glucose with those of PMA (10^{-6} M), a similar upregulation of eNOS was observed. Incubation of endothelial cells with the non-isoform specific PKC inhibitor calphostin C ($3x10^{-7}$ M), reduced eNOS protein expression almost to control values. The inhibitor alone under control conditions had no significant effect on eNOS expression (data not shown).

7.2.2 Glucose and NO Synthesis

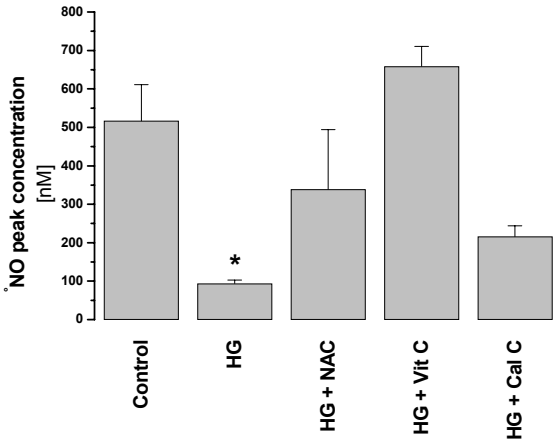

Figure 7.2

Peak concentration of °NO released upon stimulation with calcium ionophore A23187 (10^{-6}) in human aortic endothelial cells exposed to high glucose in the presence and absence of vitamin C (10^{-4} M), N-acetylcysteine ($5x10^{-5}$ M) and calphostin C ($3x10^{-7}$ M). Data are mean ± SEM (n=6) *P<0.05 vs control.
HG = high glucose; Cal C = calphostin C; NAC = N-acetylcysteine; Vit C = vitamin C

Despite the glucose-induced two-fold increase of eNOS expression, NO release following stimulation with calcium ionophore A23187 (10^{-6} M) was reduced in endothelial cells exposed to high glucose concentrations (fig. 7.2). However, in the presence of the antioxidant vitamin C (10^{-4} M) or N-acetylcysteine (NAC; $5x10^{-5}$ M) peak NO concentrations could be restored to control values. Furthermore, incubation with the PKC inhibitor calphostin C ($3x10^{-7}$ M)

doubled the concentration of free NO under hyperglycemic conditions, but failed to restore control values.

7.2.3 Effect of High Glucose on PKC Activity

To assess the effect of high glucose on PKC activity we measured its phosphorylation activity in the cytosolic and in the membrane-rich subcellular fractions. The translocation of this enzyme from the cytosol to the membrane is considered as one of the hallmarks of PKC activation (Hug and Sarre, 1993). Hyperglycemia increased membrane-associated PKC activity at the time point of 1h (191% vs control), which remained unaffected by either antioxidant, vitamin C or NAC, respectively (fig. 7.3 B). No differences in cytosolic PKC activity, between control and high glucose treated cells, had been observed . Mannitol as a hyperosmotic control had no significant effect on PKC distribution and activation (data not shown).

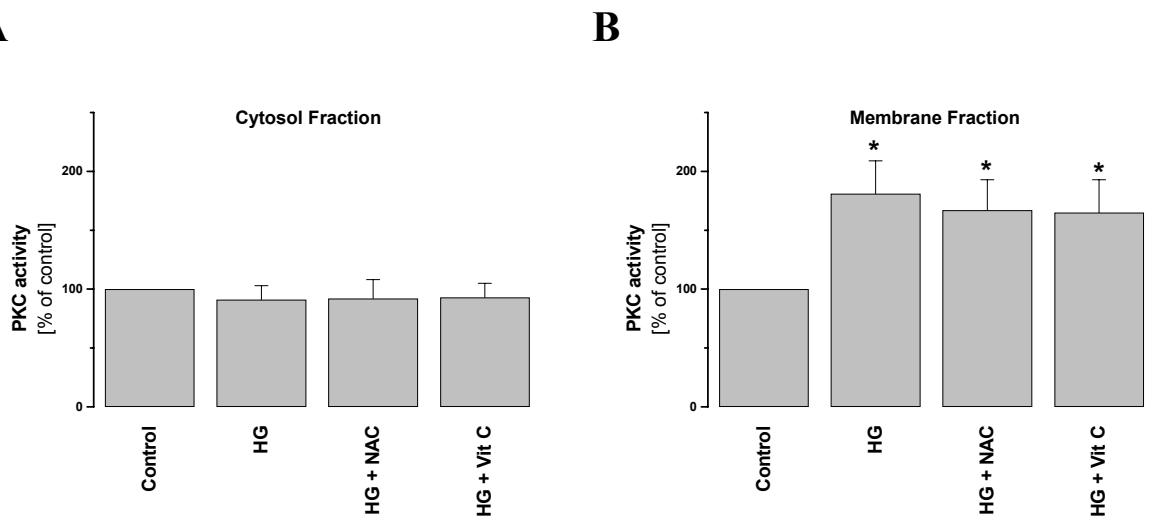

Figure 7.3

Effect on protein kinase C activity in the B) particulate and A) cytosolic fraction of human aortic endothelial cells. Elevated extracellular glucose lead to an increase of membrane-bound PKC activity after 60 min. of incubation. Neither N-acetylcysteine nor vitamin C did affect glucose-induced activation of PKC. Data are mean ± SEM (n=4). *P<0.05 vs control.
Vit C = vitamin C; NAC = N-acetylcysteine; HG = high glucose

7.2.4 Glucose and Reactive Oxygen Species Formation

The intracellular formation of ROS was measured by the cell permeable fluorescent probe dichlorodihydrofluorescein diacetate (DCFH). This dye is activated by intracellular esterases

and serves as an unspecific probe for detecting oxygen radicals. Only by specific inhibition of enzymatic ROS sources, a discrimination among the various radical species can be achieved. As shown in figure 7.4, high glucose caused a dramatic increase in the fluorescence. The antioxidants NAC and vitamin C completely restored control levels. Comparing the effects of hyperglycemia (24893±3996) with those of PMA (27450±4327) alone, a similar increase in fluorescence intensity can be observed. Accordingly, inhibition of PKC by activating NAD(P)H oxidase abolished the effect. Furthermore, diphenyleniodonium (10^{-5} M), a nonspecific inhibitor of flavoproteins, which is falsely used in several studies as proof for the involvement of NAD(P)H oxidase as a superoxide source (Inoguchi et al., 2000), blunted the response. To exclude cyclooxygenase-derived oxidants, which under some settings could increase DCFH fluorescence, the inhibitor indomethacin (10^{-5} M) was used and did not affect glucose induced ROS generation.

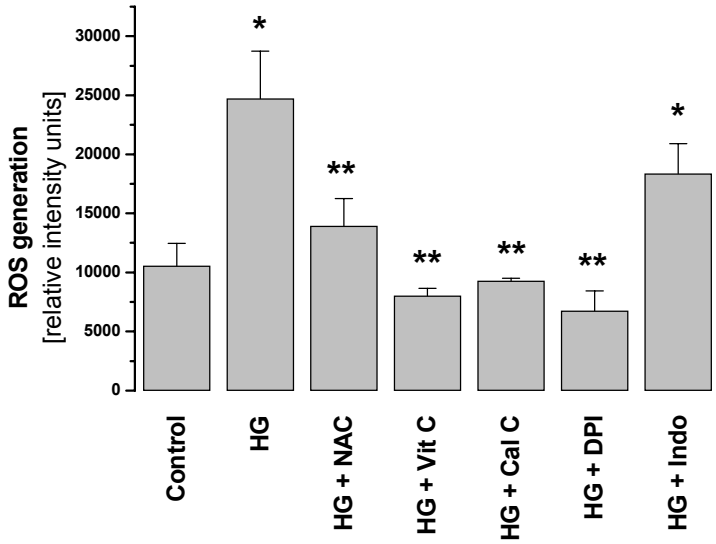

Figure 7.4

Reactive oxygen species production in human aortic endothelial cells exposed to high glucose in the presence and absence of vitamin C [10^{-4} M], N-acetylcysteine [$5x10^{-5}$ M], calphostin C[$3x10^{-7}$ M], diphenyleniodonium [10^{-6} M], and indomethacin [10^{-5} M]. Data are mean ± SEM (n=6). *P<0.05 vs control, **P<0.05 vs high glucose alone.
Vit C = vitamin C; NAC = N-acetylcysteine; Cal C = calphostin C; HG = high glucose; indo = indomethacin; DPI = diphenyleniodonium.

7.2.5 Induction of NAD(P)H Oxidase by Hyperglycemia

Since antibodies against NAD(P)H oxidase subunits were rare and some of the commercially available products only weakly detect the enzyme subunits, only the detection of $p22^{phox}$ was feasible. This subunit serves as an adapter for the cytosolic factors $p67^{phox}$ and $p47^{phox}$, and stabilizes the catalytically active $gp91^{phox}$. Thus $p22^{phox}$ is essential for the activation process of NAD(P)H oxidase. Meanwhile, several other laboratories confirmed the induction of the enzyme in diabetes and also in hypertension (Fukui et al., 1997; Griendling et al., 2000; Hink

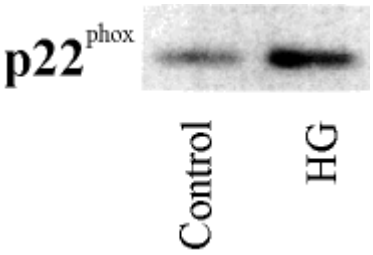

Figure 7.5

Effect of high glucose on NADPH-oxidase subunit $p22^{phox}$ expression.

HG= high glucose

et al., 2001; Guzik et al., 2002). The Western blot demonstrates a strong induction of $p22^{phox}$ upon high glucose treatment, which correlates with PKC activation (fig. 7.5).

7.2.6 Nitration of Prostacyclin Synthase

Cells grown on coated glass cover slides were stained for prostacyclin synthase. No alterations of protein expression under the different treatments had been observed (data not shown).

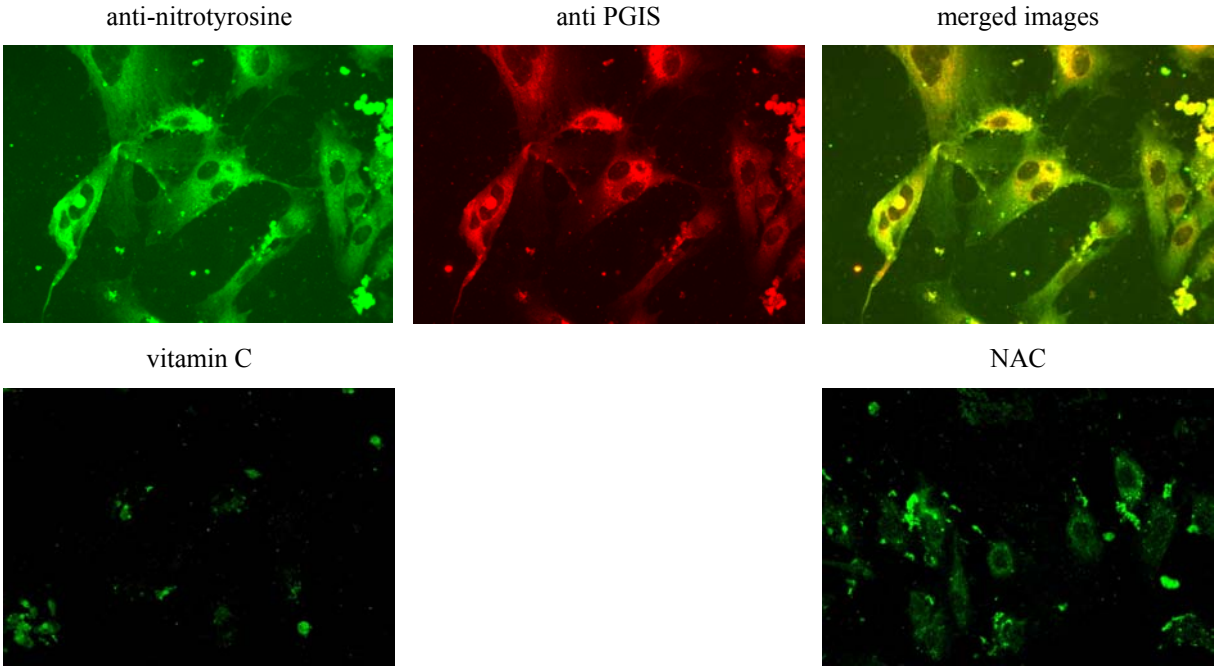

Figure 7.6
High glucose treated human aortic endothelial cells stained with anti-nitrotyrosine 1A6 monoclonal (green color) and anti-prostacyclin synthase polyclonal T6 antibody (red color). Nitrated prostacyclin synthase, as indicated by the yellow colouring of the merged images, is mainly located in the soma but not in the nucleus, whereas the fibrilary processes are mainly nitrotyrosine positive. Supplementation of the high glucose medium with NAC and vitamin C strongly reduced the nitrotyrosine staining, which was more effective in the case of vit C. Magnification 400 fold

Since the results of the eNOS expression, free NO and free radical measurements strongly indicate the formation of peroxynitrite, the immunostaining of protein-bound nitrotyrosine

was performed (fig. 7.6). A very weak labeling was observed in control cells, in contrast to the high glucose treatment, where an intense nitration was detected. Supplementation of the high glucose medium with vitamin C or NAC blunted the nitration. In parallel to the DCFH-fluorescence method vitamin C was more effective. Localization of PGIS and nitrotyrosine staining was highly coincident and strongest in the soma. The fibrillary cell protrusions were NT positive, but exhibited only a weak PGIS staining. The nuclei remained unstained.

7.2.7 Activation and Translocation of NF_kB

Activation of NF_kB requires phosphorylation and deactivation of the endogenous inhibitor I_kB. After the activation process the factor translocates into the nucleus. This can be examined by the classical electrophoretic mobility shift assay in nuclear fractions (fig. 7.7). Hyperglycemia increases NF_kB activation and the inhibition of this process by calphostin C suggests an involvement of PKC in the activation cascade. The response to high glucose was optimal after 2 to 4h, but after 24h the effect disappeared (data not shown). Interestingly, the activation was also inhibited by the antioxidant NAC. In parallel induction of COX-2 mRNA takes places (data not shown).

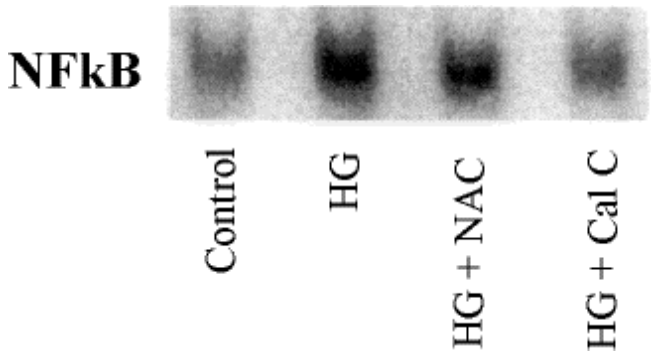

Figure 7.7

Effect of high glucose on nuclear factor-$_kB$ binding activity in nuclear fractions of human aortic endothelial cells for 2h in the presence and absence of calphostin C [$3x10^{-7}$ M] and N-acetylcysteine [$5x10^{-5}$ M].
NAC = N-acetylcysteine; Cal C = calphostin C; HG = high glucose

7.3 Discussion

The present study provides the molecular basis for understanding how hyperglycemia causes the early impairment of balance between endothelium-derived vasoactive factors, which may contribute to vascular complications in diabetes. In agreement with previous reports

(Cosentino et al. 1997; Hink et al., 2001), we found that despite the glucose induced increase of eNOS expression, NO release is reduced because of its inactivation by $^{\bullet}O_2^-$. This leads to PN formation and inhibition of PGIS by selective nitration of the active site tyrosine. Further we demonstrated that in human aortic endothelial cells high glucose causes activation of NF_kB and upregulation of COX-2 mRNA expression. Once more our results show that activation of the PKC isoenzyme family links hyperglycemia induced oxidative stress and endothelial dysfunction. Nevertheless relations and conclusions to the *in vivo* situation should be carefully evaluated, since three major biochemical pathways have been considered to be responsible for vascular damage in diabetes. These include increased glucose flux through the aldose reductase pathway (Lee et al., 1995), excessive formation of advanced glycation end products (AGE) (Brownlee, 1995), and stimulation of the diacylglycerol/PKC pathway (Koya and King, 1998). In the early hyperglycemic model, the PKC dependent pathway is the most important one because of its rapid activation. In contrast nonenzymatic AGEs and activation of AGE-receptor (RAGE) etc. occurs at later stages. This work presents a new explanation, how radicals exhibit their signal function in vasculature after high glucose challenge, supported by several lines of evidence.

The association of diabetes mellitus and PKC is well established. Incubation of endothelial cells with high glucose leads to PKC activation via an intracellular increase of diacylglycerol levels. Furthermore, activation of PKC by phorbol esters causes reduction of endothelium dependent relaxations, similar to that observed in diabetes, suggesting a common mechanism of endothelial dysfunction in response to elevated glucose levels or addition of phorbol esters (Ogata et al., 2000). Adverse effects of elevated glucose levels on acetylcholine-induced relaxation of rabbit aorta and rat pial arterioles were restored by the addition of PKC inhibitors (Mayhan and Patel, 1995; Tesfamariam et al., 1991). These *in vitro* observations are supported by studies, demonstrating, that *in vivo* treatment with PKC inhibitors ameliorates vascular complications in diabetic rats (Ishii et al., 1996). Of course signal transduction and intracellular crosstalk by PKC dependent phosphorylation is manifold and complicated. The array of substrates involves enzymes, cell-surface receptors, contractile proteins, transcription factors and other kinases (Tomlinson, 1999; Idris et al. 2001). Therefore in the present study only a few pathways had been explored as follows.

High glucose treatment of human aortic endothelial cells augmented the membrane associated PKC isoenzyme activity. Knapp and Klann (2000) had reported an $^{\bullet}O_2^-$ stimulated PKC activation via thiol oxidation. On the other hand studies on the multicomponent phagocyte

and endothelial NAD(P)H oxidase (Fontayne et al., 2002, Guzik et al. 2002) revealed that PKC activation promotes superoxide formation. Several isoforms of PKC are able to phosphorylate $p47^{phox}$, an important cytosolic subunit, thus assembling the multienzyme complex and initiating $^{\bullet}O_2^-$ formation. Two scenarios are possible, either activation of PKC by radicals or PKC promotes radical formation. However, vitamin C, an $^{\bullet}O_2^-$ scavenger as well as NAC failed to inhibit high glucose induced radical formation. Hence, it is likely that oxidant generation in human aortic endothelial cells occurs downstream of PKC activation. Treatment with the non isoenzyme specific inhibitor calphostin C prevented glucose-induced formation of ROS. Also PMA is a well accepted stimulus of NAD(P)H-oxidase (Nobuhiko et al., 2000) and commonly used to trigger the $^{\bullet}O_2^-$ burst in polymorpho-nuclear cells. Consistently PMA also induced ROS formation in the human aortic endothelial cells. High glucose further increases $^{\bullet}O_2^-$ generation not only by activation of NAD(P)H oxidase, but also by induction of the $p22^{phox}$ subunit.

Treatment of vessels from diabetic animals with SOD improved endothelium-dependent relaxations (Tesfamariam et al., 1992) and the use of vitamin C in patients with non-insulin (NIDDM) and insulin-dependent diabetes mellitus (IDDM), increased the endothelium-dependent vasodilation in the forearm circulation (Ting et al., 1996; Timimi et al., 1998).

Elevated $^{\bullet}O_2^-$ levels trap the free NO in a very efficient and nearly diffusion-limited reaction, thus eliminating a mediator important in maintaining vascular homeostasis and forming the new potent oxidant PN. Beside the messenger function of NO, it serves also as a potent antioxidant. The present study demonstrates that high glucose, via PKC induces oxidative stress and promotes a compensatory upregulation of eNOS. The latter finding is consistent with the identification of a phorbol ester-responsive element in the promotor region of human eNOS gene and the reported PKC-dependent modulation of eNOS expression. (Marsden et al., 1993; Li et al., 1998). Anyway this compensatory mechanism is not sufficient to restore control levels of free NO.

An aggravation of this process is the nitration and inhibition of PGIS by PN. PGI_2 and NO are major endothelial mediators for maintenance of vascular homeostasis, thus the loss leads to thrombosis and adhesiveness for immune cells. Both mediators were neutralized by increased levels of endothelium derived $^{\bullet}O_2^-$, serving as an antagonist. Zou and coworkers (2002b) have demonstrated that high glucose treatment of HUVEC lead to accumulation of PGH_2, caused by the inhibition of PGIS, which then stimulates the PGH_2/ TxA_2 –receptor on smooth muscle cells. This explains the changes in adhesiveness of the endothelium and the increased vascular

tone in diabetes. Formation of TxA_2 under the experimental settings, which could also explain the vasocontricting and prothrombotic effects, was not altered (data not shown). The formation and accumulation of PGH_2, belonging to the group of endothelium-derived vasoconstricting factors (EDCF), can be abolished by inhibition of COX. Several studies demonstrated, that the impaired relaxations were restored by a non-specific blockade of COX and prostanoid receptors (Tesfamariam et al. 1990, Mayhan et al., 1991).

PKC isoforms play an important role in the activation process of transcription factors, like MAP kinase cascade or NF_kB. For both signaling cascades the involvement of ROS has been implicated. NF_kB activation is in part also dependent on the phosphatase activity of calcineurin. This enzyme is inactivated by physiological amounts of $^{\bullet}O_2^-$, which in parallel increases NF_kB phosphorylation and activity. Glucose-induced NF-$_k$B activation was prevented not only by co-incubation with antioxidants but also by calphostin C. In line with our findings the demonstration that PKC activation leads to dissociation of the NF-$_k$B I_kB complex allowing NF-$_k$B to translocate to the nucleus and activate its target genes would suggest the possibility of a causal link between PKC, ROS and NF-$_k$B activation in hyperglycemia. This increased NF-$_k$B DNA binding activity may lead to changes in vascular homeostasis, endothelial function and may promote inflammatory vascular complications in diabetes as indicated by the increase in COX-2 mRNA.

In conclusion our results show that a single unifying PKC-dependent mechanism is the triggering step by which hyperglycemia-induced endothelial dysfunction and vascular inflammation can occur. Indeed, elevated glucose – via PKC- promotes oxidative stress and compensatory upregulation of the NO pathway resulting in reduced NO bioavailability, NF-$_k$B activation, and increased expression of COX-2 altering the proinflammatory prostanoid profile at later stages. Further NAD(P)H oxidase-derived $^{\bullet}O_2^-$ formation causes the NO depletion and PN formation, leading to PGIS inhibition and accumulation of the vasoconstricting prostanoid PGH_2. These findings may be relevant in understanding the intracellular signaling targets to prevent the development and progression of diabetic complications as summarized in scheme 7.1.

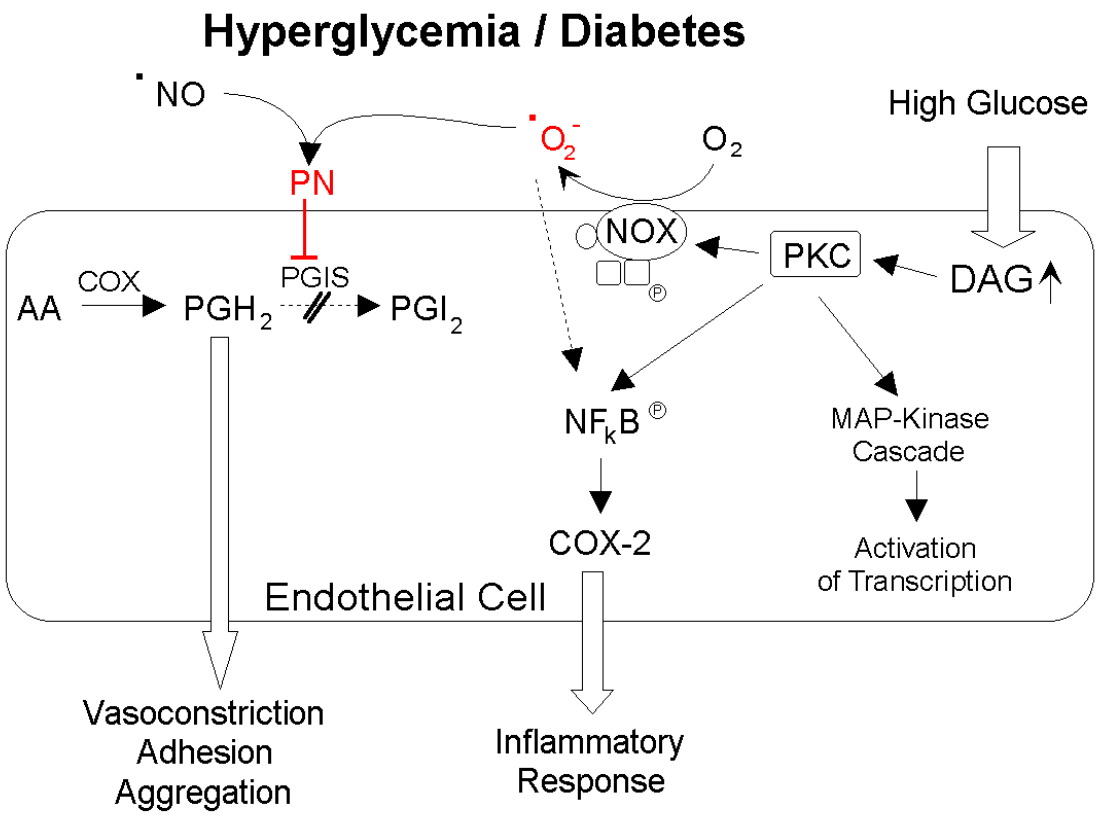
Hyperglycemia / Diabetes
NO
O_2^-
O_2
High Glucose
PN
NOX
PKC
DAG
COX
PGIS
AA
PGH_2
PGI_2
NF_kB Ⓟ
MAP-Kinase Cascade
COX-2
Activation of Transcription
Endothelial Cell
Vasoconstriction
Adhesion
Aggregation
Inflammatory Response

8 Vascular Aging

Contribution of coworkers to this work

Prof. Dr. Lüscher
Bernd van der Loo (Coordination and porphyrinic NO microsensor)
Ralf Labrugger (Western blotting and MnSOD immunoprecipitation
Juliane Kilo (Isometric tension measurement)

Multi-Imaging Center, University of Cambridge
Jeremy Skepper (Immunoelectron microscopy)

Prof. Dr. Ullrich (Supervisor)
Own contribution (Superoxide measurement and TLC NOS-activity assay)

Published in:
van der Loo B, Labugger R, Skepper JN, Bachschmid M, Kilo J, Powell JM, Palacios-Callender M, Erusalimsky JD, Quaschning T, Malinski T, Gygi D, Ullrich V, Luscher TF. Enhanced peroxynitrite formation is associated with vascular aging. J. Exp. Med. 2000 Dec 18;192(12):1731-44.

8.1 Introduction

Cardiovascular diseases increase in frequency with age, even in the absence of established risk factors (Lüscher and Noll, 1985). This suggests that aging by itself alters vascular function. The endothelium exerts a multimodal regulation of vascular smooth muscle tone and structure by the release of nitric oxide (NO), endothelium-derived hyperpolarizing factor, and prostacyclin. NO is generated from L -arginine catalyzed by NO synthases (Palmer et al., 1988; Moncada and Higgs, 1993). One of these isoenzymes, endothelial NO synthase (eNOS), is constitutively expressed in endothelial cells (Moncada, 1992). This enzyme is largely membrane associated as a result of NH_2-terminal myristoylation (Pollock et al., 1991), a reaction which regulates enzymatic biological activity (Sessa et al., 1993; Busconi and Mitchel, 1993). Endothelium-dependent relaxation

declines with increasing age (Tschudi et al., 1996). The underlying cellular and molecular mechanisms associated with age-related endothelial dysfunction have not been elucidated, but might involve: (a) changes in expression and/or activity of eNOS (Cernadas et al., 1998), (b) increased breakdown of NO due to an augmented production of $^{\bullet}O_2^-$ (Gryglewski et al., 1986), or (c) a gradual loss of antioxidant capacity (Azhar et al., 1995), which normally provides cellular protection against reactive oxygen species. The role of the L-arginine/NO pathway in the pathophysiology of vascular aging is controversial. Both reduced levels of eNOS mRNA (Challah et al., 1997) and increased eNOS enzyme expression combined with reduced activity (Cernadas et al., 1998) have been reported. Therefore, our first aim was to clarify whether age-associated endothelial dysfunction is causally related to alterations of the L -arginine/NO system. To this end, molecular analyses of eNOS expression and its subcellular localization, which might affect the biological activity of this enzyme system, were performed in aortas from young (4–6 mo), middle-aged (19 mo), and old (32–35 mo) rats and correlated to direct measurements of NO production and vascular function. Reactive oxygen species and especially are important modulators of NO activity under various pathophysiological conditions (Harrison, 1997a) and are thought to be involved in the aging process (Stadtman, 1992). In this context it seemed essential to assess the role of, which might scavenge NO to form the powerful oxidant PN (Beckman et al., 1993; Koppenol, 1999). In vivo generation of PN has not been directly demonstrated to date (Koppenol, 1999). Unlike (pK 4.8), PN (with a pK of 6.8) can easily penetrate cells in the protonated form because of its high diffusibility across phospholipid membranes (Marla et al., 1997). PN is known to initiate oxidative modification of proteins, including the nitration of aromatic rings (Beckman et al., 1992), sulfoxidation of methionin, and *S*-nitrosation of cysteine followed by disulfide formation, thereby rendering inactive certain functionally important regulatory proteins, like receptors or enzymes (Haddad et al., 1994). Nitration of tyrosine is the underlying mechanism of prostacyclin synthase inhibition by PN (Zou et al., 1997). Evidence for the in vivo formation of PN has been derived from immunohistochemical detection of NT in human atherosclerotic lesions (Beckman et al., 1994) and in the tissue of rejected human renal allografts (MacMillan-Crow et al., 1996). Recent indirect evidence (Leeuwenburg et al., 1998) suggests that specific enzymes may selectively accumulate oxidative damage during aging. This is supported by a recent study demonstrating increased nitration of the sarcoplasmic reticular Ca-ATPase isolated from the skeletal muscle of 28-mo-old F344 rats (Viner et al., 1996). Our second aim was to test the hypothesis that increased nitration of protective, antioxidant enzymes, leading to their inactivation with age, might be a contributing molecular pathway for oxidative damage to vascular tissue. We will show that the

reduced endothelium-dependent relaxation associated with aging is not due to downregulation of eNOS but rather to increased inactivation of NO by entailing altered NO bioavailability, as NO is removed through the formation of PN. The evidence for a close association between the formation of PN and age-associated vascular endothelial dysfunction provided in this study is further strengthened by the demonstration of a selective nitration of MnSOD with increased age. The paradoxical increase in eNOS expression and activity appears to be a compensatory mechanism attempting to counteract increased NO inactivation by $^{\bullet}O_2^-$.

8.2 Results

8.2.1 Weight, Heart Rate, and Blood Pressure

Body weight was higher in old and middle-aged rats than in young rats. Systolic blood pressure and heart rate were not significantly different between the three groups (table 8.1).

Parameter	Young	Middle-Aged	Old	Significance Level
Weight (g)	305 ± 8*	537 ± 7*	514 ± 20*	*P<0.0001 for Y vs. M and Y vs. O
Systolic RR (mmHg)	121 ± 8*	117 ± 4*	117 ± 2*	NS
Heart rate (bpm)	334 ± 8*	323 ± 14*	344 ± 13*	NS
Maximal relaxations (%)				
Acetylcholine	-96 ± 2*	-89 ± 2*	-62 ± 3*	*P<0.0001 for Y vs. O and M vs. O
A 23187	-76 ± 1*	-74 ± 4*	-47 ± 4*	*P<0.0001 for Y vs. O and M vs. O
Sodium nitroprusside	-111 ± 2	-107 ± 1	-105 ± 1*	NS
Maximal NO release (nmol/liter)	690 ± 50*	490 ± 70*	200 ± 30*	*P<0.0001 for Y vs. O *P<0.001 for M vs. O *P<0.01 for M vs. Y
NOS activity (pmol/min/mg)				
Total	120 ± 13*	-	216 ± 26*	*P<0.01
Ca^{++} -dependent	23 ± 10**	-	144 ± 14**	**P<0.001
Ca^{++} -independent	97 ± 15	-	72 ± 12	NS
Superoxide (cpm/mg dry wt)				
Basal	2,302 ± 323*	2,145 ± 220*	6,058 ± 445*	*P<0.0001 for Y vs. O and M vs. O
Stimulated	82,495 ± 6,033**	108,439 ± 2,612*	175,058 ± 36,080**	**P<0.01

Table 8.1

Comparison and summary of different parameters in young, middle-aged, and old rats

Y, young; M, middle-aged; O, old; RR, blood pressure; bpm, beats per minute.

8.2.2 Age-dependent Impairment of NO-mediated Vascular Endothelial Function

In old rats, NO-mediated, endotheliumdependent relaxation to acetylcholine was markedly reduced compared with young and middle-aged rats (fig. 8.1 A, and tab. 8.1). Furthermore, aging was

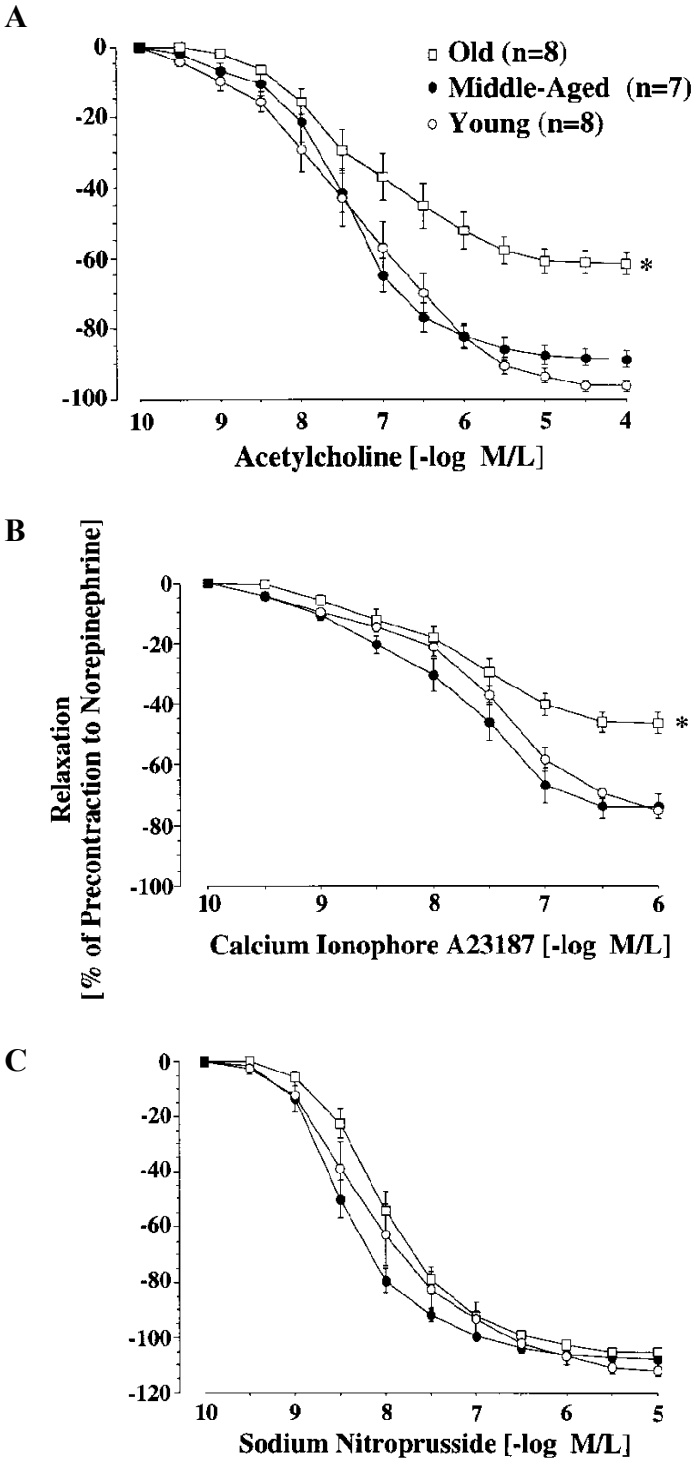

Figure 8.1
Age-dependent changes in endothelium-dependent and –independent relaxation of the rat aorta. Line graphs show concentration –response curves to A) acetylcholine, B) calcium ionophore A23187, and C) sodium nitroprusside (SNP). Relaxation to both endothelium-dependent agonists was reduced in old aortas ($P<0.0001$). Endothelium-independent relaxation was unaffected.

also associated with comparable reductions of NO-mediated, endothelium- dependent relaxation to the calcium ionophore A23187 (fig. 8.1 B, and tab. 8.1). In contrast, there was no impairment of endothelium-independent relaxation to SNP in aged animals (fig. 8.1 C, and tab 8.1).

8.2.3 Age-associated Upregulation of the eNOS Enzyme System

Fig. 8.2 A depicts typical amperograms for each age group of direct *in situ ex vivo* measurements of NO on the aortic endothelial surface after maximal stimulation with A23187 (10^{-6} M). A receptor-independent agonist was chosen for stimulation in order to delineate changes of eNOS activity rather than possible age-associated changes of receptormediated signal transduction. The porphyrinic microsensor, with its fast response time (0.1–10 ms), high sensitivity for NO, and lack of sensitivity to secondary species such as nitrate/nitrite, was chosen to provide the most precise, direct measurements of endogenous NO (Malinski and Taha, 1992). Maximal NO levels were lower in aortas obtained from old and middle aged animals compared with those from young rats (fig. 8.2, and tab. 8.1).

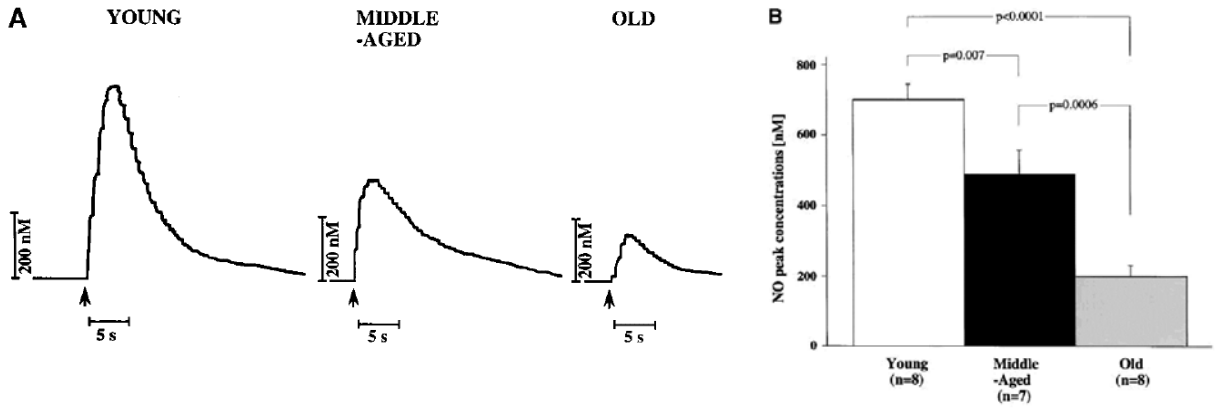

Figure 8.2
Age-from dependent changes in aortic NO release. A) Representative amperograms of NO release from isolated and perfused aortas. NO release was induced by calcium ionophore A23187 (10^{-6} M) and measured in situ on the endothelial surface using a porphyrinic microsensor. B) Bar graph showing peak concentration of NO.

As NO in vascular endothelial cells is synthesized by eNOS, we investigated the possibility that age-dependent changes might be related to alterations in the expression and/or activity of the eNOS enzyme system. To this end, we determined eNOS protein expression selectively in homogenates of endothelium using a new extraction method. Strikingly, we found that eNOS protein expression steeply increased in an age-dependent manner, nearly sevenfold in old rats compared with young ones (fig. 8.3 A) and nearly threefold in middle-aged animals (young versus old, middle- aged versus old, and young versus middle-aged; P = 0.0001). The age-dependent increase in eNOS expression was in sharp contrast to the decrease in NO detection. In contrast to eNOS, there was no iNOS expression detectable in all age groups (data not shown). Analysis of the subcellular distribution of eNOS protein expression revealed that, in all age groups, eNOS was exclusively associated with the particulate, subcellular membrane fraction (fig. 8.3 A) containing the biological activity of the enzyme (Sessa et al., 1993; Busconi and Michel, 1993). No eNOS was found in the cytosolic fraction. To confirm that eNOS overexpression was also associated with a higher activity, we determined eNOS activity by the conversion of l-[^{14}C]arginine into l-[^{14}C]citrulline. Using this test we found that both total NOS activity and eNOS activity were significantly greater in old than in young rats (fig. 8.3 B, and tab. 8.1). The sevenfold increase in eNOS activity in old aortas parallels the increase in enzyme expression. In conclusion, fully active eNOS is upregulated with age, although the bioavailability of its intended product, NO, is significantly diminished. However, citrulline formation may not be stoichiometrically related to NO production, as a partial conversion of NOS to its oxidase form will also yield l-citrulline as an end product (Vasquez-Vivar et al., 1999).

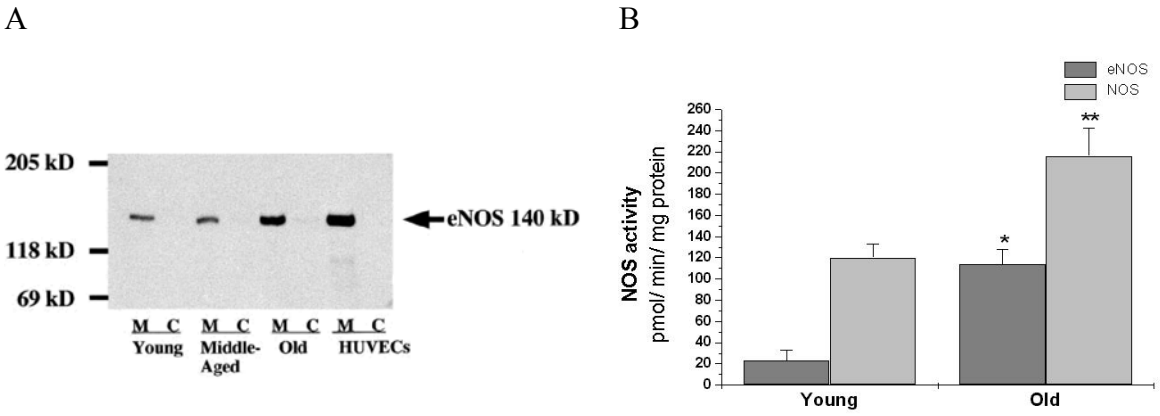

Figure 8.3

A Subcellular analysis of eNOS as detected by immunoblotting. Membrane-associated (M) and cytosolic (C) eNOS expression. Cytosolic and membrane fractions were prepared from homogenates of each age group and analyzed by immunoblotting. Data are representative of three experiments. HUVECs, human umbilical vein endothelial cells. **B** Activity of total NOS and eNOS in aortas from young and old rats. Activity was measured in homogenates of aortic tissue by determination of the rate of conversion of l-[^{14}C]arginine to l-[^{14}C]citrulline. Significance: eNOS, $^{**}P < 0.001$; total NOS, $^{*}P < 0.01$

8.2.4 Age-associated Increased Vascular Superoxide Formation.

$^{\bullet}O_2^-$ is the main oxidant for NO (Dinerman et al., 1993). Therefore, we investigated the possibility that increased tissue levels of $^{\bullet}O_2^-$ might be the cause of the inactivation of NO. Using a lucigenin enhanced chemiluminescence method, we found a threefold increase of basal and a twofold increase of stimulated (A23187 10^{-6} M) $^{\bullet}O_2^-$-generated chemiluminescence in old aortas compared with young ones (fig. 8.4 A, and tab. 8.1).

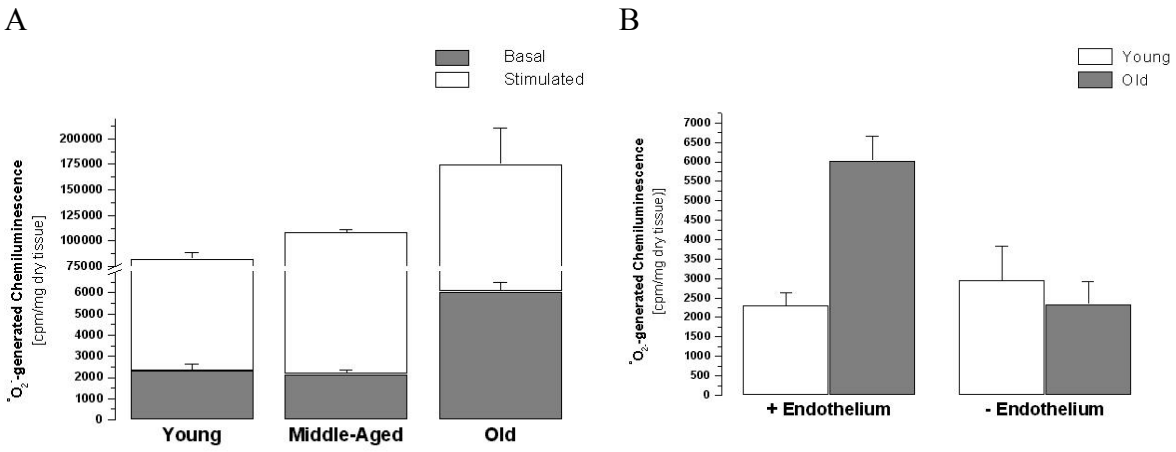

Figure 8.4

Age-dependent $^{\bullet}O_2^-$ production. (**A**) Bar graph showing both basal amount of chemiluminescence generated by $^{\bullet}O_2^-$ in aorta from young, middle-aged, and old rats ($^{*}P < 0.0001$ versus basal values for young and middle-aged rats) and maximal generation of chemiluminescence after stimulation with calcium ionophore A23187 (10^{-6} M). (**B**) The influence of endothelium: aortic rings from young and old ($n = 6$ each) rats were mechanically denuded, and the basal chemiluminescence signal was compared with that from intact aortas.

This assay, in the absence of added NADH, largely reflects $^{\bullet}O_2^-$ production. To identify the source of $^{\bullet}O_2^-$, aortic rings were mechanically denuded. Thereafter, $^{\bullet}O_2^-$-generated chemiluminescence fell from 6,058±445 to 2,293±625 cpm/mg (P= 0.02), suggesting that the endothelium is the primary source of $^{\bullet}O_2^-$ generation (fig. 8.4 B). Values for young denuded aortas (3,019±835 cpm/mg) did not significantly differ from those obtained from young aortas with an intact endothelium (2,302±323 cpm/mg; NS). This suggests that in young aortas there is only a low, basal production of $^{\bullet}O_2^-$ and also that the age-associated increase in $^{\bullet}O_2^-$ occurs within the endothelium.

8.2.5 Increased Vascular Deposition of Nitrated Proteins in Distinct Cellular and Subcellular Compartments of the Vasculature.

We then sought to prove that PN was indeed formed after the trapping of NO by $^{\bullet}O_2^-$ in the aging vasculature and, if so, to clarify its biological effects on antioxidative enzymes. Therefore, we studied the distribution of 3-NT residues, which are typical end products of the reaction of PN with biological compounds. As shown in fig. 8.5, aortic tissue sections from old animals exhibited a markedly increased specific immunostaining with a monoclonal antibody to NT compared with young animals. In the endothelium of old aortas (fig. 8.5 A), significant amounts of NT accumulated in the nucleus, the cytosol, and the mitochondria compared with young aortas (fig. 8.5 B). The extracellular matrix of the intima (fig. 8.5 E) and vascular smooth muscle cells within the media (fig. 8.5 G) of old aorta also had an enhanced immunolabeling compared with young tissue (fig. 8.5, D and F, respectively). Depending on the subcellular compartment examined, a two to sixfold increased labeling of old aorta was observed. A particularly high labeling density for NT was found in the mitochondria of endothelial cells (data not shown). It is of importance to note that these vessels do not exhibit any particular signs of atherosclerosis, as confirmed by electron microscopy.

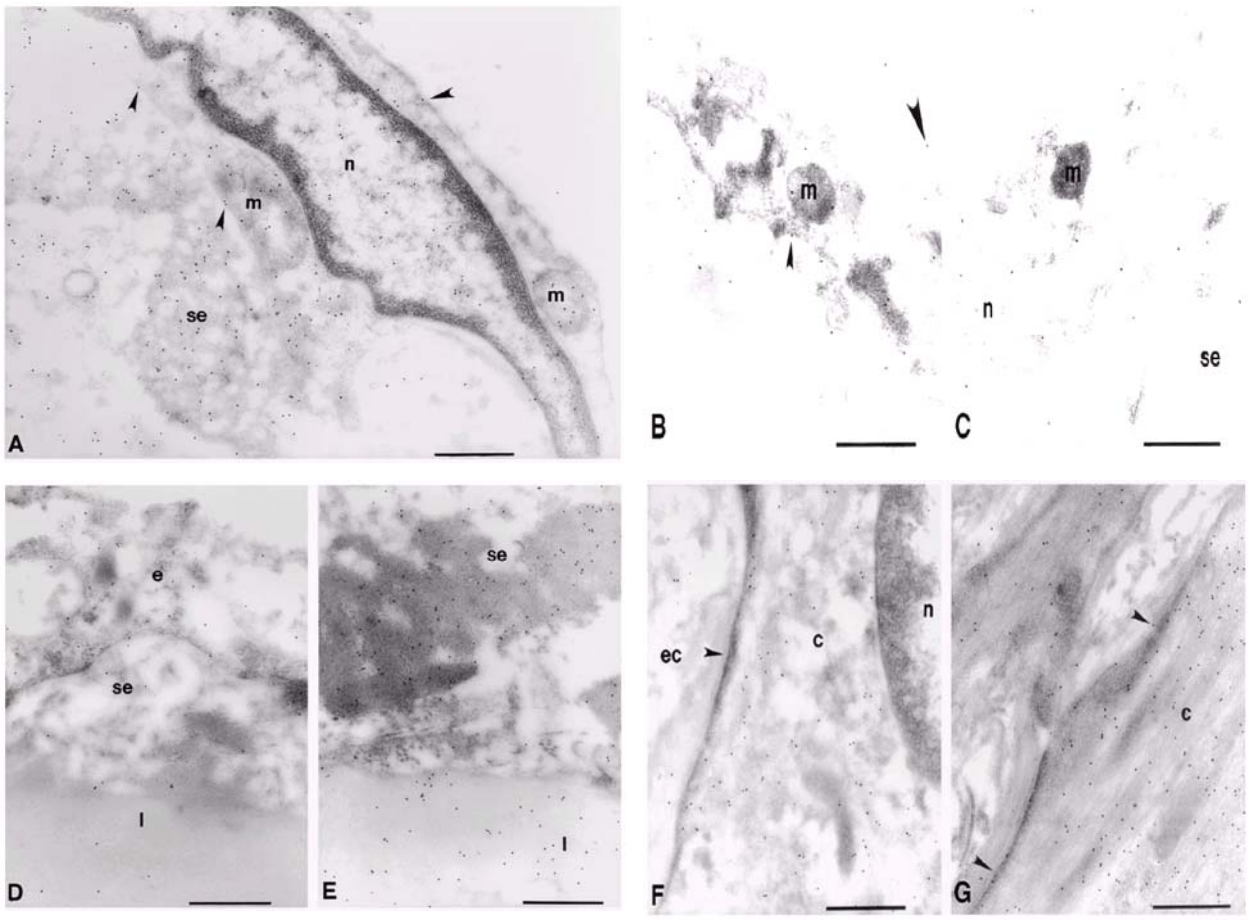

Figure 8.5
The accumulation of 3-NT is increased in the aorta of the old rat compared with that of the young rat. Representative electron micrographs show the pattern of immunogold labeling for 3-NT in thin sections of young (B, D, and F) and old (A, E, and G) aortas. Primary antibody binding sites were visualized with goat anti–mouse IgG conjugated to 10-nm gold particles. (A) Intima of the aorta from an old rat. Label is densest over mitochondria (m) and strong over nucleoplasm (n) and over endothelial cell cytoplasm. Sparse labeling is associated with the luminal plasmalemma (large arrowheads) and stronger label is present over the abluminal plasmalemma (small arrowheads). Strong labeling is seen in the subendothelial space (se). (B) Intima of the aorta from a young rat. Label is lower over mitochondria and cytoplasm and sparse over the luminal plasmalemma (large arrowhead) and the abluminal plasmalemma (small arrowhead). (C) Intima of an old rat. The primary antisera against NT was preincubated with 2x10-5 NT for 1 h before labeling as in A and B. Label density is reduced to levels lower than those seen in the young rats in all compartments. (D) Intima of a young rat showing low levels of labeling over the endothelium (e) and sparse labeling over the subendothelial space and the first elastic lamellae (l). (E) Subendothelial space and the first elastic lamellae of an old rat. Labeling density is much greater in both compartments and is particularly dense over aggregates of electron dense material seen in the subendothelial space. (F) Smooth muscle cell in the medial layer of the aorta of a young rat. Label is strongest over the cytoplasm (c) and low over the nucleoplasm and extracellular space (ec) and seldom seen over the sarcolemma (arrowhead). (G) Smooth muscle cell in the medial layer of the aorta from an old rat. Labeling is much stronger over the cytoplasm and is frequently seen over the sarcolemma (arrowheads). Bars, 0.5 µm. Original magnifications: 322,000.

8.2.6 Increased Nitration of MnSOD as a Molecular Marker for Age-associated Mitochondrial Oxidative Stress in the Vasculature.

Immunoelectron microscopy strongly supported that the most significant generation of oxidants, namely $^{\bullet}O_2^-$ and PN, occurs within the mitochondria and in particular, in those within the endothelium. This is of particular interest as, in a different pathophysiological context, the nitration

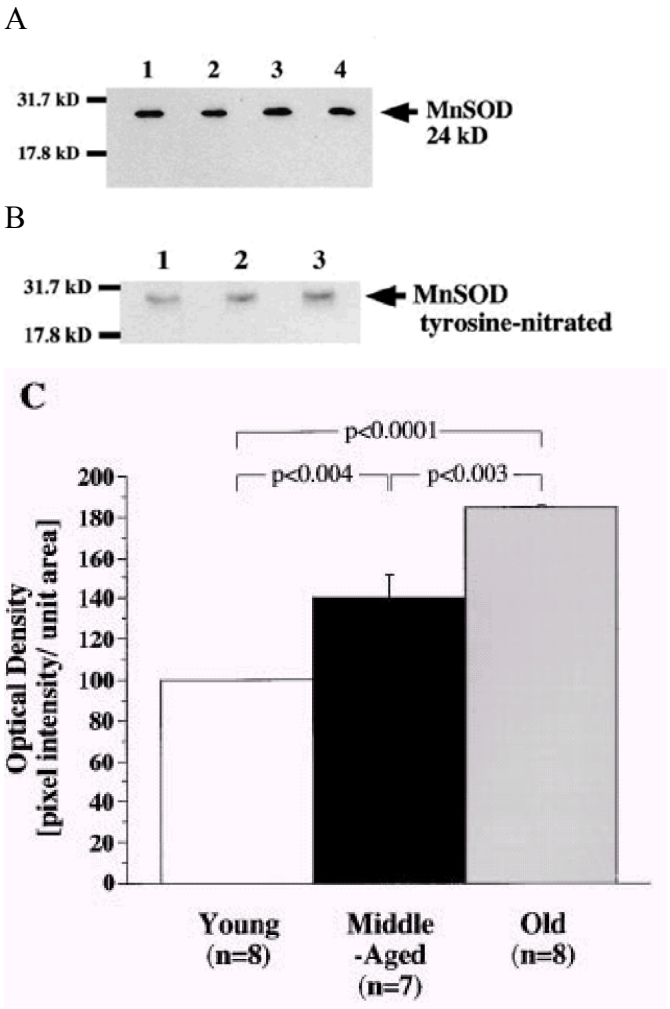

Figure 8.6
Total protein expression and age-associated increased nitration of mitochondrial MnSOD. Western blot of MnSOD (A) from young (lane 1), middle-aged (lane 2), and old (lane 3) aortas. Extracted proteins were separated on 15% SDS-PAGE gels and examined by Western blot with a polyclonal antibody against MnSOD. Recombinant MnSOD served as a positive control (lane 4). Molecular weight markers are indicated (in kD) on the left. (B) Nitrotyrosine-containing immunoprecipitated MnSOD from young (lane 1), middle-old (lane 2), and old (lane 3) rats were separated by 15% SDS-PAGE gels and analyzed by Western blot with a polyclonal antibody against nitrotyrosine. Films were exposed for 15 s to 3 min. (C) Quantitative analysis of tyrosine-nitrated MnSOD.

and inactivation of mitochondrial MnSOD had been reported (MacMillan-Crow et al., 1996). Therefore, it was considered important that the effect of aging on this mitochondrial enzyme was analyzed further. Surprisingly, immunoblot analysis of aortic homogenates from different age groups with polyclonal anti-MnSOD antibody revealed no significant change in enzyme expression (fig. 8.6 A). We then confirmed nitration of tyrosine residues in MnSOD by immunoblot analysis of MnSOD, which had been immunoprecipitated from aortic tissue with a polyclonal anti-MnSOD antibody. Indeed, immunodetection with polyclonal antiNT antibody showed increased levels of tyrosinenitrated MnSOD in old and middle-aged aortas compared with young ones (fig. 8.6 B). Densitometric analysis of the Western blots showed that nitration of MnSOD significantly increased with age in old aortic tissue (Fig. 8.6 C). To ensure that the same amounts of protein were loaded, a silver staining was performed before each Western blot analysis (not shown).

8.3 Discussion

This study provides new insights into the mechanisms of endothelial dysfunction that occur with age and offers a coherent picture of the underlying biochemical events. In agreement with previous reports, we found that detectable levels of NO were clearly reduced with age but, for the first time, we demonstrate that decreased NO production is a consequence neither of a reduced expression of the NO producing enzymes nor of a reduced activity in the l-arginine/ NO pathway, as both are sevenfold higher in aged compared with young aortas. As this was accompanied by a threefold higher activity in endothelial $^{\bullet}O_2^-$ production, the age-associated, decreased endothelial NO levels, and hence impaired vascular relaxation, must be a consequence of the known rapid reaction between the two radicals. The resulting formation of PN is confirmed by enhanced $^{\bullet}O_2^-$ vascular nitration. The conclusion that NO must be inactivated by is supported by three observations: (a) in the old aorta, reduced NO levels occur in the presence of increased eNOS expression and activity; (b) increased $^{\bullet}O_2^-$ levels with aging occur concomitantly with decreased NO levels; and (c) $^{\bullet}O_2^-$ rapidly reacts with NO to form PN, and this reaction is reflected by tyrosine nitration in proteins such as MnSOD.

Based on these new findings, we hypothesize an age related gradual change in a distinct network of different signals, including up- and/or down regulation which controls vascular function. Mitochondria and an increased one-electron oxidation of respiratory chain components may be involved in the initial reactions. As a consequence, the protective mechanisms that preserve endothelial function are dramatically “switched on” (i.e., upregulation of the eNOS enzyme system), but the balance between vascular protection and damage cannot be preserved, as it is in young animals. As the functional responses to the receptor-dependent and -independent endothelium-dependent vasodilators acetylcholine and A23187, respectively, were superimposable, age-associated endothelial dysfunction is not related to an alteration of the signal transduction pathway, but instead to reduced bioavailability of NO.

Paradoxically, both eNOS protein expression and l-arginine turnover were increased sevenfold in aortas from old animals. Previous work demonstrated a marginal increase in eNOS protein expression, but not activity, in the aorta of 20-month-old male Wistar rats (Cernades et al., 1998). The increase described here is much more dramatic and might be due to the considerably higher age of the animals used in this study and to our new technique for the isolation of vascular endothelium. In addition, we found that eNOS activity was similarly increased, demonstrating the functional integrity and in fact overactivity of the l-arginine/NO pathway even at extreme age.

This conclusion is further strengthened by the subcellular distribution of eNOS. Association of eNOS with the cell membrane determines the biological activity of the enzyme, and its location in caveolae may facilitate NO signaling to adjacent smooth muscle cells (Busconi and Michel, 1993). It is likely that the eNOS enzyme system is overactivated in aged blood vessels as a compensatory mechanism to counterbalance endothelial dysfunction induced by age-dependent oxidative stress. Another reason for increased eNOS expression might be hemodynamic forces such as shear stress, which have been shown to upregulate eNOS in vitro (Ranjan et al., 1995). However, neither blood pressure, heart rate, nor hematocrit value changed with age in these animals. In contrast to eNOS, there was no significant difference in both iNOS activity and expression between young and old animals, suggesting that iNOS does not contribute to the compensatory mechanism of NOS upregulation. The major and crucial finding of this study is the markedly increased $^{\bullet}O_2^-$ production (most of which was derived from the endothelium) with aging. The use of lucigenin to detect $^{\bullet}O_2^-$ in tissue has recently become a subject of controversy, as lucigenin may itself enhance $^{\bullet}O_2^-$ formation (Tarpey et al., 1999, Liochev and Fridovich, 1997). However, if autoxidation of lucigenin had in part contributed to $^{\bullet}O_2^-$ generation, this would have been applicable to the same extent to all age groups and would not affect the relative differences observed. The increased $^{\bullet}O_2^-$ production led to an inactivation of equimolar amounts of NO by the formation of PN, which, in turn, exhibits new messenger functions. The highest density of immunogold labeling for 3-nitrotyrosine was found in the mitochondria, in particular in those within the endothelium, indicating that nitration was dominant in these organelles and supporting their importance in the cascade of events contributing to the aging process. This may well have distinct pathophysiological consequences. Although we did not directly investigate mitochondria, it is reasonable to assume that mitochondria themselves may be a major source of $^{\bullet}O_2^-$ and PN in the aging vascular system (Beckman and Ames, 1998). Autoxidation of components of the respiratory chain would lead to the formation of $^{\bullet}O_2^-$, which is the one-electron reduction product of oxygen. Increased $^{\bullet}O_2^-$ production is unsuccessfully counter-balanced by the enhanced expression and activity of NO-synthesizing enzymes. At least in the chronic process of vascular aging, this directly involves eNOS but not iNOS, although in situations of acute oxidative stress, iNOS may also be induced (Crespo et al., 1999). PN nitrates an essential tyrosine residue in Mn-SOD with the participation of manganese catalysis. In fact, our results suggest that the nitration of tyrosine within Mn-SOD might be a mechanism leading to a significant reduction of its activity (Mac-Millan-Crow et al., 1998), and a possible further increase of $^{\bullet}O_2^-$formation. Nitration and dityrosine formation, both of which can easily be mediated by PN, are both required to completely inhibit MnSOD. However, a partial

inhibition of this crucial enzyme may also have important biological consequences (MacMillan-Crow, L.A., personal communication). MnSOD is the major antioxidant enzyme in the mitochondria of all mammals, and it is an endogenous nitration target in human renal allograft rejection (MacMillan-Crow et al., 1996). This study is the first to suggest that the degree of nitration of this enzyme may also be a molecular footprint of vascular aging. Proof for a pivotal role of MnSOD is provided by a recent report showing that genetic inactivation of Mn-SOD in mutant mice results in premature death (Melov et al., 1998), and that treatment with the SOD mimetic manganese–tetrakisbenzoic acid-porphyrin (MnTBAP) dramatically prolongs their survival. Manganese porphyrins also have a high capacity for the elimination of peroxynitrite (Lee et al., 1998). Our findings suggest that mitochondrial MnSOD may be a potentially important and novel drug target for the alleviation of vascular aging. It is of particular interest to the design of future therapeutic strategies to combat nitration-associated vascular aging to note that manganese porphyrins become even more efficient reductases for peroxynitrite when coupled with the biological antioxidants vitamin C, vitamin E, and glutathione, all of which serve as electron sources for the reduction of peroxynitrite (Lee et al., 1998). Although 3-nitrotyrosyl labeling would be in line with a mitochondrial source of $^{\bullet}O_2^-$, other sources, such as NADPH-oxidase (Channock et al., 1994), xanthin oxidase, or eNOS (Cosentino et al., 1998a) itself, also have to be considered as contributors to $^{\bullet}O_2^-$ and PN formation. eNOS, in the absence of cofactors such as tetrahydrobiopterin, or in case of insufficient substrate supply, will exhibit oxidase activity (Vasquez-Vivar et al., 1999). The dramatic increase in activity and expression of eNOS seen in the aged aorta may eventually not (or not only) be beneficial as an attempt by the organism to maintain endothelial function, but rather be detrimental, with eNOS becoming part of a redox system that increases electron transfer to oxygen. However, attempts to identify eNOS as the enzymatic source of $^{\bullet}O_2^-$ will be hampered by the fact that selective inhibitors of its oxidase activity are not available to date. It remains to be determined whether eNOS plays a more pathological or a more protective role in vascular aging. As eNOS expression and citrulline formation from l-arginine are dramatically increased with age, the diminished formation of free NO must be primarily a consequence of augmented $^{\bullet}O_2^-$ generation. The link between increased $^{\bullet}O_2^-$production and decreased NO release is stringent in view of the known chemistry, kinetics, and diffusion properties of both free radicals. This reaction is currently accepted as the main biological source of PN responsible for tyrosine nitration (Goldstein et al., 2000, Reiter et al., 2000). This would also be in agreement with our measurements of $^{\bullet}O_2^-$ and nitrated proteins. Future work will be concerned with the identification of nitrated PGIS, the only other enzyme for which nitration by reaction with PN

and subsequent inactivation has been reported (Zou and Bachschmid, 1999d), and which has been associated with endothelial dysfunction in atherosclerosis (Beckman et al., 1994) and ischemia-reperfusion damage (Liu et al., 1997). The analysis presented here sets the basis for future studies in the field of vascular aging, in particular for those aimed at preventing age-related vascular dysfunction. Based on the knowledge of the mechanisms involved in the aging process of the endothelium, which is crucial to maintain normal vascular function, strategies to prevent this process should be designed and tested. New therapeutic interventions to prevent vascular aging might have enormous medical consequences given the strong age dependency of cardiovascular diseases.

9 Vascular Aging and NAD(P)H-Oxidase

Contribution of coworkers to this work:

Prof. Dr. Lüscher (Coordination)
Bernd van der Loo (PKC activity measurement)

Prof. Dr. Ullrich (Supervisor)
Own contribution (Quantitative RT-PCR)

Bachschmid M, van der Loo B, Thurau S. Luscher T, Ullrich V. Oxidative stress-associated vascular aging is independent of the Protein Kinase C/ NAD(P)H oxidase pathway. Submitted to “Mechanisms in Aging and Development”.

9.1 Introduction

The strong correlation between age and the incidence of cardiovascular diseases, in the absence of other risk factors, suggests that aging per se alters vascular function. In agreement with the "oxidative stress hypothesis" of aging, a markedly increased $^{\bullet}O_2^-$ production followed by NO conversion to PN occurring with aging has been shown (van der Loo et al., 2000). However, the molecular mechanisms responsible for this age-dependent increased formation of $^{\bullet}O_2^-$ remain obscure. In the setting of other risk factors for the development of cardiovascular diseases, such as diabetes mellitus (Ishii et al., 1998), hypertension (Rajagopalan et al., 1996), and hypercholesterolemia (O' Hara et al., 1993) the PKC-/NAD(P)H oxidase pathway appears to be responsible for enhanced oxidative stress. Hink and coworkers (2001) have recently shown that in diabetes mellitus, PKC inhibition may restore endothelial function.
Endothelial NAD(P)H oxidase differs in terms of structure and biochemical activity from the phagocyte oxidase. It consists of membrane-bound (cytochrome b558, containing $p22^{phox}$ and gp91phox) as well as cytosolic components ($p40^{phox}$, $p47^{phox}$ and $p67^{phox}$) which assemble by transfer of the cytosolic components to the membrane, followed by association with cytochrome b558 to become fully active. PKC, after becoming activated itself by translocation from the cytosol to the

membrane (Hug and Sarre, 1993), is known to activate the NAD(P)H oxidase (Griendling et al., 2000), which, in turn, increases the production of $^{\bullet}O_2^-$ by a one electron reduction of molecular oxygen using NAD(P)H as the electron donor (Babior, 1999).

We wanted to investigate the hypothesis that an age-associated augmented PKC activity and hence increased assembly of components of the NAD(P)H oxidase may also be a molecular pathway for oxidative damage during the process of vascular aging.

9.2 Results

9.2.1 Age-associated increased vascular superoxide formation

Using the lucigenin-enhanced chemiluminescence assay, which, in the absence of added NADH, largely reflects $^{\bullet}O_2^-$ production, we found a 3-fold increase of basal - generated chemiluminescence in old aortas as compared with young and middle-aged ones (data not shown). In young and middle-aged aortas there is only a low, basal production of $^{\bullet}O_2^-$.

9.2.2 PKC activity

To assess the effect of aging on PKC activity we measured its phosphorylation activity in the cytosolic and in the membrane-rich subcellular fractions. The translocation of this enzyme from the cytosol to the membrane is considered as one of the hallmarks of PKC activation (Hug and Sarre, 1993). The levels of total PKC activity found in the cytosolic (fig. 9.1 A) and membrane fractions (fig. 9.1 B) of aortic tissue pooled from middle-aged and old animals did not significantly differ from those in young aortas. In particular, no age-dependent increased translocation from the cytosol to the plasma membrane could be observed.

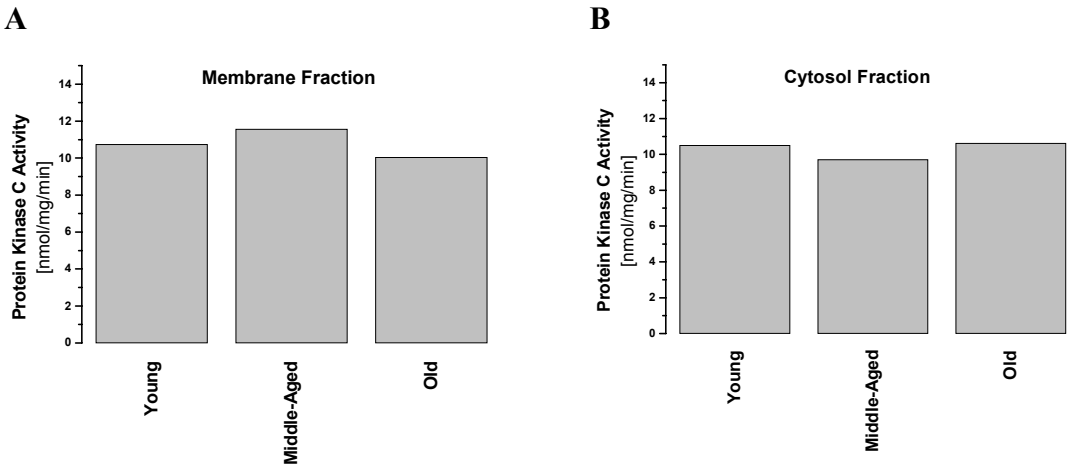

Figure 9.1
Bar graphs showing the effect of age on protein kinase C (PKC) activity in the particulate (A) and cytosolic (B) fraction. Age did not affect the PKC activity in fractionated homogenates from rat aorta. Data are mean of pooled tissue samples (n=6)

9.2.3 p47phox and p67phox detection and expression

NAD(P)H oxidase activity requires the assembly of $p47^{phox}$ and $p67^{phox}$, the latter of which is a limiting factor in enzyme activity. Therefore, $p47^{phox}$ and $p67^{phox}$ mRNA in rat aorta were amplified by RT-PCR, and a 123 bp ($p47^{phox}$) and a 137 bp ($p67^{phox}$) product were validated by size, melting point analysis with the light cycler and sequencing. Both semiquantitative (Fig. 9.2 A and 9.2 B) and quantitative (Fig. 9.2D) RT-PCR analysis revealed no statistically significant changes of $p47^{phox}$ (crossing points: Young = 26.9±0.18; Old = 27.54±0.64) and $p67^{phox}$ (Crossing points: Young = 33.05±0.6; Old = 32.28±1.1) expression with increasing age. Melting point analysis confirmed the high specificity of the amplified products (Fig. 9.2C).

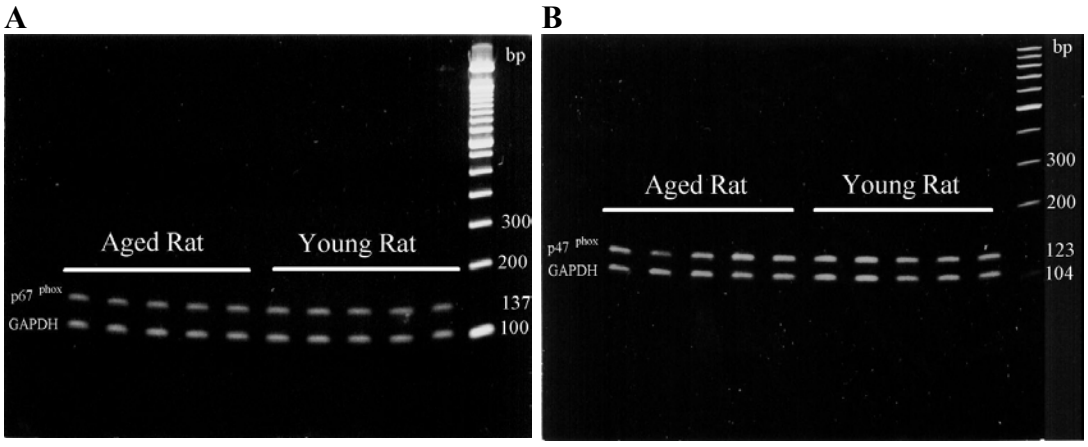

C

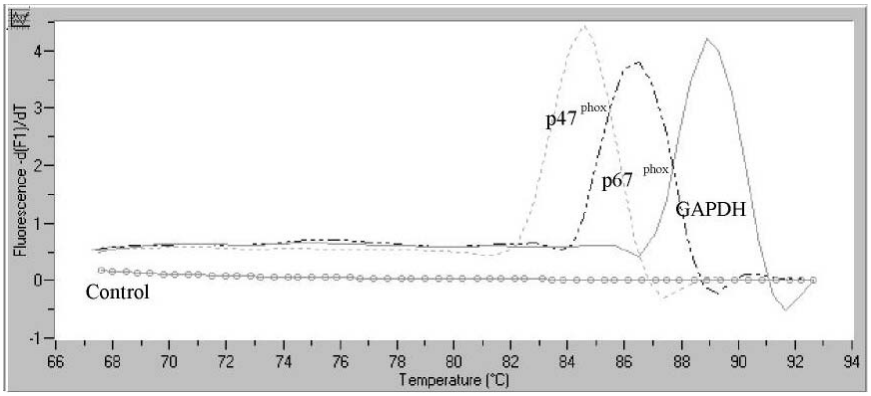

D

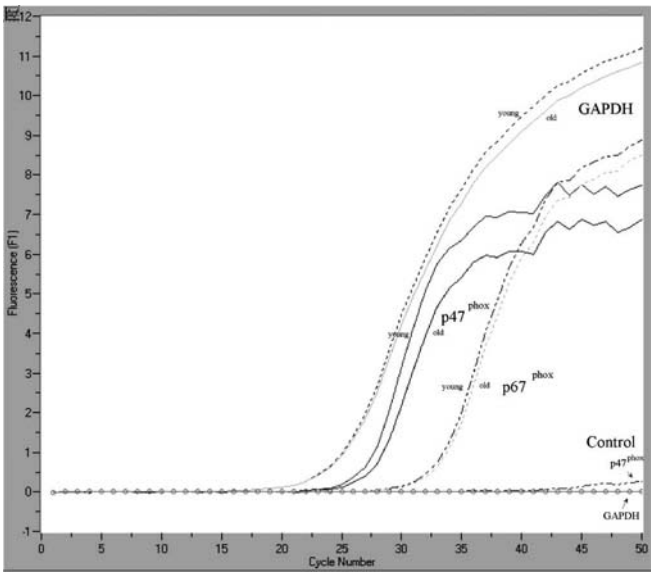

Figure 9.2
RT-PCR analysis of $p47^{phox}$ (**A**) and $p67^{phox}$ (**B**). 2 µg of total RNA were subjected to RT-PCR and then analyzed by TBE buffered polyacrylamide gel electrophoresis. Positions and sizes of the DNA markers (in base pairs) are shown.
Representative RT-PCR Light Cycler™ analysis of $p47^{phox}$, $p67^{phox}$ and GADPH in aortic homogenates from a young and an old rat performed with CYBR Green™ (**C**). Melting point analysis for specificity control of the amplified products (**D**).

9.3 Discussion

Our study was performed in 3-year-old rats, which do not exhibit hypertension, diabetes or atherosclerosis. It was initiated by the finding that aging results in a markedly increased vascular $^{\bullet}O_2^-$ production. PKC-mediated activation of the NAD(P)H-oxidase has been shown to be a major source for $^{\bullet}O_2^-$ in the pathophysiological setting of other known risk factors for the development of cardiovascular diseases (Cai and Harrison, 2000). However, in contrast to our expectations, translocation of PKC activity from the cytosol to the membrane was not increased as a function of age. Furthermore, $p47^{phox}$ and $p67^{phox}$, essential components of the NAD(P)H oxidase, remained unchanged with age. $p47^{phox}$ plays a crucial role

in vascular NAD(P)H oxidase activation (Li et al., 2002) as it regulates the electron transfer from FAD to cytochrom b558, eventually leading to $^{\bullet}O_2^-$ generation (Babior, 1999). Although it has been shown that $p47^{phox}$ alone is not absolutely necessary for NAD(P)H oxidase activation (Koshkin et al., 1996), $p67^{phox}$ is indispensable (Cross and Curnutte, 1995). Therefore, one may assume that our results largely reflect the status of NAD(P)H oxidase as a whole.

Recently, it has been shown that incubation of aortic vessels derived from 1-year-old rats with the NAD(P)H oxidase inhibitors DPI and apocynin resulted in a significant decrease in $^{\bullet}O_2^-$ production (Hamilton et al., 2001). However, those inhibitors are not specific for NAD(P)H oxidase and may also act on other oxidases.

We conclude that the major source of $^{\bullet}O_2^-$ in the setting of vascular aging originates from a different oxidase activity. Xanthine oxidase (Marczin et al., 1996), a malfunctioning endothelial NO synthase (Cosentino et al., 1998), or mitochondrial respiratory chain components (Beckman and Ames, 1998) are oxidase systems which may account for the age-associated enhanced production of $^{\bullet}O_2^-$ According to many reports on reactive oxygen species production with age, the primary source may be a modified electron transport chain in the mitochondria (Beckman and Ames, 1998). This assumption was indirectly supported by our finding of tyrosine-nitrated mitochondrial Mn-SOD in these aged rats (van der Loo et al., 2000), which suggests the formation of mitochondrial derived PN and hence probably mitochondrial $^{\bullet}O_2^-$ as a primary reactant. A more direct proof for the source of $^{\bullet}O_2^-$ remains a challenge for future research. However, an exact discrimination between these alternative oxidase activities is hampered by the lack of specific inhibitors (Wang et al., 1993).

We suggest that vascular aging is a distinct process well different from the pathophysiological situation seen in the context of other cardiovascular risk factors, where a decisive role for PKC-mediated activation of the NAD(P)H oxidase system has previously been described (Rajagopalan et al., 1996; O'Hara et al., 1993; Hink et al., 2001). Eventually understanding the mechanisms of vascular aging would elicit pharmacological efforts to interfere with this process and remains a challenge for future research.

10 General Discussion

This work was initiated by the observation that treatment with PN inhibits PGIS with a concomitant appearance of a protein band that positively reacts with an antibody against NT. This study has confirmed tyrosine nitration of PGIS as the underlying mechanism of enzyme inhibition and has provided evidence for a broad physiological and pathophysiological significance of this new posttranslational protein modification. Our results focus on superoxide as a messenger, which combines with NO to exert tyrosine nitration. It turned out that the important process of endothelial activation is primarily based on superoxide generation, which can be mediated by xanthine oxidase (endotoxin), NADPH-oxidase (hyperglycemia/ diabetes), mitochondria (aging) or NO-synthase - oxidase (still under debate, e.g. aging). The results of this study are discussed under the aspects of

chemistry and biochemistry of PGIS nitration
superoxide as a messenger and
endothelial cell activation type I

10.1 Nitration of PGIS

Prerequisite of this study was the development of a method for the reliable and sensitive detection of both NT and nitrated PGIS. Two different methods have been established: The immunoprecipitation of nitrated proteins, followed by Western blotting and immunostaining of PGIS and the total hydrolysis of microsomes and homogenates followed by HPLC analysis. Both methods revealed the unusually high stability of the enzyme towards digestion and unfolding.

Only chemically based methods allow a real quantification and identification of NT. Antibodies directed against small epitopes such as the nitro group can lead to unwanted cross-reactivities, thus leading to false positive results. HPLC analysis in connection with UV/VIS- and electrochemical detection provides a sensitive and specific method. Commonly applied acidic hydrolysis was inappropriate, since under acidic pH, even traces of nitrite lead to artefactual nitration (Frost et al., 2000). Therefore, total digestion with pronase was used and revealed an unusual high

resistance of the core protein. Only after 72h, the digestion was almost complete. The disadvantage of this procedure was the high accumulation of amino acids from the self-digested proteases, which had to be supplemented at several times. This led to loss of sensitivity in HPLC analysis. To overcome this problem, alkaline hydrolysis was applied. Shorter incubation times for complete hydrolysis were required and after this improvement of the experimental conditions the sensitivity was well suited for biological samples. Optical absorbance at 362 nm and the electrochemical potential of 800 mV confirmed the NT specificity. NT -analysis of microsomes correlated well with the applied PN concentrations and the amount of nitrated PCS detected by immunoblotting. Also samples of LPS treated bovine coronary arteries yielded higher concentrations of NT, compared to controls. However, this was not yet a sufficient proof for a nitration of PGIS and another method was required.

Immunoprecipitation of nitrated proteins with a monoclonal antibody serves as a very sensitive detection method, but specificity should be confirmed independently. When the antibody was blocked with either nitrated peptides or nitrotyrosine the antibody reactivity as well as the reduction of the nitro-group with Na-dithionite to aminotyrosine were abolished,. Treatment with “soft” reducing agents like ß-mercaptoethanol or DTT had no effect on nitrotyrosine formation as established by HPLC analysis. Further observations demonstrated that protein denaturation was essential for NT epitope presentation and antibody binding. The stripping procedure of blot membranes always increased sensitivity and specificity of the anti NT antibody. Therefore, a denaturating immunoprecipitation method using high stringent buffers and heat denaturation of the antigen gave reproducible results. The IP was dependent on the concentration of PN and the amount of protein. Sensitive and reliable detection of nitrated PGIS was achieved in vascular tissue homogenates or lysed endothelial cells. The precipitates were further digested by trypsin, and the resulting peptides were identified by MALDI-TOF-MS. This often resulted in a poor yield of the sequence recovery analysis, best explained by the high proteolytic stability of the enzyme (approx. up to 50% at best per experiment of the expected peptide yield). using this technique , The exact positioning of the nitro-group was impossible, since the high laser energy and the matrix molecules yield extensive fragmentation of nitrated peptides. Nevertheless, the specificity of the IP for nitrated PGIS was confirmed. This powerful method revealed that PGIS is already nitrated at

submicromolar concentrations of either exogenously or endogeously generated PN and paralleled decreased plasma levels of 6-keto-$PGF_{1\alpha}$. In Several models, such as hypoxia-reoxygenation, hyperglycemia and endotoxemia altered levels of nitrated PGIS were demonstrated. Thus, this work gives a reference for PGIS nitration in the endothelium and its participation in physiologically relevant signaling processes as a target enzyme in the redoxregulation of the vessel system. Next to the oxidation of thiols or methionine residues the nitration of tyrosine in PGIS can be considered as a new pathway in redox regulation.

10.2 Superoxide as a Messenger

As a consequence of the definite establishment of tyrosine nitration in PGIS as a regulatory mechanism one has to conclude that the triggering event for this regulation is the generation of $^{\bullet}O_2^-$ in conjunction with NO. This new concept seems controversial at first glance since, to date, $^{\bullet}O_2^-$ has been claimed as an ubiquitous reactive oxygen intermediate which is generated during many redox processes in the cell. However, the presence of high concentrations of $^{\bullet}O_2^-$ in cells, in mitochondria and even extracellularly makes it necessary to have strictly controlled $^{\bullet}O_2^-$ levels which may range as low as 10^{-10} mol/l under normal conditions. Therefore, on top of these resting levels, certain enzymes would be able to provide elevated levels of $^{\bullet}O_2^-$ which then may be responsible for selective actions of the radical.

The low chemical reactivity of $^{\bullet}O_2^-$ hardly allows oxidative modifications of biological molecules. Upon reaction with NO, however, the resulting PN represents a very reactive molecule and therefore PN would act as a potent mediator of oxidative modifications such as sulfhydryl groups oxidation or tyrosine nitration. In the case of PGIS the high specificity for this process also involves a compartmental component since the production of NO occurs in the near neighbourhood of PGIS for which a localisation in the caveolae has been shown. If a source of $^{\bullet}O_2^-$ in the same environment existed the resulting local concentrations of PN could be sufficiently high and would therefore add specificity to the process of nitration. It should be mentioned that PN is also a candidate for the conversion of methionine to methionine

sulfoxide and for the oxidation of zinc finger proteins (Daiber et al., 2002) so that the nitration of tyrosine is only one of three reactions performed by peroxynitrite.

In search of potential sources for $^{\bullet}O_2^-$ one has to consider at first the many reports showing NADPH oxidase as an important enzyme in leukocytes which also has been found in various isoforms in other cells like fibroblasts or smooth muscle. It has also been associated with the activation of the angiotensin-II receptor in the endothelium. Another source is xanthine oxidase which has been known since a long time but has always been considered as a degradation product of xanthine dehydrogenase. This enzyme can be converted to its oxidase form either by thiol oxidation or proteolytic attack (Harrison, 1997b). Xanthine oxidase may also be attached to the endothelial membrane after release from liver and transport in the blood stream (White et al., 1996; Radi et al., 1997). $^{\bullet}O_2^-$ formation requires the presence of xanthine or hypoxanthine as hydrogen donors, which, under pathophysiological conditions, can be provided from ATP breakdown in quite high concentrations. Under those conditions mitochondria would be damaged and the respiratory chain would be able to transfer electrons to oxygen, thereby giving rise to $^{\bullet}O_2^-$. This has been found under several pathophysiological conditions involving damaged mitochondria. Finally the discovery of NO synthase as an oxidase has provided a new pathway for $^{\bullet}O_2^-$ generation. This seems to require an oxidative modification of NO synthase since an oxidative release of zinc under monomerisation of the enzyme would generate the oxidase form (Zou et al., 2002a; Xia et al., 1998). Thus there are four mechanisms known to date which could provide superoxide anions in a defined way and in quantities sufficient for PN formation when NO production has been increased in the presence of calcium or the MAP38 kinase phosphorylation cascade. The model of LPS -treated coronary segments suggests that xanthine oxidase is a major $^{\bullet}O_2^-$ -generating system. Allopurinol can be used as a selective inhibitor but more work is required to identify the exact role of xanthine oxidase in this process. One definitely can rule out other reactive oxygen species since the involvement of PN is clearly indicated by the inhibitory effect of added Cu/Zn-SOD. To prove the involvement of $^{\bullet}O_2^-$ this is still the most specific tool. Thus for our present investigations the fluorescent and luminescent probes for $^{\bullet}O_2^-$ like lucigenin, coelenteracine or L0-12 have been used in association with the inhibitory action of SOD. For future work it will be important to identify the primary source of $^{\bullet}O_2^-$ since one can imagine situations in which a

primary source is followed by the activation of secondary and even third mechanisms of $^{\bullet}O_2^-$ formation. The latter would apply for xanthine dehydrogenase or NO synthase which can be converted by oxidation to their oxidase forms. Mitochondria could also get oxidized at critical SH groups of the permeability transition pore and then could join the $^{\bullet}O_2^-$ burst as a very powerful generator of this species. In summary our results indicate that $^{\bullet}O_2^-$ in conjunction with NO forms PN as the highly reactive oxidant of $^{\bullet}O_2^-$ in cellular systems. The recent discovery in our laboratory that $^{\bullet}O_2^-$ can inhibit calcineurin by oxidation of its ferrous active form represents a second mechanism how a peroxide intermediate is generated by electron transfer to $^{\bullet}O_2$. This then possesses enough oxidizing energy to change the structure of macromolecules as a signal transduction mechanism.

10.3 Endothelial Cell Activation Type I

This thesis work demonstrates that activation of different sources of $^{\bullet}O_2^-$ leads to the same effects on the vessel tone and vascular homeostasis as by inhibition of PGI_2-synthesis. This is the most important result of this work, since it describes a detailed and cohered elucidation of how free radicals can modulate endothelial cell activity. Elevated $^{\bullet}O_2^-$ levels lead to a complete inversion of the endothelial properties, without induction of any gene or expression of new protein. This conversion is typically finished in less then 1h. Many reports and hypotheses deal with such findings, but they never gave an exact molecular explanation. The use of Different terms is also misleading like endothelial dysfunction, priming or stunning. Actually, all effects are based on the activation of the endothelium and ,as an appropriated term, “endothelial cell activation” (ECA) should be used. Two types where described in literature, but the aim of this study was to concentrate on the initiation of ECA, which is also called ECA Type I. This phase is characterized by endothelial cell retraction from each other, expression of P-selectin and the release of von Willebrand factor. Such events are independent of *de novo* protein synthesis and are essentially completed within 1 h. A second stage (ECA Type II) becomes apparent after about one hour and involves induction and expression of early genes like the adhesion molecules ICAM or VCAM, proinflammatory cytokines and regulatory enzymes like NOS-2 and COX-2. As a consequence white cells can tightly adhere and emigrate into tissues, NO and

prostaglandins are formed in excess and cytokines may modulate the further inflammatory response. This type has already been well characterized previously and was not in the focus of this study.

The following scheme summarizes and explains the signalling pathways:

1. Physiological Situation

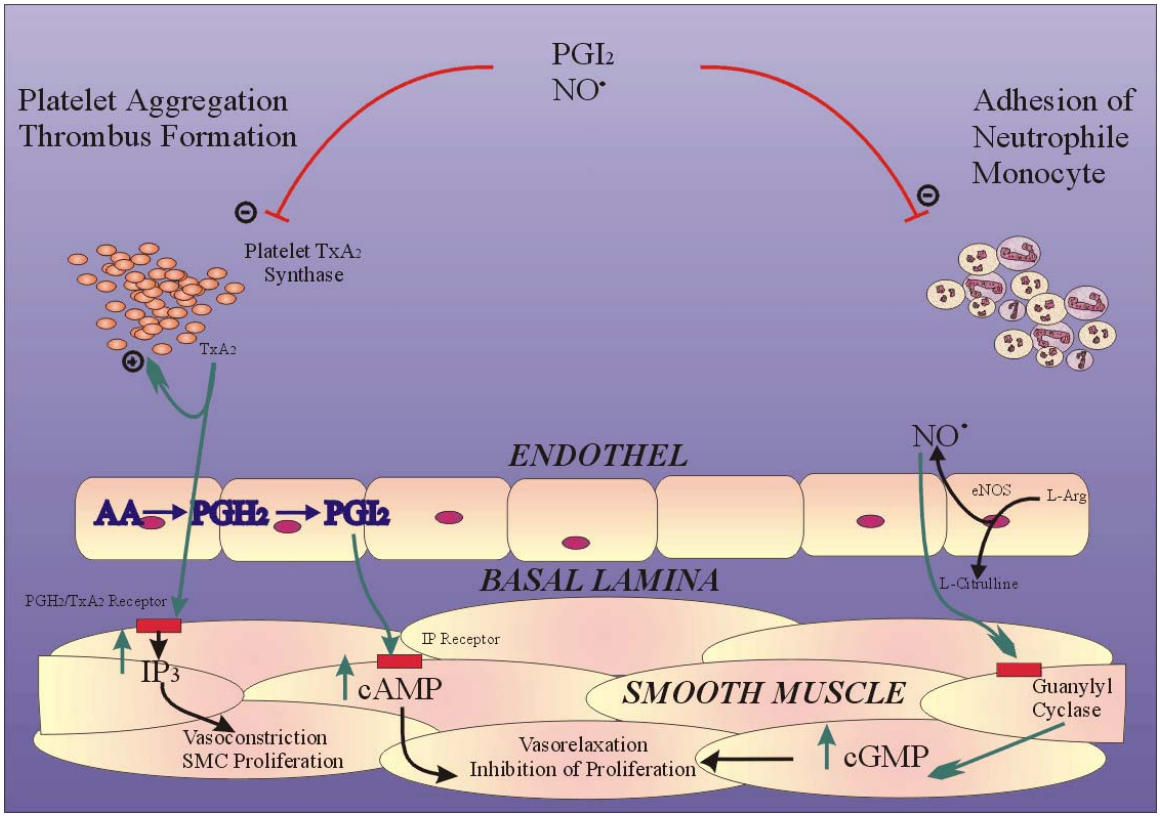

2. Pathohysiological Situation

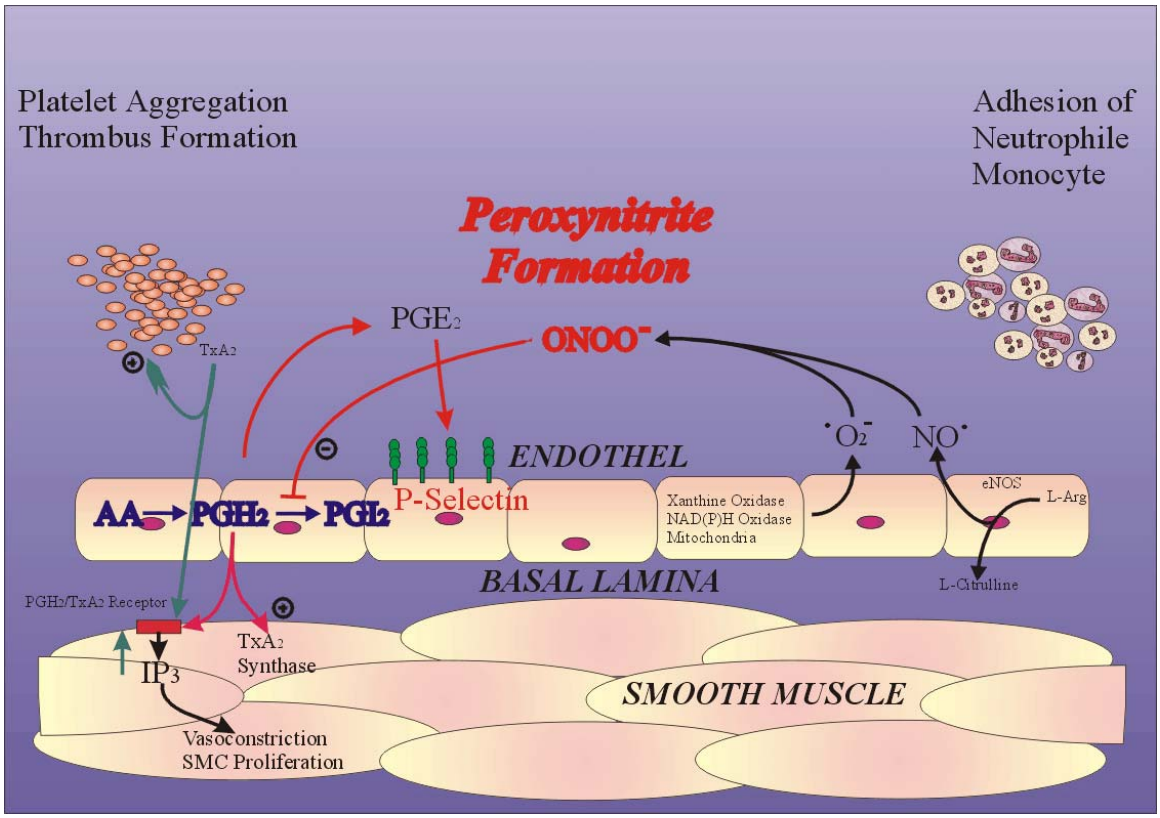

If physiological conditions start to change, i. e. in the context of local invasion of pathogens, reduced oxygen supply, high glucose etc., corresponding $^{\bullet}O_2^-$ sources are activated. The study demonstrates, for endotoxemia that a further agonist like Ang II or bradykinin is required to trigger a parallel generation of NO to form PN.

Two effects will now change the balance of endothelium-derived relaxing factors. The first and most obvious effect is the trapping of NO, neutralizing its biological activity. The second effect concerns the newly formed PN, which nitrates PGIS at already very low concentrations. This reaction involves the catalysis by an active -site located heme–thiolate complex (P450). Otherwise millimolar concentrations of PN are required for tyrosine nitration. Nitration at the Y430 near the active site may hamper the substrate access to the heme, thus reducing the amount of synthesized PGI_2.

Constitutive COX converts free arachidonic acid in a two step reaction to PGH_2, which serves as substrate for the enzymes of the prostaglandin metabolism. The capacity of COX-1 remains unchanged and thus PGH_2 accumulates. This molecule acts on the TxA_2/PGH_2 receptor leading to smooth muscle contraction and platelet

activation. Since PGH_2 is an unstable metabolite, being converted to PGE_2, and thus triggering the expression of P-selectin.

This model gives a satisfactory explanation how the single messenger molecule $^{\bullet}O_2^-$ changes vascular homeostasis, by guiding and completing the endothelial cell activation type I. According to our results one can describe ECA type I as a shift of the relaxing factors NO and PGI_2 to PGH_2 as a potent vasoconstricting messenger.

11 Outlook

Biological regulation obeys the classical Yin-Yang principle, which is also reflected in the modern laws of cybernetics. Phosphorylation-dephosphorylation is the best example of a reversible protein modification by which many biological pathways are controlled and embedded in regulatory networks.

Redox reactions emerge as a possible second mechanism, in which oxidation of thiols or methionines to disulfides or sulfoxides can modify enzyme activities in one way and reduction restores the original activity. Nitrotyrosine formation as shown for PGI_2-synthase could be established as an oxidative reaction leading to inhibition, but the reversal has not yet been observed. We hypothesize that, in the case of the prostacyclin synthase, such a mechanism involving a nitroreductase may also exist. Unpublished observations provide a first hint for the reactivation of PGIS in physiology. After some hours PGI_2 levels were restored in endothelial cell culture, although the half lifetime of PGIS is over twenty four hours and mRNA- as well as protein levels remained unchanged. This suggests the "reactivation" of the enzyme by a mechanism apparently independent of a *de novo* synthesis of the enzyme. First reports for such a concept came from the laboratory of Murad (Kamisaki et al., 1998). He discovered that the nitration of BSA was reduced after incubation of the protein together with NADPH and spleen homogenate from endotoxin treated rats. The new putative enzyme was termed "nitrotyrosine denitrase". In contrast nitrated proteins can be also rapidly degraded by the proteasome pathway (Souza et al., 2000), which seems not to be the case for PGIS.

Since P450 enzymes are generally associated with a reductase, such an activity could be involved in the reduction of nitrotyrosine. This process would require redox-equivalents from NADPH, as it was demonstrated by the experiments of Murad and coworkers. In the case of PGIS a possible associated reductase is still unknown. However, any two-electron transfer could generate the nitroso-derivative which, in direct neighborhood of a phenolic group, is known to migrate to form R-O-N=O which then hydrolyses to nitrite and the starting phenol. This putative reduction/migration and splitting could then also constitute a complete cycle of redoxregulation for the nitration of tyrosine. In order for tyrosine nitration in PGIS becoming generally accepted as a reversible postranslational modification, this mechanism we here propose has to be investigated in future work. This then would perfectly fulfill the cybernetic laws and serve as an impressive model of redox-regulation and modulation of endothelial properties.

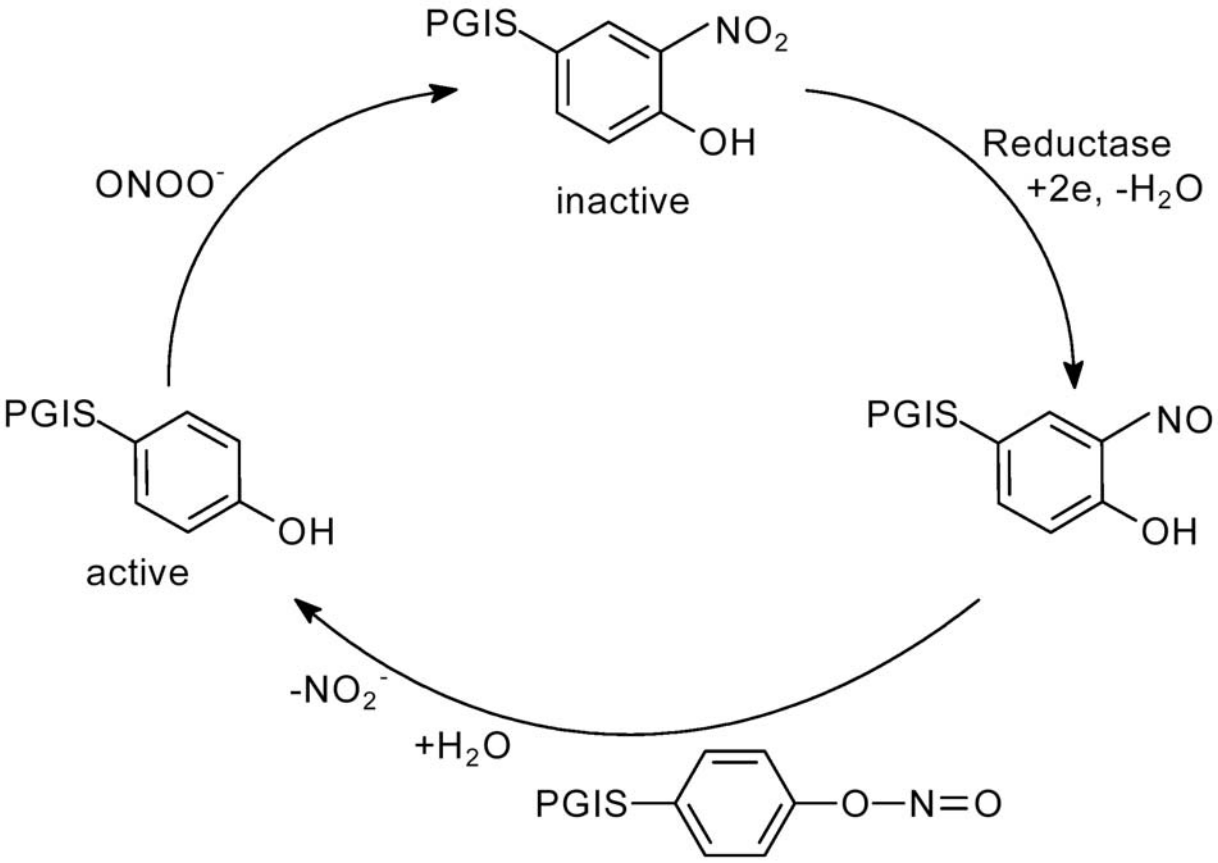
PGIS
NO2
OH
inactive
Reductase
+2e, -H2O
PGIS
NO
OH
PGIS
OH
active
ONOO-
-NO2-
+H2O
PGIS
O—N=O

12 Zusammenfassung

Diese Arbeit wurde durch die Beobachtung initiiert, dass sich die Prostacyclin Synthase durch Peroxynitrit hemmen läst und mit dem Auftreten einer Nitrierung einhergeht. Die vorliegende Studie bestätigt die Tyrosin-Nitrierung der Prostacyclin Synthase als zugrundeliegenden Mechanismus für die Enzymhemmung und liefert zahlreiche Hinweise für die physiologische und pathophysiologische Bedeutung als posttranslationale Modifikation. Unsere Befunde konzentrieren sich auf die Signalmolekülfunktion von Superoxid, welches nach der Kombination mit NO zur Nitrierung von speziell exponierten Tyrosinen führt. Es stellte sich heraus, dass der Prozess der endothelialen Aktivierung hauptsächlich auf der Bildung von Superoxid beruht, welches von der Xanthin-Oxidase (Entzündung), NADPH-Oxidase (Hyperglykämie/ Diabetes), den Mitochondrien (Alterung) oder der NO-Synthase-Oxidase (wird für die Alterung noch debattiert) stammt. Die Resultate dieser Studie wurden diskutiert unter dem Aspekt der:

1. Chemie und Biochemie der Tyrosin-Nitrierung in der Prostacyclin-Synthase (PGIS)
2. Bedeutung von Superoxid als Signalmolekül
3. Rolle von Peroxynitrite bei der endothelialen Zellaktivierung

Die wichtigsten Ergebnisse sind im Folgenden zusammengefasst:

1. Nitrierung der Prostacyclin Synthase

    - Für diese Studie wurden zwei zuverlässige und empfindliche Methoden für den Nachweis der PGIS-Nitrierung und Nitrierung im allgemeinen etabliert. Zum einen die Immunoprezipitation der nitrierten PGIS und zum anderen die Totalhydrolyse von Homogenaten mit nachfolgender HPLC-Analyse.
    - Beide Methoden in Verbindung mit MALDI-TOF Massenspektroskopie, bestätigten die durch Peroxynitrit hervorgerufene Nitrierung der PGIS.

- Die angewandte Methodik bestätigte eine hohe Stabilität der PGIS gegenüber proteolytischer Zersetzung und Denaturierung.
- Erhöhte Nitrierung der PGIS konnte in einigen Modelsystemen, wie zum Beispiel Hypoxie-Reoxygenierung, Hyperglykämie und Endotoxämie nachgewiesen werden.

2. Superoxid als Signalmolekül
    - Unsere Resultate zeigen, dass Superoxid in Verbindung mit NO Peroxynitrit bildet, welches als höchst reaktive Form des Superoxid-Radikals in zellulären Systemen fungiert.
    - Im frühen Stadium der Entzündung in bovinen Koronargefäßen, konnte die Xanthin-Oxidase als maßgebliche Superoxid-Quelle identifiziert werden.
    - Am Alterungsprozess der Blutgefäße sind die Mitochondrien ein entscheidender Bildungsort für Superoxid, zum Teil bedingt durch die Reduktion von funktioneller Mn-SOD.
    - Die Superoxid-Generierung in der Hyperglykämie/ Diabetes wird durch die Induktion der NADPH-Oxidase und über ihre Aktivierung durch die Protein Kinase C verursacht.

3. Die Aktivierung der Endothelzelle - Typ I
    - Diese Arbeit belegt, dass verschiedene endogene Superoxid-Quellen zur 1. Phase in der Endothelzellaktivierung führen können und damit die Funktion des Endothels modulieren.
    - Erhöhte vaskuläre Superoxid-Spiegel invertieren innerhalb einer Stunde die endothelialen Eigenschaften, ohne dabei die Gen- bzw. Proteinexpression zu verändern.
    - Die gesteigerte Superoxid-Freisetzung führt nach der Reaktion mit NO zur gesteigerten Peroxynitrit Bildung, welches die PGIS nitriert und inaktiviert. Dadurch werden die zwei wichtigen Signalmoleküle NO und PGI_2, die zum Erhalt der vaskulären Homöostase unerlässlich sind,

stark reduziert. Im Gegenzug akkumuliert das Substrat der PGIS, Prostaglandin Endoperoxid H_2, welches vasokonstriktorische Eigenschaften über seine Aktivierung des TP-Rezeptors besitzt. Dadurch wird das Gleichgewicht der endothelialen Mediatoren zugunsten der Vasokonstriktion verschoben.

13 References

Azhar, S.; Cao, L. and Reaven, E. Alteration of the adrenal antioxidant defense system during aging in rats. *J. Clin. Invest* 96: 1414-1424; 1995

Babior, B.M. NADPH oxidase: an update. *Blood* 93: 1464-1476; 1999

Bauer, S.H.; Wiechers, M.F.; Bruns, K.; Przybylski, M. and Stuermer, C.A. Isolation and identification of the plasma membrane-associated intracellular protein reggie-2 from goldfish brain by chromatography and Fourier-transform ion cyclotron resonance mass spectrometry. *Anal. Biochem.* 298: 25-31; 2001

Baynes, J.W. Role of oxidative stress in development of complications in diabetes. *Diabetes* 40: 405-412; 1991

Beckman, J.S.; Minor, R.L., Jr.; White, C.W.; Repine, J.E.; Rosen, G.M. and Freeman, B.A. Superoxide dismutase and catalase conjugated to polyethylene glycol increases endothelial enzyme activity and oxidant resistance. *J Biol. Chem.* 263: 6884-6892; 1988

Beckman, J.S.; Beckman, T.W.; Chen, J.; Marshall, P.A. and Freeman, B.A. Apparent hydroxyl radical production by peroxynitrite: implications for endothelial injury from nitric oxide and superoxide. *Proc. Natl. Acad. Sci. U. S. A* 87: 1620-1624; 1990

Beckman, J.S.; Ischiropoulos, H.; Zhu, L.; van der, W.M.; Smith, C.; Chen, J.; Harrison, J.; Martin, J.C. and Tsai, M. Kinetics of superoxide dismutase- and iron-catalyzed nitration of phenolics by peroxynitrite. *Arch. Biochem. Biophys.* 298: 438-445; 1992

Beckman, J.S.; Carson, M.; Smith, C.D. and Koppenol, W.H. ALS, SOD and peroxynitrite. *Nature* 364: 584; 1993

Beckman, J.S.; Ye, Y.Z.; Anderson, P.G.; Chen, J.; Accavitti, M.A.; Tarpey, M.M. and White, C.R. Extensive nitration of protein tyrosines in human atherosclerosis detected by immunohistochemistry. *Biol. Chem. Hoppe-Seyler* 375: 81-88; 1994

Beckman, J.S. and Koppenol, W.H. Nitric oxide, superoxide, and peroxynitrite: the good, the bad, and ugly. *Am. J. Physiol* 271: C1424-C1437; 1996

Beckman, K.B. and Ames, B.N. Mitochondrial aging: open questions. *Ann. N. Y. Acad. Sci.* 854: 118-127; 1998

Benninghoff, A. Anatomie. Drenckhahn, D., Zenker, W. (Eds.). *Urban & Schwarzenberg* 15th ed.: 652-685; 1994

Bhagat, K.; Moss, R.; Collier, J. and Vallance, P. Endothelial "stunning" following a brief exposure to endotoxin: a mechanism to link infection and infarction? *Cardiovasc. Res.* 32: 822-829; 1996

Bhagat, K. and Vallance, P. Inflammatory cytokines impair endothelium-dependent dilatation in human veins in vivo. *Circulation* 96: 3042-3047; 1997

Boneberg, E.M.; Zou, M.H. and Ullrich, V. Inhibition of cyclooxygenase-1 and -2 by R(-)- and S(+)-ibuprofen. *J. Clin. Pharmacol.* 36: 16S-19S; 1996

Boyle, W.J.; Smeal, T.; Defize, L.H.; Angel, P.; Woodgett, J.R.; Karin, M. and Hunter, T. Activation of protein kinase C decreases phosphorylation of c-Jun at sites that negatively regulate its DNA-binding activity. *Cell* 64: 573-584; 1991

Brandes, R.P.; Barton, M.; Philippens, K.M.; Schweitzer, G. and Mugge, A. Endothelial-derived superoxide anions in pig coronary arteries: evidence from lucigenin chemiluminescence and histochemical techniques. *J. Physiol* 500 (Pt 2): 331-342; 1997

Brandes, R.P.; Koddenberg, G.; Gwinner, W.; Kim, D.; Kruse, H.J.; Busse, R. and Mugge, A. Role of increased production of superoxide anions by NAD(P)H oxidase and xanthine oxidase in prolonged endotoxemia. *Hypertension* 33: 1243-1249; 1999

Bredeweg, R.A.; Rothman, L.D. and Pfeiffer, C.D. Chemical reactivation of silica columns. *Anal. Chem.* 51: 2061-2063; 1979

Brennan, M.L.; Wu, W.; Fu, X.; Shen, Z.; Song, W.; Frost, H.; Vadseth, C.; Narine, L.; Lenkiewicz, E.; Borchers, M.T.; Lusis, A.J.; Lee, J.J.; Lee, N.A.; Abu-Soud, H.M.; Ischiropoulos, H. and Hazen, S.L. A tale of two controversies: defining both the role of peroxidases in nitrotyrosine formation in vivo using eosinophil peroxidase and myeloperoxidase-deficient mice, and the nature of peroxidase-generated reactive nitrogen species. *J. Biol. Chem.* 277: 17415-17427; 2002

Brown, G.C. Regulation of mitochondrial respiration by nitric oxide inhibition of cytochrome c oxidase. *Biochim. Biophys. Acta* 1504: 46-57; 2001

Brownlee, M. Advanced protein glycosylation in diabetes and aging. *Annu. Rev. Med.* **46:** 223-234; 1995

Brune, B.; Schmidt, K.U. and Ullrich, V. Activation of soluble guanylate cyclase by carbon monoxide and inhibition by superoxide anion. *Eur. J Biochem.* 192: 683-688; 1990

Busconi, L. and Michel, T. Endothelial nitric oxide synthase. N-terminal myristoylation determines subcellular localization. *J. Biol. Chem.* 268: 8410-8413; 1993

Cai, H. and Harrison, D.G. Endothelial dysfunction in cardiovascular diseases: the role of oxidant stress. *Circ. Res.* 87: 840-844; 2000

Cernadas, M.R.; Sanchez, d.M.; Garcia-Duran, M.; Gonzalez-Fernandez, F.; Millas, I.; Monton, M.; Rodrigo, J.; Rico, L.; Fernandez, P.; de Frutos, T.; Rodriguez-Feo, J.A.; Guerra, J.; Caramelo, C.; Casado, S. and Lopez, F. Expression of constitutive and inducible nitric oxide synthases in the vascular wall of young and aging rats. *Circ. Res.* 83: 279-286; 1998

Challah, M.; Nadaud, S.; Philippe, M.; Battle, T.; Soubrier, F.; Corman, B. and Michel, J.B. Circulating and cellular markers of endothelial dysfunction with aging in rats. *Am. J. Physiol* 273: H1941-H1948; 1997

Chanock, S.J.; El Benna, J.; Smith, R.M. and Babior, B.M. The respiratory burst oxidase. *J. Biol. Chem.* 269: 24519-24522; 1994

Chen, W.; Pawelek, T.R. and Kulmacz, R.J. Hydroperoxide dependence and cooperative cyclooxygenase kinetics in prostaglandin H synthase-1 and -2. *J Biol. Chem.* 274: 20301-20306; 1999

Cheng, G.; Cao, Z.; Xu, X.; van Meir, E.G. and Lambeth, J.D. Homologs of gp91phox: cloning and tissue expression of Nox3, Nox4, and Nox5. *Gene* 269: 131-140; 2001

Cines, D.B.; Pollak, E.S.; Buck, C.A.; Loscalzo, J.; Zimmerman, G.A.; McEver, R.P.; Pober, J.S.; Wick, T.M.; Konkle, B.A.; Schwartz, B.S.; Barnathan, E.S.; McCrae, K.R.; Hug, B.A.; Schmidt, A.M. and Stern, D.M. Endothelial cells in physiology and in the pathophysiology of vascular disorders. *Blood* 91: 3527-3561; 1998

Cosentino, F.; Patton, S.; d'Uscio, L.V.; Werner, E.R.; Werner-Felmayer, G.; Moreau, P.; Malinski, T. and Luscher, T.F. Tetrahydrobiopterin alters superoxide and nitric oxide release in prehypertensive rats. *J Clin. Invest* 101: 1530-1537; 1998

Cosentino, F. and Luscher, T.F. Endothelial dysfunction in diabetes mellitus. *J. Cardiovasc. Pharmacol.* 32 Suppl 3: S54-S61; 1998

Crespo, E.; Macias, M.; Pozo, D.; Escames, G.; Martin, M.; Vives, F.; Guerrero, J.M. and Acuna-Castroviejo, D. Melatonin inhibits expression of the inducible NO synthase II in liver and lung and prevents endotoxemia in lipopolysaccharide-induced multiple organ dysfunction syndrome in rats. *FASEB J.* 13: 1537-1546; 1999

Cross, A.R. and Curnutte, J.T. The cytosolic activating factors p47phox and p67phox have distinct roles in the regulation of electron flow in NADPH oxidase. *J. Biol. Chem.* 270: 6543-6548; 1995

Crow, J.P. and Beckman, J.S. Reactions between nitric oxide, superoxide, and peroxynitrite: footprints of peroxynitrite in vivo. *Adv. Pharmacol.* 34: 17-43; 1995

Daiber, A.; Zou, M.H.; Bachschmid, M. and Ullrich, V. Ebselen as a peroxynitrite scavenger in vitro and ex vivo. *Biochem. Pharmacol.* 59: 153-160; 2000a

Daiber, A.; Herold, S.; Schoneich, C.; Namgaladze, D.; Peterson, J.A. and Ullrich, V. Nitration and inactivation of cytochrome P450BM-3 by peroxynitrite. Stopped-flow measurements prove ferryl intermediates. *Eur. J. Biochem.* 267: 6729-6739; 2000b

Daiber, A.; Schoneich, C.; Schmidt, P.; Jung, C. and Ullrich, V. Autocatalytic nitration of P450CAM by peroxynitrite. *J. Inorg. Biochem.* 81: 213-220; 2000c

Daiber, A.; Frein, D.; Namgaladze, D. and Ullrich, V. Oxidation and nitrosation in the nitrogen monoxide/superoxide system. *J Biol. Chem.* 277: 11882-11888; 2002

Darley-Usmar, V.M.; Hogg, N.; O'Leary, V.J.; Wilson, M.T. and Moncada, S. The simultaneous generation of superoxide and nitric oxide can initiate lipid peroxidation in human low density lipoprotein. *Free Radic. Res. Commun.* 17: 9-20; 1992

DeRubertis, F.R. and Craven, P.A. Activation of protein kinase C in glomerular cells in diabetes. Mechanisms and potential links to the pathogenesis of diabetic glomerulopathy. *Diabetes* 43: 1-8; 1994

DeWitt, D.L.; Day, J.S.; Sonnenburg, W.K. and Smith, W.L. Concentrations of prostaglandin endoperoxide synthase and prostaglandin I2 synthase in the endothelium and smooth muscle of bovine aorta. *J Clin. Invest* 72: 1882-1888; 1983

Dinerman, J.L.; Lowenstein, C.J. and Snyder, S.H. Molecular mechanisms of nitric oxide regulation. Potential relevance to cardiovascular disease. *Circ. Res.* 73: 217-222; 1993

Dogne, J.M.; de, L., X; Delarge, J.; David, J.L. and Masereel, B. New trends in thromboxane and prostacyclin modulators. *Curr. Med. Chem.* 7: 609-628; 2000

Edens, W.A.; Sharling, L.; Cheng, G.; Shapira, R.; Kinkade, J.M.; Lee, T.; Edens, H.A.; Tang, X.; Sullards, C.; Flaherty, D.B.; Benian, G.M. and Lambeth, J.D. Tyrosine cross-linking of extracellular matrix is catalyzed by Duox, a multidomain oxidase/peroxidase with homology to the phagocyte oxidase subunit gp91phox. *J Cell Biol.* 154: 879-891; 2001

Faour, W.H.; He, Y.; He, Q.W.; de Ladurantaye, M.; Quintero, M.; Mancini, A. and Di Battista, J.A. Prostaglandin E(2) regulates the level and stability of cyclooxygenase- 2 mRNA through activation of p38 mitogen-activated protein kinase in interleukin-1 beta-treated human synovial fibroblasts. *J Biol. Chem.* 276: 31720-31731; 2001

Fontayne, A.; Dang, P.M.; Gougerot-Pocidalo, M.A. and El Benna, J. Phosphorylation of p47phox sites by PKC alpha, beta II, delta, and zeta: effect on binding to p22phox and on NADPH oxidase activation. *Biochemistry* 41: 7743-7750; 2002

Forth, W., Henschler, D., Rummel, W. and Starke, K. Allgemeine und spezielle Pharmakologie und Toxikologie. *Spektrum Akademischer Verlag* 7th ed.: 414; 1998

Frost, M.T.; Halliwell, B. and Moore, K.P. Analysis of free and protein-bound nitrotyrosine in human plasma by a gas chromatography/mass spectrometry method that avoids nitration artifacts. *Biochem. J* 345 Pt 3: 453-458; 2000

Fukui, T.; Ishizaka, N.; Rajagopalan, S.; Laursen, J.B.; Capers, Q.; Taylor, W.R.; Harrison, D.G.; de Leon, H.; Wilcox, J.N. and Griendling, K.K. p22phox mRNA expression and NADPH oxidase activity are increased in aortas from hypertensive rats. *Circ. Res.* 80: 45-51; 1997

Furchgott, R.F.; Cherry, P.D.; Zawadzki, J.V. and Jothianandan, D. Endothelial cells as mediators of vasodilation of arteries. *J Cardiovasc. Pharmacol.* 6 Suppl 2: S336-S343; 1984

Gaston, B. Nitric oxide and thiol groups. *Biochim. Biophys. Acta* 1411: 323-333; 1999

Goldstein, S.; Czapski, G.; Lind, J. and Merenyi, G. Tyrosine nitration by simultaneous generation of (.)NO and O-(2) under physiological conditions. How the radicals do the job. *J. Biol. Chem.* 275: 3031-3036; 2000

Goligorsky, M.S.; Noiri, E.; Tsukahara, H.; Budzikowski, A.S. and Li, H. A pivotal role of nitric oxide in endothelial cell dysfunction. *Acta Physiol Scand.* 168: 33-40; 2000

Graff, G. Preparation of PGG2 and PGH2. *Methods Enzymol.* 86: 376-385; 1982

Griendling, K.K. and Harrison, D.G. Dual role of reactive oxygen species in vascular growth. *Circ. Res.* 85: 562-563; 1999

Griendling, K.K.; Sorescu, D. and Ushio-Fukai, M. NAD(P)H oxidase: role in cardiovascular biology and disease. *Circ. Res.* 86: 494-501; 2000

Grunfeld, S.; Hamilton, C.A.; Mesaros, S.; McClain, S.W.; Dominiczak, A.F.; Bohr, D.F. and Malinski, T. Role of superoxide in the depressed nitric oxide production by the endothelium of genetically hypertensive rats. *Hypertension* 26: 854-857; 1995

Gryglewski, R.J.; Palmer, R.M. and Moncada, S. Superoxide anion is involved in the breakdown of endothelium-derived vascular relaxing factor. *Nature* 320: 454-456; 1986

Guzik, T.J.; Mussa, S.; Gastaldi, D.; Sadowski, J.; Ratnatunga, C.; Pillai, R. and Channon, K.M. Mechanisms of increased vascular superoxide production in human diabetes mellitus: role of NAD(P)H oxidase and endothelial nitric oxide synthase. *Circulation* 105: 1656-1662; 2002

Gyllenhammar, H. Lucigenin chemiluminescence in the assessment of neutrophil superoxide production. *J. Immunol. Methods* 97: 209-213; 1987

Haddad, I.Y.; Pataki, G.; Hu, P.; Galliani, C.; Beckman, J.S. and Matalon, S. Quantitation of nitrotyrosine levels in lung sections of patients and animals with acute lung injury. *J. Clin. Invest* 94: 2407-2413; 1994

Hailer, N.P.; Oppermann, E.; Leckel, K.; Cinatl, J.; Markus, B.H. and Blaheta, R.A. Prostaglandin E2 induces expression of P-selectin (CD62P) on cultured human umbilical vein endothelial cells and enhances endothelial binding of CD4-T-cells. *Transplantation* 70: 236-240; 2000

Hamilton, C.A.; Brosnan, M.J.; McIntyre, M.; Graham, D. and Dominiczak, A.F. Superoxide excess in hypertension and aging: a common cause of endothelial dysfunction. *Hypertension* 37: 529-534; 2001

Hammarstrom, S. Enzymatic synthesis of 15-hydroperoxythromboxane A2 and 12-hydroperoxy- 5,8,10-heptadecatrienoic acid. *J. Biol. Chem.* 255: 518-521; 1980

Harold, J.G.; Siegel, R.J.; Edwalds, G.M.; Satoh, P. and Fishbein, M.C. Immunohistochemical localization of 6-keto-PGF1-alpha in canine coronary vasculature. *Prostaglandins* 29: 19-23; 1985

Harrison, D.G. Cellular and molecular mechanisms of endothelial cell dysfunction. *J. Clin. Invest* 100: 2153-2157; 1997a

Harrison, R. Human xanthine oxidoreductase: in search of a function. *Biochem. Soc. Trans.* 25: 786-791; 1997b

Hecker, M.; Hatzelmann, A. and Ullrich, V. Preparative HPLC purification of prostaglandin endoperoxides and isolation of novel cyclooxygenase-derived arachidonic acid metabolites. *Biochem. Pharmacol.* 36: 851-855; 1987

Hink, U.; Li, H.; Mollnau, H.; Oelze, M.; Matheis, E.; Hartmann, M.; Skatchkov, M.; Thaiss, F.; Stahl, R.A.; Warnholtz, A.; Meinertz, T.; Griendling, K.; Harrison, D.G.; Forstermann, U. and Munzel, T. Mechanisms underlying endothelial dysfunction in diabetes mellitus. *Circ. Res.* 88: E14-E22; 2001

Houston, M.; Estevez, A.; Chumley, P.; Aslan, M.; Marklund, S.; Parks, D.A. and Freeman, B.A. Binding of xanthine oxidase to vascular endothelium. Kinetic characterization and oxidative impairment of nitric oxide-dependent signaling. *J Biol. Chem.* 274: 4985-4994; 1999

Hug, H. and Sarre, T.F. Protein kinase C isoenzymes: divergence in signal transduction? *Biochem. J.* 291 (Pt 2): 329-343; 1993

Huie, R.E. and Padmaja, S. The reaction of no with superoxide. *Free Radic. Res. Commun.* 18: 195-199; 1993

Hunt, B.J. and Jurd, K.M. Relation between endothelial-cell activation and infection, inflammation, and infarction. *Lancet* 350: 293; 1997

Idris, I.; Gray, S. and Donnelly, R. Protein kinase C activation: isozyme-specific effects on metabolism and cardiovascular complications in diabetes. *Diabetologia* 44: 659-673; 2001

Inoguchi, T.; Battan, R.; Handler, E.; Sportsman, J.R.; Heath, W. and King, G.L. Preferential elevation of protein kinase C isoform beta II and diacylglycerol levels in the aorta and heart of diabetic rats: differential reversibility to glycemic control by islet cell transplantation. *Proc. Natl. Acad. Sci. U. S. A* 89: 11059-11063; 1992

Inoguchi, T.; Li, P.; Umeda, F.; Yu, H.Y.; Kakimoto, M.; Imamura, M.; Aoki, T.; Etoh, T.; Hashimoto, T.; Naruse, M.; Sano, H.; Utsumi, H. and Nawata, H. High glucose level and free fatty acid stimulate reactive oxygen species production through protein kinase C--dependent activation of NAD(P)H oxidase in cultured vascular cells. *Diabetes* 49: 1939-1945; 2000

Ishii, H.; Jirousek, M.R.; Koya, D.; Takagi, C.; Xia, P.; Clermont, A.; Bursell, S.E.; Kern, T.S.; Ballas, L.M.; Heath, W.F.; Stramm, L.E.; Feener, E.P. and King, G.L. Amelioration of vascular dysfunctions in diabetic rats by an oral PKC beta inhibitor. *Science* 272: 728-731; 1996

Ishii, H.; Koya, D. and King, G.L. Protein kinase C activation and its role in the development of vascular complications in diabetes mellitus. *J. Mol. Med.* 76: 21-31; 1998

Jones, R.D.; Hancock, J.T. and Morice, A.H. NADPH oxidase: a universal oxygen sensor? *Free Radic. Biol. Med.* 29: 416-424; 2000

Kamisaki, Y.; Wada, K.; Bian, K.; Balabanli, B.; Davis, K.; Martin, E.; Behbod, F.; Lee, Y.C. and Murad, F. An activity in rat tissues that modifies nitrotyrosine-containing proteins. *Proc. Natl. Acad. Sci. U. S. A* 95: 11584-11589; 1998

Klein, T.; Ullrich, V.; Pfeilschifter, J. and Nusing, R. On the induction of cyclooxygenase-2, inducible nitric oxide synthase and soluble phospholipase A2 in rat mesangial cells by a nonsteroidal anti-inflammatory drug: the role of cyclic AMP. *Mol. Pharmacol.* 53: 385-391; 1998

Knapp, L.T. and Klann, E. Superoxide-induced stimulation of protein kinase C via thiol modification and modulation of zinc content. *J. Biol. Chem.* 275: 24136-24145; 2000

Knowles, R.G. and Salter, M. Measurement of NOS activity by conversion of radiolabeled arginine to citrulline using ion-exchange separation. *Methods Mol. Biol.* 100: 67-73; 1998

Koppenol, W.H. Chemistry of peroxynitrite and its relevance to biological systems. *Met. Ions. Biol. Syst.* 36: 597-619; 1999

Koshkin, V.; Lotan, O. and Pick, E. The cytosolic component p47(phox) is not a sine qua non participant in the activation of NADPH oxidase but is required for optimal superoxide production. *J. Biol. Chem.* 271: 30326-30329; 1996

Koya, D. and King, G.L. Protein kinase C activation and the development of diabetic complications. *Diabetes* **47:** 859-866; 1998

Kromer, B.M. and Tippins, J.R. The vasoconstrictor effect of 8-epi prostaglandin F2alpha in the hypoxic rat heart. *Br. J Pharmacol.* 126: 1171-1174; 1999

Kumar, V.B.; Bernardo, A.E.; Alshaher, M.M.; Buddhiraju, M.; Purushothaman, R. and Morley, J.E. Rapid assay for nitric oxide synthase using thin-layer chromatography. *Anal. Biochem.* 269: 17-20; 1999

Lassegue, B.; Sorescu, D.; Szocs, K.; Yin, Q.; Akers, M.; Zhang, Y.; Grant, S.L.; Lambeth, J.D. and Griendling, K.K. Novel gp91(phox) homologues in vascular smooth muscle cells : nox1 mediates angiotensin II-induced superoxide formation and redox- sensitive signaling pathways. *Circ. Res.* 88: 888-894; 2001

Lee, J.; Hunt, J.A. and Groves, J.T. Manganese porphyrins as redox-coupled peroxynitrite reductase. *J. Am. Chem. Soc.* 120: 6053-6061; 1998

Leeuwenburgh, C.; Hansen, P.; Shaish, A.; Holloszy, J.O. and Heinecke, J.W. Markers of protein oxidation by hydroxyl radical and reactive nitrogen species in tissues of aging rats. *Am. J. Physiol* 274: R453-R461; 1998

Lefer, A.M. and Lefer, D.J. Pharmacology of the endothelium in ischemia-reperfusion and circulatory shock. *Annu. Rev. Pharmacol. Toxicol.* 33: 71-90; 1993

Li, H.; Oehrlein, S.A.; Wallerath, T.; Ihrig-Biedert, I.; Wohlfart, P.; Ulshofer, T.; Jessen, T.; Herget, T.; Forstermann, U. and Kleinert, H. Activation of protein kinase C alpha and/or epsilon enhances transcription of the human endothelial nitric oxide synthase gene. *Mol. Pharmacol.* 53: 630-637; 1998

Li, J.M.; Mullen, A.M.; Yun, S.; Wientjes, F.; Brouns, G.Y.; Thrasher, A.J. and Shah, A.M. Essential role of the NADPH oxidase subunit p47(phox) in endothelial cell superoxide production in response to phorbol ester and tumor necrosis factor-alpha. *Circ. Res.* 90: 143-150; 2002

Li, Y.; Huang, T.T.; Carlson, E.J.; Melov, S.; Ursell, P.C.; Olson, J.L.; Noble, L.J.; Yoshimura, M.P.; Berger, C.; Chan, P.H. and . Dilated cardiomyopathy and neonatal lethality in mutant mice lacking manganese superoxide dismutase. *Nat. Genet.* 11: 376-381; 1995

Li, Y. and Trush, M.A. Diphenyleneiodonium, an NAD(P)H oxidase inhibitor, also potently inhibits mitochondrial reactive oxygen species production. *Biochem. Biophys. Res. Commun.* 253: 295-299; 1998

Liochev, S.I. and Fridovich, I. Lucigenin (bis-N-methylacridinium) as a mediator of superoxide anion production. *Arch. Biochem. Biophys.* 337: 115-120; 1997

Liu, P.; Hock, C.E.; Nagele, R. and Wong, P.Y. Formation of nitric oxide, superoxide, and peroxynitrite in myocardial ischemia-reperfusion injury in rats. *Am. J. Physiol* 272: H2327-H2336; 1997

Lum, H. and Roebuck, K.A. Oxidant stress and endothelial cell dysfunction. *Am. J Physiol Cell Physiol* 280: C719-C741; 2001

Luscher, T.F. and Noll, G. The pathogenesis of cardiovascular disease: role of the endothelium as a target and mediator. *Atherosclerosis* 118 Suppl: S81-S90; 1995

MacMillan-Crow, L.A.; Crow, J.P.; Kerby, J.D.; Beckman, J.S. and Thompson, J.A. Nitration and inactivation of manganese superoxide dismutase in chronic rejection of human renal allografts. *Proc. Natl. Acad. Sci. U. S. A* 93: 11853-11858; 1996

MacMillan-Crow, L.A.; Crow, J.P. and Thompson, J.A. Peroxynitrite-mediated inactivation of manganese superoxide dismutase involves nitration and oxidation of critical tyrosine residues. *Biochemistry* 37: 1613-1622; 1998

MacMillan-Crow, L.A. and Thompson, J.A. Immunoprecipitation of nitrotyrosine-containing proteins. *Methods Enzymol.* 301: 135-145; 1999

Mais, D.E.; Saussy, D.L., Jr.; Chaikhouni, A.; Kochel, P.J.; Knapp, D.R.; Hamanaka, N. and Halushka, P.V. Pharmacologic characterization of human and canine thromboxane A2/prostaglandin H2 receptors in platelets and blood vessels: evidence for different receptors. *J. Pharmacol. Exp. Ther.* 233: 418-424; 1985

Malinski, T. and Taha, Z. Nitric oxide release from a single cell measured in situ by a porphyrinic-based microsensor. *Nature* 358: 676-678; 1992

Mannick, J.B.; Schonhoff, C.; Papeta, N.; Ghafourifar, P.; Szibor, M.; Fang, K. and Gaston, B. S-Nitrosylation of mitochondrial caspases. *J. Cell Biol.* 154: 1111-1116; 2001

Marczin, N.; Antonov, A.; Papapetropoulos, A.; Munn, D.H.; Virmani, R.; Kolodgie, F.D.; Gerrity, R. and Catravas, J.D. Monocyte-induced downregulation of nitric oxide synthase in cultured aortic endothelial cells. *Arterioscler. Thromb. Vasc. Biol.* 16: 1095-1103; 1996

Marla, S.S.; Lee, J. and Groves, J.T. Peroxynitrite rapidly permeates phospholipid membranes. *Proc. Natl. Acad. Sci. U. S. A* 94: 14243-14248; 1997

Marsden, P.A.; Heng, H.H.; Scherer, S.W.; Stewart, R.J.; Hall, A.V.; Shi, X.M.; Tsui, L.C. and Schappert, K.T. Structure and chromosomal localization of the human constitutive endothelial nitric oxide synthase gene. *J. Biol. Chem.* 268: 17478-17488; 1993

Mayhan, W.G.; Simmons, L.K. and Sharpe, G.M. Mechanism of impaired responses of cerebral arterioles during diabetes mellitus. *Am. J. Physiol* 260: H319-H326; 1991

Mayhan, W.G. and Patel, K.P. Acute effects of glucose on reactivity of cerebral microcirculation: role of activation of protein kinase C. *Am. J. Physiol* 269: H1297-H1302; 1995

Melov, S.; Schneider, J.A.; Day, B.J.; Hinerfeld, D.; Coskun, P.; Mirra, S.S.; Crapo, J.D. and Wallace, D.C. A novel neurological phenotype in mice lacking mitochondrial manganese superoxide dismutase. *Nat. Genet.* 18: 159-163; 1998

Moncada, S.; Palmer, R.M. and Higgs, E.A. Nitric oxide: physiology, pathophysiology, and pharmacology. *Pharmacol. Rev.* 43: 109-142; 1991

Moncada, S. The 1991 Ulf von Euler Lecture. The L-arginine: nitric oxide pathway. *Acta Physiol. Scand.* 145: 201-227; 1992

Moncada, S. and Higgs, A. The L-arginine-nitric oxide pathway. *N. Engl. J. Med.* 329: 2002-2012; 1993

Mullarkey, C.J.; Edelstein, D. and Brownlee, M. Free radical generation by early glycation products: a mechanism for accelerated atherogenesis in diabetes. *Biochem. Biophys. Res. Commun.* 173: 932-939; 1990

Mulsch, A.; Bauersachs, J.; Schafer, A.; Stasch, J.P.; Kast, R. and Busse, R. Effect of YC-1, an NO-independent, superoxide-sensitive stimulator of soluble guanylyl cyclase, on smooth muscle responsiveness to nitrovasodilators. *Br. J Pharmacol.* 120: 681-689; 1997

Namgaladze, D.; Hofer, H.W. and Ullrich, V. Redox control of calcineurin by targeting the binuclear Fe(2+)-Zn(2+) center at the enzyme active site. *J Biol. Chem.* 277: 5962-5969; 2002

Narumiya, S.; Sugimoto, Y. and Ushikubi, F. Prostanoid receptors: structures, properties, and functions. *Physiol Rev.* 79: 1193-1226; 1999

O' Hara, Y.; Peterson, T.E. and Harrison, D.G. Hypercholesterolemia increases endothelial superoxide anion production. *J. Clin. Invest* 91: 2546-2551; 1993

Oberley, L.W. Free radicals and diabetes. *Free Radic. Biol. Med.* 5: 113-124; 1988

Ogata, N.; Yamamoto, H.; Kugiyama, K.; Yasue, H. and Miyamoto, E. Involvement of protein kinase C in superoxide anion-induced activation of nuclear factor-kappa B in human endothelial cells. *Cardiovasc. Res.* 45: 513-521; 2000

Palmer, R.M.; Ashton, D.S. and Moncada, S. Vascular endothelial cells synthesize nitric oxide from L-arginine. *Nature* 333: 664-666; 1988

Pasquet, J.P.; Zou, M.H. and Ullrich, V. Peroxynitrite inhibition of nitric oxide synthases. *Biochimie* 78: 785-791; 1996

Pfeiffer, S. and Mayer, B. Lack of tyrosine nitration by peroxynitrite generated at physiological pH. *J. Biol. Chem.* 273: 27280-27285; 1998

Pfeiffer, S.; Schmidt, K. and Mayer, B. Dityrosine formation outcompetes tyrosine nitration at low steady-state concentrations of peroxynitrite. Implications for tyrosine modification by nitric oxide/superoxide in vivo. *J. Biol. Chem.* 275: 6346-6352; 2000

Pfeiffer, S.; Lass, A.; Schmidt, K. and Mayer, B. Protein tyrosine nitration in cytokine-activated murine macrophages. Involvement of a peroxidase/nitrite pathway rather than peroxynitrite. *J. Biol. Chem.* 276: 34051-34058; 2001a

Pfeiffer, S.; Lass, A.; Schmidt, K. and Mayer, B. Protein tyrosine nitration in mouse peritoneal macrophages activated in vitro and in vivo: evidence against an essential role of peroxynitrite. *FASEB J.* 15: 2355-2364; 2001b

Pober, J.S. Warner-Lambert/Parke-Davis award lecture. Cytokine-mediated activation of vascular endothelium. Physiology and pathology. *Am. J Pathol.* 133: 426-433; 1988

Pollock, J.S.; Forstermann, U.; Mitchell, J.A.; Warner, T.D.; Schmidt, H.H.; Nakane, M. and Murad, F. Purification and characterization of particulate endothelium-derived relaxing factor synthase from cultured and native bovine aortic endothelial cells. *Proc. Natl. Acad. Sci. U. S. A* 88: 10480-10484; 1991

Prescott, S.M.; McIntyre, T.M. and Zimmerman, G.A. Events at the vascular wall: the molecular basis of inflammation. *J Investig. Med.* 49: 104-111; 2001

Pritchard, K.A., Jr.; Ackerman, A.W.; Gross, E.R.; Stepp, D.W.; Shi, Y.; Fontana, J.T.; Baker, J.E. and Sessa, W.C. Heat shock protein 90 mediates the balance of nitric oxide and superoxide anion from endothelial nitric-oxide synthase. *J Biol. Chem.* 276: 17621-17624; 2001

Pueyo, M.E.; Arnal, J.F.; Rami, J. and Michel, J.B. Angiotensin II stimulates the production of NO and peroxynitrite in endothelial cells. *Am. J Physiol* 274: C214-C220; 1998

Radi, R.; Rubbo, H.; Bush, K. and Freeman, B.A. Xanthine oxidase binding to glycosaminoglycans: kinetics and superoxide dismutase interactions of immobilized xanthine oxidase-heparin complexes. *Arch. Biochem. Biophys.* 339: 125-135; 1997

Rajagopalan, S.; Kurz, S.; Munzel, T.; Tarpey, M.; Freeman, B.A.; Griendling, K.K. and Harrison, D.G. Angiotensin II-mediated hypertension in the rat increases vascular superoxide production via membrane NADH/NADPH oxidase activation. Contribution to alterations of vasomotor tone. *J. Clin. Invest* 97: 1916-1923; 1996

Rand, M.J. and Li, C.G. The inhibition of nitric oxide-mediated relaxations in rat aorta and anococcygeus muscle by diphenylene iodonium. *Clin. Exp. Pharmacol. Physiol* 20: 141-148; 1993

Ranjan, V.; Xiao, Z. and Diamond, S.L. Constitutive NOS expression in cultured endothelial cells is elevated by fluid shear stress. *Am. J. Physiol* 269: H550-H555; 1995

Reaume, A.G.; Elliott, J.L.; Hoffman, E.K.; Kowall, N.W.; Ferrante, R.J.; Siwek, D.F.; Wilcox, H.M.; Flood, D.G.; Beal, M.F.; Brown, R.H., Jr.; Scott, R.W. and Snider, W.D. Motor neurons in Cu/Zn superoxide dismutase-deficient mice develop normally but exhibit enhanced cell death after axonal injury. *Nat. Genet.* 13: 43-47; 1996

Reed, J.W.; Ho, H.H. and Jolly, W.L. Chemical syntheses with a quenched flow reactor. Hydroxytrihydroborate and peroxynitrite. *J. Am. Chem. Soc.* 96: 1248-1249; 1974

Reiter, C.D.; Teng, R.J. and Beckman, J.S. Superoxide reacts with nitric oxide to nitrate tyrosine at physiological pH via peroxynitrite. *J. Biol. Chem.* 275: 32460-32466; 2000

Rhoden, K.J. and Barnes, P.J. Effect of hydrogen peroxide on guinea-pig tracheal smooth muscle in vitro: role of cyclo-oxygenase and airway epithelium. *Br. J Pharmacol.* 98: 325-330; 1989

Ruderman, N.B.; Williamson, J.R. and Brownlee, M. Glucose and diabetic vascular disease. *FASEB J.* 6: 2905-2914; 1992

Ryan, M.G.; Balendran, A.; Harrison, R.; Wolstenholme, A. and Bulkley, G.B. Xanthine oxidoreductase: dehydrogenase to oxidase conversion. *Biochem. Soc. Trans.* 25: 530S; 1997

Salmon, J.A. and Flower, R.J. Preparation and assay of prostacyclin synthase. *Methods Enzymol.* 86: 91-99; 1982

Salmon, J.A. and Flower, R.J. Extraction and thin-layer chromatography of arachidonic acid metabolites. *Methods Enzymol.* 86: 477-493; 1982

Sano, T.; Umeda, F.; Hashimoto, T.; Nawata, H. and Utsumi, H. Oxidative stress measurement by in vivo electron spin resonance spectroscopy in rats with streptozotocin-induced diabetes. *Diabetologia* 41: 1355-1360; 1998

Saussy, D.L., Jr.; Mais, D.E.; Burch, R.M. and Halushka, P.V. Identification of a putative thromboxane A2/prostaglandin H2 receptor in human platelet membranes. *J Biol. Chem.* 261: 3025-3029; 1986

Schmidt, P., Youhnovski, N., Daiber, A., Balan, A., Arsic, M., Bachschmid, M., Przybylski, M. and Ullrich, V. Specific nitration at tyrosine-430 revealed by high resolution mass spectrometry as basis for redox regulation of bovine prostacyclin synthase. Submitted to *J. Biol. Chem.* 2002

Scott, G.S. and Hooper, D.C. The role of uric acid in protection against peroxynitrite-mediated pathology. *Med. Hypotheses* **56:** 95-100; 2001

Segal, A.W. The NADPH oxidase and chronic granulomatous disease. *Mol. Med. Today* 2: 129-135; 1996

Sessa, W.C.; Barber, C.M. and Lynch, K.R. Mutation of N-myristoylation site converts endothelial cell nitric oxide synthase from a membrane to a cytosolic protein. *Circ. Res.* 72: 921-924; 1993

Shevchenko, A.; Jensen, O.N.; Podtelejnikov, A.V.; Sagliocco, F.; Wilm, M.; Vorm, O.; Mortensen, P.; Shevchenko, A.; Boucherie, H. and Mann, M. Linking genome and proteome by mass spectrometry: large-scale identification of yeast proteins from two dimensional gels. *Proc. Natl. Acad. Sci. U. S. A* 93: 14440-14445; 1996

Shevchenko, A.; Wilm, M.; Vorm, O. and Mann, M. Mass spectrometric sequencing of proteins silver-stained polyacrylamide gels. *Anal. Chem.* 68: 850-858; 1996

Shimizu, S.; Ishii, M.; Yamamoto, T.; Kawanishi, T.; Momose, K. and Kuroiwa, Y. Bradykinin induces generation of reactive oxygen species in bovine aortic endothelial cells. *Res. Commun. Chem. Pathol. Pharmacol.* 84: 301-314; 1994

Siddhanta, U.; Presta, A.; Fan, B.; Wolan, D.; Rousseau, D.L. and Stuehr, D.J. Domain swapping in inducible nitric-oxide synthase. Electron transfer occurs between flavin and heme groups located on adjacent subunits in the dimer. *J Biol. Chem.* 273: 18950-18958; 1998

Siegle, I.; Nusing, R.; Brugger, R.; Sprenger, R.; Zecher, R. and Ullrich, V. Characterization of monoclonal antibodies generated against bovine and porcine prostacyclin synthase and quantitation of bovine prostacyclin synthase. *FEBS Lett.* 347: 221-225; 1994

Smith, W.L.; DeWitt, D.L. and Allen, M.L. Bimodal distribution of the prostaglandin I2 synthase antigen in smooth muscle cells. *J Biol. Chem.* 258: 5922-5926; 1983

Sobotta, J. Histologie. Welsch, U. (Ed.). *Urban & Schwarzenberg* 5th ed.: 128; 1997

Sohn, H.Y.; Raff, U.; Hoffmann, A.; Gloe, T.; Heermeier, K.; Galle, J. and Pohl, U. Differential role of angiotensin II receptor subtypes on endothelial superoxide formation. *Br. J Pharmacol.* 131: 667-672; 2000

Song, Y.; Cardounel, A.J.; Zweier, J.L. and Xia, Y. Inhibition of superoxide generation from neuronal nitric oxide synthase by heat shock protein 90: implications in NOS regulation. *Biochemistry* 41: 10616-10622; 2002

Souza, J.M.; Choi, I.; Chen, Q.; Weisse, M.; Daikhin, E.; Yudkoff, M.; Obin, M.; Ara, J.; Horwitz, J. and Ischiropoulos, H. Proteolytic degradation of tyrosine nitrated proteins. *Arch. Biochem. Biophys.* 380: 360-366; 2000

Spisni, E.; Griffoni, C.; Santi, S.; Riccio, M.; Marulli, R.; Bartolini, G.; Toni, M.; Ullrich, V. and Tomasi, V. Colocalization prostacyclin (PGI_2) synthase--caveolin-1 in endothelial cells and new roles for PGI_2 in angiogenesis. *Exp. Cell Res.* 266: 31-43; 2001

Stadtman, E.R. Protein oxidation and aging. *Science* 257: 1220-1224; 1992

Stamler, J.S.; Simon, D.I.; Jaraki, O.; Osborne, J.A.; Francis, S.; Mullins, M.; Singel, D. and Loscalzo, J. S-nitrosylation of tissue-type plasminogen activator confers vasodilatory and antiplatelet properties on the enzyme. *Proc. Natl. Acad. Sci. U. S. A* 89: 8087-8091; 1992a

Stamler, J.S.; Simon, D.I.; Osborne, J.A.; Mullins, M.E.; Jaraki, O.; Michel, T.; Singel, D.J. and Loscalzo, J. S-nitrosylation of proteins with nitric oxide: synthesis and characterization of biologically active compounds. *Proc. Natl. Acad. Sci. U. S. A* 89: 444-448; 1992b

Stevens, T.; Garcia, J.G.; Shasby, D.M.; Bhattacharya, J. and Malik, A.B. Mechanisms regulating endothelial cell barrier function. *Am. J Physiol Lung Cell Mol. Physiol* 279: L419-L422; 2000

Sun, J.; Xin, C.; Eu, J.P.; Stamler, J.S. and Meissner, G. Cysteine-3635 is responsible for skeletal muscle ryanodine receptor modulation by NO. *Proc. Natl. Acad. Sci. U. S. A* 98: 11158-11162; 2001

Takahashi, K.; Nammour, T.M.; Fukunaga, M.; Ebert, J.; Morrow, J.D.; Roberts, L.J.; Hoover, R.L. and Badr, K.F. Glomerular actions of a free radical-generated novel prostaglandin, 8- epi-prostaglandin F2 alpha, in the rat. Evidence for interaction with thromboxane A2 receptors. *J. Clin. Invest* 90: 136-141; 1992

Tarpey, M.M.; White, C.R.; Suarez, E.; Richardson, G.; Radi, R. and Freeman, B.A. Chemiluminescent detection of oxidants in vascular tissue. Lucigenin but not coelenterazine enhances superoxide formation. *Circ. Res.* 84: 1203-1211; 1999

Tesfamariam, B.; Brown, M.L.; Deykin, D. and Cohen, R.A. Elevated glucose promotes generation of endothelium-derived vasoconstrictor prostanoids in rabbit aorta. *J. Clin. Invest* 85: 929-932; 1990

Tesfamariam, B.; Brown, M.L. and Cohen, R.A. Elevated glucose impairs endothelium-dependent relaxation by activating protein kinase C. *J. Clin. Invest* 87: 1643-1648; 1991

Tesfamariam, B. and Cohen, R.A. Free radicals mediate endothelial cell dysfunction caused by elevated glucose. *Am. J. Physiol* 263: H321-H326; 1992a

Tesfamariam, B. and Cohen, R.A. Role of superoxide anion and endothelium in vasoconstrictor action of prostaglandin endoperoxide. *Am. J. Physiol* 262: H1915-H1919; 1992b

Thorup, C.; Kornfeld, M.; Winaver, J.M.; Goligorsky, M.S. and Moore, L.C. Angiotensin-II stimulates nitric oxide release in isolated perfused renal resistance arteries. *Pflugers Arch.* 435: 432-434; 1998

Timimi, F.K.; Ting, H.H.; Haley, E.A.; Roddy, M.A.; Ganz, P. and Creager, M.A. Vitamin C improves endothelium-dependent vasodilation in patients with insulin-dependent diabetes mellitus. *J. Am. Coll. Cardiol.* 31: 552-557; 1998

Ting, H.H.; Timimi, F.K.; Boles, K.S.; Creager, S.J.; Ganz, P. and Creager, M.A. Vitamin C improves endothelium-dependent vasodilation in patients with non-insulin-dependent diabetes mellitus. *J. Clin. Invest* 97: 22-28; 1996

Tomlinson, D.R. Mitogen-activated protein kinases as glucose transducers for diabetic complications. *Diabetologia* 42: 1271-1281; 1999

Tschudi, M.R.; Barton, M.; Bersinger, N.A.; Moreau, P.; Cosentino, F.; Noll, G.; Malinski, T. and Luscher, T.F. Effect of age on kinetics of nitric oxide release in rat aorta and pulmonary artery. *J. Clin. Invest* 98: 899-905; 1996

Ullrich, V.; Castle, L. and Weber, P. Spectral evidence for the cytochrome P450 nature of prostacyclin synthetase. *Biochem. Pharmacol.* 30: 2033-2036; 1981

Ullrich, V. and Bachschmid, M. Superoxide as a messenger of endothelial function. *Biochem. Biophys. Res. Commun.* 278: 1-8; 2000

Ullrich, V.; Zou, M.H. and Bachschmid, M. New physiological and pathophysiological aspects on the thromboxane A(2)-prostacyclin regulatory system. *Biochim. Biophys. Acta* 1532: 1-14; 2001

Vallance, P.; Leone, A.; Calver, A.; Collier, J. and Moncada, S. Accumulation of an endogenous inhibitor of nitric oxide synthesis in chronic renal failure. *Lancet* 339: 572-575; 1992

van Dalen, C.J.; Winterbourn, C.C.; Senthilmohan, R. and Kettle, A.J. Nitrite as a substrate and inhibitor of myeloperoxidase. Implications for nitration and hypochlorous acid production at sites of inflammation. *J. Biol. Chem.* 275: 11638-11644; 2000

van der Loo, B.; Labugger, R.; Skepper, J.N.; Bachschmid, M.; Kilo, J.; Powell, J.M.; Palacios-Callender, M.; Erusalimsky, J.D.; Quaschning, T.; Malinski, T.; Gygi, D.; Ullrich, V. and Luscher, T.F. Enhanced peroxynitrite formation is associated with vascular aging. *J. Exp. Med.* 192: 1731-1744; 2000

Vane, J.R.; Anggard, E.E. and Botting, R.M. Regulatory functions of the vascular endothelium. *N. Engl. J Med.* 323: 27-36; 1990

Vanhoutte, P.M. Aging and endothelial dysfunction. *Eur. Heart Journ* 136: 481-483; 2002

Vasquez-Vivar, J.; Hogg, N.; Martasek, P.; Karoui, H.; Pritchard, K.A., Jr. and Kalyanaraman, B. Tetrahydrobiopterin-dependent inhibition of superoxide generation from neuronal nitric oxide synthase. *J. Biol. Chem.* 274: 26736-26742; 1999

Viner, R.I.; Ferrington, D.A.; Huhmer, A.F.; Bigelow, D.J. and Schoneich, C. Accumulation of nitrotyrosine on the SERCA2a isoform of SR Ca-ATPase of rat skeletal muscle during aging: a peroxynitrite-mediated process? *FEBS Lett.* 379: 286-290; 1996

Viner, R.I.; Williams, T.D. and Schoneich, C. Peroxynitrite modification of protein thiols: oxidation, nitrosylation, and S-glutathiolation of functionally important cysteine residue(s) in the sarcoplasmic reticulum Ca-ATPase. *Biochemistry* 38: 12408-12415; 1999

Wang, Y.X.; Poon, C.I.; Poon, K.S. and Pang, C.C. Inhibitory actions of diphenyleneiodonium on endothelium-dependent vasodilatations in vitro and in vivo. *Br. J. Pharmacol.* 110: 1232-1238; 1993

White, C.R.; Darley-Usmar, V.; Berrington, W.R.; McAdams, M.; Gore, J.Z.; Thompson, J.A.; Parks, D.A.; Tarpey, M.M. and Freeman, B.A. Circulating plasma xanthine oxidase contributes to vascular dysfunction in hypercholesterolemic rabbits. *Proc. Natl. Acad. Sci. U. S. A* 93: 8745-8749; 1996

Xia, Y.; Tsai, A.L.; Berka, V. and Zweier, J.L. Superoxide generation from endothelial nitric-oxide synthase. A Ca2+/calmodulin-dependent and tetrahydrobiopterin regulatory process. *J Biol. Chem.* 273: 25804-25808; 1998

Ye, Y.Z.; Strong, M.; Huang, Z.Q. and Beckman, J.S. Antibodies that recognize nitrotyrosine. *Methods Enzymol.* 269: 201-209; 1996

Yura, T.; Fukunaga, M.; Khan, R.; Nassar, G.N.; Badr, K.F. and Montero, A. Free-radical-generated F2-isoprostane stimulates cell proliferation and endothelin-1 expression on endothelial cells. *Kidney Int.* 56: 471-478; 1999

Zajicek, J.; Wing, M.; Skepper, J. and Compston, A. Human oligodendrocytes are not sensitive to complement. A study of CD59 expression in the human central nervous system. *Lab Invest* 73: 128-138; 1995

Zhang, H.; Schmeisser, A.; Garlichs, C.D.; Plotze, K.; Damme, U.; Mugge, A. and Daniel, W.G. Angiotensin II-induced superoxide anion generation in human vascular endothelial cells: role of membrane-bound NADH-/NADPH-oxidases. *Cardiovasc. Res.* 44: 215-222; 1999

Zou, M.H. and Ullrich, V. Peroxynitrite formed by simultaneous generation of nitric oxide and superoxide selectively inhibits bovine aortic prostacyclin synthase. *FEBS Lett.* 382: 101-104; 1996

Zou, M.; Martin, C. and Ullrich, V. Tyrosine nitration as a mechanism of selective inactivation of prostacyclin synthase by peroxynitrite. *Biol. Chem.* 378: 707-713; 1997

Zou, M.H.; Klein, T.; Pasquet, J.P. and Ullrich, V. Interleukin 1beta decreases prostacyclin synthase activity in rat mesangial cells via endogenous peroxynitrite formation. *Biochem. J.* 336 (Pt 2): 507-512; 1998

Zou, M.; Jendral, M. and Ullrich, V. Prostaglandin endoperoxide-dependent vasospasm in bovine coronary arteries after nitration of prostacyclin synthase. *Br. J Pharmacol.* 126: 1283-1292; 1999a

Zou, M.; Yesilkaya, A. and Ullrich, V. Peroxynitrite inactivates prostacyclin synthase by heme-thiolate-catalyzed tyrosine nitration. *Drug Metab Rev.* 31: 343-349; 1999b

Zou, M.H.; Leist, M. and Ullrich, V. Selective nitration of prostacyclin synthase and defective vasorelaxation in atherosclerotic bovine coronary arteries. *Am. J. Pathol.* 154: 1359-1365; 1999c

Zou, M.H. and Bachschmid, M. Hypoxia-reoxygenation triggers coronary vasospasm in isolated bovine coronary arteries via tyrosine nitration of prostacyclin synthase. *J Exp. Med.* 190: 135-139; 1999d

Zou, M.H.; Daiber, A.; Peterson, J.A.; Shoun, H. and Ullrich, V. Rapid reactions of peroxynitrite with heme-thiolate proteins as the basis for protection of prostacyclin synthase from inactivation by nitration. *Arch. Biochem. Biophys.* 376: 149-155; 2000

Zou, M.H.; Shi, C. and Cohen, R.A. Oxidation of the zinc-thiolate complex and uncoupling of endothelial nitric oxide synthase by peroxynitrite. *J. Clin. Invest* 109: 817-826; 2002a

Zou, M.H.; Shi, C. and Cohen, R.A. High glucose via peroxynitrite causes tyrosine nitration and inactivation of prostacyclin synthase that is associated with thromboxane/prostaglandin H(2) receptor-mediated apoptosis and adhesion molecule expression in cultured human aortic endothelial cells. *Diabetes* 51: 198-203; 2002b